RAPID OSCILLATIONS

IN CATACLYSMIC VARIABLES

Sue Allen

Thesis submitted for the degree of
Master of Science
at the University of Cape Town

July 1986

ACKNOWLEDGEMENTS

I am indebted to my supervisor, Professor B. Warner, for his guidance and patience and for securing me financial support for this work.

I am grateful to the Director of the South African Astronomical Observatory, Dr M. Feast, for the allocation of observing time and for allowing me to use the Observatory Library over an extended period. Thanks also to Mrs E. Lastovica and Dr L. Balona, and especially to Drs D. Kilkenny and I. Coulson for constant encouragement and for putting up with a "squatter" in their office.

Dr D. O'Donoghue wrote all the computer programs used in the data analysis, and gave me great moral support and much of his time.

My thanks go to Mrs P. Dobbie and Mrs C. Barends for help with the worst of the typing, and to Dr I. Coulson for proofreading the manuscript.

I am grateful to the Council for Scientific and Industrial Research for the support of a post-graduate research scholarship, and to the University of Cape Town for a research associateship.

ABSTRACT

Coherent and quasi-periodic rapid oscillations have been seen in the optical and X-ray light curves of more than 30 cataclysmic variables to date. The observational characteristics of these oscillations are reviewed, and current models discussed. To put the observations in context, a detailed review is given of the canonical model of cataclysmic variables and the variations that give rise to its various sub-classes.

Observations of two systems of particular interest are presented, and their contributions to the modelling of rapid oscillations are discussed.

High-speed photometry of the very bright nova-like variable CPD-48^{o}1577 (IX Velorum) is shown to reveal low-amplitude oscillations with periods between 24 and 31 seconds. The oscillations are present in more than half of the runs, making this variable an attractive target for simultaneous observations in different wavelength bands.

The dwarf nova Z Cha is one of four cataclysmic variables which show rapid oscillations as well as primary eclipses. Photometry of Z Cha, archived at the University of Cape Town over a period of ten years, is searched for rapid oscillations. Two runs show oscillations, with periods of 24 and 28 seconds. They exhibit eclipse-related phase changes which show qualitative repetition within a run, but significant long-term variation. This behaviour

has not been seen in any other cataclysmic variable, and makes Z Cha a potentially powerful discriminating tool for models of oscillation and superoutburst.

CONTENTS

CHAPTER 1

A GENERALISED MODEL

1.1 INTRODUCTION

The term "cataclysmic variables" originally referred to stellar systems that have been observed to outburst - a spectacular increase in brightness over a period of days or even hours. More intensive studies of these stars have made it clear that many other systems, which have not been known to outburst, also belong to the class. On the other hand, some stars (eg. supernovae) originally included as cataclysmic variables, have since been excluded. Despite such re-classifications, cataclysmic variables are a fairly well-defined group with common properties. It is now universally accepted that they are binary systems in which one star is transferring matter in a steady stream to the other, often forming a disk of accreted material around it. They comprise the novae, recurrent novae, dwarf novae, nova-like variables and magnetic variables, a total of several hundred known stars.

In this chapter I shall summarise the essential characteristics of cataclysmic variables (CV's) and review in some detail the canonical model which applies to these apparently disparate star types. Chapter 2 deals with the classification of CV's into classes (and subclasses), and presents some of the current models for these classes as variations of the canonical model. Chapter 3 reviews the

properties of rapid oscillations in cataclysmic variables and describes current attempts to explain this behaviour.

Chapters 5 and 6 present high-speed, white light photometry of two CV's, analysis of rapid oscillations present in these data and conclusions that may be drawn. Chapter 4 is a brief outline of the methods of data capture, reduction and analysis used.

1.2 OBSERVATIONAL CHARACTERISTICS OF CATACLYSMIC VARIABLES

Much use has been made here of reviews by Warner [1976], Robinson [1976a] and Cordova and Mason [1983].

Essential characteristics of CV's can be summarised as follows:

i) Optical spectrum: A typical CV has a combination spectrum, with contributions from various parts of the system (principally the disk, bright spot and secondary). Although the spectra vary considerably, they generally feature a blue continuum, on which are superimposed strong, broad emission lines of HI, HeI and HeII.

Typically the widths of such lines, interpreted as Doppler shifts, imply radial velocities of many hundreds or even thousands of kilometres per second. Other common, though not universal, spectral features include CaII (H and K) and the CIII - NIII (λ4640-50) group of lines. Many systems have absorption features that correspond to spectra of cool main-sequence stars (spectral class G, K or M), and a few systems have extremely broad Balmer absorption lines

(eg. UX UMa). Line profiles may be single-peaked or double-peaked, and may change from one to the other around the orbital cycle (eg. in RU Peg).

ii) X-ray spectrum: Gravitational considerations based on the canonical CV model predict that these systems should be X-ray sources. About 50 CV's observed in the hard X-ray region of the spectrum (of energy $\geq$ 2 keV) have shown detectable flux (King and Shaviv [1984a]). Several have also shown emission in the ultra-soft X-ray region ($\sim$ 0.05 keV). Time variations of these emissions suggest that the two X-ray components are distinct in nature.

iii) Periodic light variations: Periodic variations of CV brightness may be divided into two broad groups: orbital variations on timescales of hours, and "rapid oscillations" on timescales of minutes or seconds.

The most obvious orbital variations are eclipses, during which the light intensity from a CV may drop by as much as 90% on a timescale of minutes or less. Unfortunately, relatively few CV's exhibit eclipses. More commonly, the orbital period of a system may be deduced by the presence of an "orbital hump" in the light curve, a gentle brightening which may extend over half the orbital cycle. In CV's which do eclipse, the eclipses occur at or just after the orbital hump. The orbital period may also be determined (or verified) if periodic variations occur in the spectra or polarization properties of a CV. Since CV's are not classified according to orbital period, it is a

remarkable observation that their periods are distinctly grouped, with a well-defined lower limit of 1.35 hours (EF Eri) and a noticeable gap between 2.10 hours (YZ Cnc) and 3.09 hours (AM Her). Excluding recurrent novae, which may have orbital periods of several hundred days, the longest observed period is 1.904 days for GK Per (Bianchini et al [1981]).

Rapid oscillations are present in the light curves of many CV's. They range in period (~ 7 s to ~ 1000 s) and stability, and may modulate the optical light curve by as much as 40% (Shafter and Targan [1982]).

iv) Aperiodic light variations: Here again, two broad distinctions may be made according to timescale of variations. All CV's exhibit small-amplitude brightness changes on a timescale of minutes or even seconds, a distinctive property known as flickering. In systems where an orbital hump is present, the flickering amplitude is larger on the hump. On a timescale of days or longer, aperiodic variations include outbursts (previously definitive), long minima (eg. VY Scl) and standstills at intermediate brightness that may continue for years (eg. Z Cam).

1.3 THE CANONICAL MODEL

The basic CV model was suggested by Crawford and Kraft [1956] and principally amended by Warner and Nather [1971] and Smak [1971]. It is shown schematically in Fig 1.1. Two

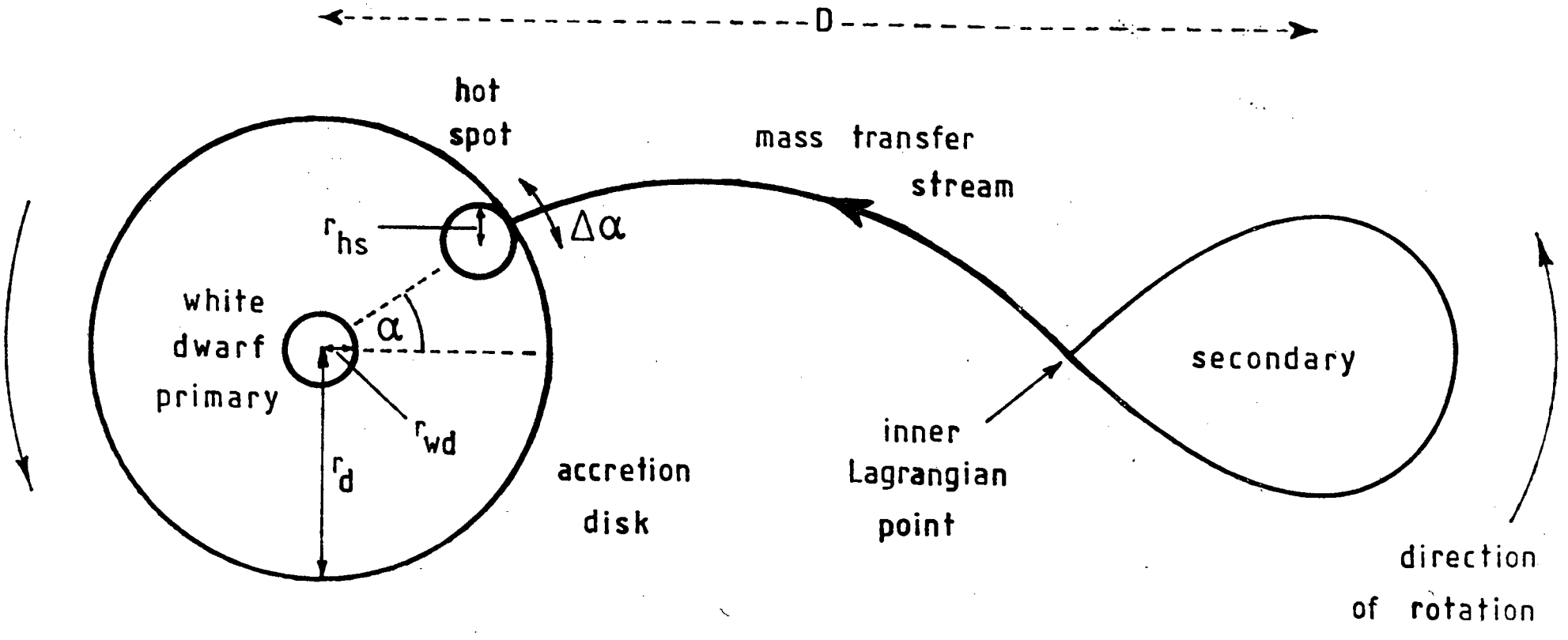

Figure 1.1 Diagram of a generalised cataclysmic variable (not drawn to scale).

$\frac{D}{r_{wd}} \sim 50$, $\frac{D}{r_d} \sim 5$, $\frac{r_{wd}}{r_{hs}} \sim 1$.

stars, gravitationally bound, revolve about their common centre of mass. This point lies on the line joining the centres of the two stars, its exact position depending on their relative masses. One star, known as the secondary, is usually a red dwarf of spectral type G or K which fills its Roche lobe. This lobe is a droplet-shaped region whose boundary is the zeroth equipotential of effective gravity for the enclosed star, ie. matter inside the Roche lobe is gravitationally bound to the star; matter outside it is not. In the CV model, the secondary is overflowing its Roche lobe. Matter leaves the star via the inner Lagrangian point (the "droplet" apex) since the gravitational attraction of the other star is stronger immediately outside this point than anywhere else on the secondary Roche lobe. Once outside the secondary, this matter forms a narrow stream, accelerated by gravitational attraction towards the primary star, a compact white dwarf which has ceased to burn hydrogen and is electron-degenerate. The path of the stream must be such that total angular momentum of the system about the centre of mass is conserved. This means that matter approaching the primary has too much angular momentum to impact directly onto it, but instead orbits at a certain radius, forming an accretion disk. Where the stream of material reaches the outer part of the disk, its large velocity relative to the disk material generates a strongly shocked impact region called a "hot spot".

Observations suggest that different classes of CV have different physical properties: for instance, only the outer part of the disk is present in intermediate polars, while AM Her stars do not have disks at all. More will be said of such variations in the next chapter.

I shall now consider each part of the idealised system shown in Fig 1.1, reviewing the evidence for its nature.

i) The secondary: Gallagher and Oinas [1974] used the photometric and spectroscopic properties of nova GK Per to calculate the radius of its secondary star, and to show that this was at least as large as the radius of its Roche lobe. However, Warner [1976] points out that CV secondaries cannot significantly overfill their Roche lobes, or their mass transfer rates would be unstable. Thus it seems likely that the Roche lobes are filled almost exactly, and this fact is now generally deduced from the occurrence of mass transfer.

The implication that the secondary is distorted in shape is supported by sinusoidal variations in light intensity at infrared wavelengths in, for instance, U Gem (Frank et al [1981]) and EM Cyg (Jameson el al [1981]). These are interpreted as being due to the changing aspect of a non-spherical secondary, but are not present in the optical light curves since these are dominated by light from the disk and/or hot spot. As we shall see in Section 1.4, it is fundamentally important to mass determinations of CV's to establish whether the secondary lies on the main sequence in the HR diagram, ie. whether its spectral type and

luminosity are consistent for a red dwarf. There is such evidence for SS Cyg (Joy [1956]). Also, Z Cam can be consistently modelled by assuming a mass - luminosity (M - L) relationship characteristic of main sequence stars (Kraft el al [1969]), and EM Cyg obeys the equivalent mass - radius (M - R) relationship (Robinson [1976b]). In addition, Faulkner el al [1972] derived a theoretical relationship between orbital period, P, and density of the secondary, ρ_2, in CV's where $M_2 < M_1$:

$$P \sqrt{<\rho_2>} = 3.83 \times 10^4$$

where P is in seconds and ρ_2 in g cm^{-3}.

This equation yields values of ρ_2 that are characteristic of the lower main sequence for CV's with orbital periods less than 10 hours. This is very reasonable, since longer-period CV's probably do not contain main sequence secondaries. They have sufficiently large orbital separations (and hence Roche lobes) to prevent mass transfer except from an evolved secondary. For example, spectra of T CrB, with an orbital period of 227.5 days, clearly show the presence of an M giant.)

More recently, Patterson [1984] has derived an empirical mass - radius relationship:

$$\frac{R}{R_\odot} = \begin{cases} \left(\frac{M}{M_\odot}\right)^{0.88\pm0.02} & 0.1 < \frac{M}{M_\odot} \lesssim 0.8 \\ 0.98\left(\frac{M}{M_\odot}\right)^{1.00} & 0.8 < \frac{M}{M_\odot} < 1.4 \end{cases}$$

which differs from the traditional theoretical main sequence relationship:

$$\frac{R}{R_\odot} = 0.96\left(\frac{M}{M_\odot}\right)^{1.00} \qquad 0.2 \lesssim \frac{M}{M_\odot} \lesssim 1.5 \qquad \ldots (1)$$

in that it predicts slightly lower masses for the secondaries of short-period CV's. Patterson's relationship is closely followed not only by CV secondaries but also by nearby field stars, supporting the hypothesis that both types are the same, viz. lower main sequence dwarfs.

On the assumption that short-period CV secondaries are lobe-filling, lower main sequence stars, their properties may be deduced as spectral types G or K, luminosity class V and masses from 0.1 to 1.0 $M_\odot$. We shall see later how such estimates are made.

ii) <u>The Primary</u>: Cataclysmic variables are modelled as having white dwarf primaries. There are several reasons for this. Firstly, Crawford and Kraft [1956], Greenstein [1957] and others noted that these stars did not lie on the main sequence, being underluminous by several magnitudes. Secondly, as early as 1943 Elvey and Babcock realised that

the shapes of some emission lines were characteristic of rotational Doppler shifts, but that the implied rotational velocities would be too high for a normal star to sustain without breaking up. Thirdly, compelling evidence for the presence of a white dwarf is the observation of rapid, coherent oscillations of period 7 to 71 seconds in a total of 21 CV's (Warner [1986a]). Since gravitationally-controlled processes obey the well-known period - density relationship

$$P \propto (G\rho)^{-\frac{1}{2}}$$

it can be shown that such oscillations arise in regions where $\rho \sim 10^6$ g cm^{-3}, a density characteristic of electron-degenerate material. Thus whether we postulate a rotational or pulsational origin for rapid oscillations in CV's, we must conclude they arise on or near a white dwarf.

iii) The accretion disk: In CV's which have an observable secondary spectrum, the radial velocity variations of this spectrum are out of phase with variations in the emission lines which must therefore be produced in the primary or surrounding disk (Warner [1979]). The emission lines may be produced over large regions of the disk, but their broad wings must arise from the inner parts where material moves most rapidly. The continuum light is produced mainly by the hot spot (eg. U Gem) or the disk as a whole (eg. UX UMa) or by some combination of the two.

Such a spectrum is theoretically predicted by Lynden-Bell and Pringle [1974], who show that light from a disk should have two main components:

i) a component from the disk itself, with spectral intensity as a function of frequency given by

$$F_\nu \propto \nu^{\frac{4}{3}} [\exp (h\nu/kT) -1]^{-1}$$

which becomes $F_\nu \propto \nu^{1/3}$ for small ν, and

ii) a component from the boundary layer between the white dwarf and the inner disk, with a rapidly variable blue continuum and emission peaking in the ultraviolet.

The standard steady-state disk model was proposed by Shakura and Sunyaev [1973]. They pointed out that accretion can only occur from a disk to a compact object if the accreted material loses angular momentum. Since the total disk momentum must remain constant, this excess angular momentum must be transported outwards. The result is a radial spreading of the disk, both inwards and outwards. At steady state, material of the inner disk accretes steadily onto the central star, while the outermost layers are stripped off by tidal interaction with the secondary, and may be recycled within the system.

What is the mechanism of momentum transfer? It is essentially unknown, but usually modelled as a viscosity,

ie. an effect whose magnitude is proportional to a velocity gradient. The constant of proportionality, the coefficient of viscosity, can be deduced from the observed accretion rate. Its value for CV's is typically $\eta \geq 10^6$ g cm^{-1} s^{-1} (Petterson [1983]), far higher than can be explained by particle viscosity alone, which gives $\eta < 10^2$ g cm^{-1} s^{-1} for ionised hydrogen at $T < 10^7$ K (Rossi and Olbert [1970]). Proposed mechanisms for this large viscosity include the action of magnetic fields in the disk, and turbulence, neither of which is well understood.

Shakura and Sunyaev first introduced the parameter α to characterise the efficiency of the angular momentum transfer mechanism, whatever its nature.

$$\alpha = \frac{v_t}{v_s} + \frac{H^2}{4\pi\rho v_s^2}$$

where v_t is the turbulent speed, v_s the speed of sound, H the magnetic induction and ρ the density of the disk. α may vary over the disk, but it is very likely that $\alpha \leq 1$ in all cases, and may be only a fraction of that value (eg. Cox and Everson [1982], Pringle [1981]). Its significance is that disks with $\alpha << 1$ are "quiet" thermal disks, whereas $\alpha \sim 1$ gives significant non-thermal disk radiation.

The Shakura-Sunyaev model predicts the physical properties of disks in some detail. In particular, a disk is concave, with thickness given approximately by $h \sim r^Y$

where $\gamma \sim 9/8$. This important property is the basis of CV models where radiation is reprocessed from the disk surface in order to explain the phase-behaviour of rapid oscillations. The disk is thin, even at the outer edge (Petterson [1983] finds $h_{max} \sim 10^{10}$ cm), being only a few percent of the radius. Its mass has been estimated as $M_D \leq 10^{-8} M_\odot$ (eg. Bath and Pringle [1981]), so self-gravity is negligible. Optically thick, the disk radiates approximately a blackbody spectrum from its outer parts, giving the well-observed $\nu^{1/3}$ frequency dependence over much of the visible spectrum.

Cordova and Mason [1982] show that the steady state disk model gives excellent agreement with outburst observations of SS Cyg, an apparently disk-dominated CV.

Warner [1976] points out that there is no physical restriction that forces a disk to be in the steady state. Mass may be lost from the system at the hot spot or disk edge, and the disk may change its size with variations in mass transfer rate from the secondary. Indeed, Smak [1979] and Robinson [1976a] list cataclysmic variables which exhibit apparent variations in disk size and light distribution. Most, though not all, such changes are related to outburst cycle, and more will be said of them in the next chapter. It is noteworthy that time-dependent disk models are most sensitive to the viscosity parameter α, while steady state disks are insensitive (Bath and Pringle [1981]).

iv) The primary/accretion disk boundary: The boundary region between the primary and the disk in CV's is the most likely source of high-energy radiation (X-rays), since the gravitational field of the white dwarf is strongest here.

The current model of X-ray emission from highly magnetic white dwarfs (in AM Her stars) will be discussed in Chapter 2. X-ray emission from non-magnetic, disk-dominated systems is more difficult to explain. Fabian et al [1976] invoked a standing shock, due to accretion, formed at a fixed height above the white dwarf. Gas reaching the shock would lose much of its kinetic energy in the form of bremsstrahlung before moving through the region below the shock, and coming to rest on the white dwarf surface. Pringle and Savonije [1979] predict that the X-ray spectrum should be sensitive to accretion rate, $\dot{M}$. For $\dot{M} \gtrsim 2\times10^{16}$ g s^{-1}, the electron density in the shock region becomes so large that Compton scattering degrades essentially all the hard X-rays to soft X-rays. Thus the brightest hard X-ray sources among CV's are probably not those with the highest mass transfer rates. Tylenda [1981b] finds similar results using a model of turbulent viscosity as an X-ray generator, instead of strong shocks. More recently, Patterson and Raymond [1985] have improved these models by allowing for variation of density with height in the optically thin boundary region. While agreement with observation is fairly good, the theory is still far from complete.

The boundary region is also highly significant as the probable source of rapid oscillations in CV's. Of this, more will be said in Chapter 3.

v) The atmosphere of the accretion disk: The emission lines observed in CV's (HI, HeI, HeII, CaII, etc) must have their source in an ionised, optically thin region of the disk. Liang and Price [1977] and Schwarzenberg-Czerny [1981] suggest that such conditions arise in the disk "chromosphere". This is a region surrounding the disk which is ionised as a result of high-energy radiation from the central parts, near the white dwarf. Other authors (eg. Williams [1980], Tylenda [1981a] show that the emission lines (except HeI and HeII) may arise from the outer parts of the disk, which are optically thin for low mass transfer rates ($M \leq 10^{-8}\ M_{\odot}\ yr^{-1}$).

vi) The mass transfer stream and hot spot: Gas particles within a disk have sufficiently short mean free paths that the disk behaves as a fluid, and hydrodynamical models are appropriate. By contrast, the path of gas streaming from the inner Lagrangian point to the disk may be determined to a high degree of accuracy (~ 0.1% uncertainty) by using single-particle trajectories (eg. Kruszewski [1964], Smak [1971]). Lubow and Shu [1975] point out that this is possible only in regions where the particle trajectories do not tend to cross one another, so that these models cannot be used to predict the width of the gas stream nor to describe its interaction with the disk.

In the simplest case, the gas stream is pictured as acquiring supersonic speed relative to gas in the disk. At the point of collision incoming gas particles lose much of their kinetic energy, and a region of shock-heating (the "hot spot") is formed. Various authors (eg. Bath et al [1983b]) have noted that "hot spot" is something of a misnomer, since the inner regions of the disk are significantly hotter than this region, and "bright spot" would be a better term. The continuum radiation from the spot may be comparable with that from the entire disk, and U Gem is an example of a CV whose optical light curve is dominated by "spot light". Smak [1971] made use of this fact to determine the mean geometrical parameters of the hot spot in U Gem.

More recently, Cook and Warner [1984] have revealed the variability of the hot spot in Z Cha. This system exhibits eclipses of two types, depending on the shape and duration of egress. Cook and Warner interpret these as eclipses of a hot spot whose extent, shape and position may vary on a timescale of days or even hours. They find its position relatively stable at a distance of one-third the orbital separation from the white dwarf, while its position angle, α, varies from 22° to 31° (see Fig 1.1) and its angular extent, $\Delta\alpha$, from 14° to 40°. It may even extend into the inner parts of the disk, suggesting that at times the gas stream producing it may be very broad indeed.

It is worth noting at this point that, since most of the disk is optically thick, the observed brightness of the spot should depend on orbital phase. Indeed this is so, as is evidenced by the presence of "orbital humps" in the light curves of many CV's.

The gas stream is very important to the structure and evolution of a cataclysmic variable. Warner [1976] regards the mass transfer rate as probably the most critical single factor governing the properties of CV's. It affects photometric properties such as the luminosity of the hot spot and the frequency of outbursts. Savonije [1983] shows that it gives rise to a changing orbital separation, the sign of which depends on the relative masses of the primary and secondary. In most CV's the primary appears to be the more massive component, in which case mass transfer tends to increase the orbital separation (Webbink [1982]). Such an increase in orbital separation would soon halt mass transfer, and various mechanisms have been invoked to counteract this effect by releasing angular momentum from the system. The first was put forward by Paczynski [1967]. He showed that gravitational radiation from a CV could decrease its angular momentum at a rate depending only on the orbital period, and predicted a corresponding rate of mass transfer. More recent calculations (eg. by Savonije [1983]) show that this mechanism yields mass transfer rates of 10^{-11} to 10^{-10} $M_{\odot}$ yr^{-1}, as long as the secondary is a main sequence dwarf. This range agrees well with the

transfer rates determined by Patterson [1985] for CV's with orbital period $P \lesssim 3$ hours. However, CV's with $P \gtrsim 3$ hours have transfer rates significantly higher than the upper limit of 10^{-10} $M_\odot$ yr^{-1}, so it is clear that a more efficient process must be responsible for angular momentum loss in these stars. The most likely mechanism is that of magnetic braking, originally suggested by Eggleton [1976]. In this model, angular momentum is lost via stellar wind from the secondary, the material being forced to follow the magnetic field lines of the secondary corona, and hence to corotate with it out to great distances. Recent authors (eg. Vilhu [1984]) conclude that this mechanism may well yield sufficiently high rates of mass transfer to agree with observation, especially since the "observed" rates may be inaccurate by a factor of 5 (Verbunt and Wade [1984]).

1.4 DETERMINATIONS OF PHYSICAL PROPERTIES

Determining the physical properties of CV's (the masses of the individual stars, their luminosities, radii, separation and so forth) is a most challenging task, principally because of the difficulties in separating light from the various parts of a single system. It is thus worthwhile to mention some of the techniques used (and their results) in grappling with this daunting detective puzzle.

i) Masses: For unambiguous mass determinations, a CV must be both a double-lined spectroscopic binary and an eclipsing binary. The former property allows for

determination of the mass ratio ($q \equiv M_1/M_2$), while the latter implies the system is seen "edge-on", giving an inclination angle of $i \gtrsim 67^\circ$. Then, since the orbital period is known, simple geometrical and physical arguments lead to solution for M_1 and M_2. This method was used by Robinson [1974] to give $M_1 = 0.70 \pm 0.18\ M_\odot$ and $M_2 = 0.90 \pm 0.17\ M_\odot$ for EM Cyg. Unfortunately, EM Cyg and U Gem are the only CV's which are both double-lined spectroscopic binaries and eclipsing binaries, so the technique is not generally applicable. It can be used in one other system, Z Cam, since the inclination angle of this system is known to within about 5° despite the fact that eclipses are not observed. For this system, Robinson calculates $M_1 \simeq 1.20\ M_\odot$ and $M_2 \simeq 0.85\ M_\odot$.

A less direct method of somewhat greater generality was proposed by Robinson [1976b]. It can be applied to any CV with orbital period $\lesssim$ 10 hours, providing one knows either the mass ratio (q) or the mass function and orbital inclination ($M_2 \sin^3 i / (1+q)^2$ and i). This includes all double-lined spectroscopic binaries and single-lined spectroscopic binaries of known inclination: six systems in all. Robinson derives two independent equations relating M_2 and q. These are:

$$M_2{}^2 = 0.996 \times 10^{-8} \frac{P^2 (1+q) (0.38-0.2 \log q)^3}{q\zeta^3} \qquad \ldots (2)$$

and

$$\frac{M_2 \sin^3 i}{(1+q)^2} = \frac{P K_1{}^3}{2\pi G}$$

where P is orbital period, K_1 the amplitude of radial velocity variations of the primary, and G the universal gravitational constant. Solar units have been used for mass and radius. ζ is the constant of proportionality in the dependence of radius on mass obeyed by lower main sequence stars ($R/R_\odot = \zeta\ M/M_\odot$), and may be empirically determined to have the value $\zeta \simeq 0.96$ (equation (1)). The appearance of this constant in equation (2) arises from the assumption that the secondary of the CV is a main sequence star, as justified earlier (section 1.3). If q is known, equation (2) is immediately soluble to give M_2 and hence M_1. Alternatively, if i and K_1 are known, the two equations may be solved simultaneously to give M_2 and q. Robinson's technique yields white dwarf masses ranging from 0.73 to 1.26 $M_\odot$ in the six systems analysed, and his values for EM Cyg and Z Cam agree well with direct determinations.

Warner [1973] proposed a method which, if not as accurate as Robinson's, is more generally applicable. It makes the same basic assumption, viz. that the secondary is

a lower main sequence star almost exactly filling its Roche lobe. He derives

$$\frac{K_1}{v \sin i} = \frac{f^2(q)q^3}{q(1+q)^2} \qquad \ldots (3)$$

where v sin i is the projected rotational velocity of the disk and f is a tabulated, empirical function of q. The left-hand side of equation (3) is an observable quantity for all single-lined binaries; thus q can be determined. M_2 is then independently determined by solving two simultaneous equations in M_2 and R_2. One is the empirical mass - radius relationship for lower main sequence stars, while the other uses the theoretical Roche lobe calculations by Plavec [1968]. Warner's method, which can be applied to any spectroscopic binary showing disk emission, suffers primarily from the observational ambiguity of measurements of v sin i, as Warner himself points out. Particular ambiguity arises in the CV's with ultra-short periods ($\lesssim$ 2 hours), which have small radial velocity amplitudes that may easily be confused with S-wave emission from the hot spot (Warner [1979]). Recently some headway has been made by Shafter [1983], who suggests that reliable values of v sin i may be obtained by measuring the width of the Hα emission line at a particular height above the continuum. This height is chosen so that a fixed fraction (ξ) of the total line flux lies below it. Shafter's preliminary

results indicate that $\xi \approx 0.65$ may be a useful value of this parameter for all cataclysmic variables.

All the above techniques agree on one point: the masses of the white dwarfs in cataclysmic variables are higher than those of lone white dwarfs, which are generally less than 0.65 $M_\odot$ (Warner [1972]). Livio and Soker [1984] examine possible selection effects in some detail, and conclude that the mass difference is significant. They offer a tentative explanation based on their examination of the current model of CV formation, in which the secondary spirals in towards the core of a giant or supergiant inside a common convective envelope. They argue that a CV is more likely to evolve from a supergiant than a giant, and that the core (which is destined to become the white dwarf primary) is correspondingly more massive in the supergiant case.

ii) Mass transfer rates: Early attempts to determine the rate of mass transfer in CV's were based on the assumption that neither mass nor angular momentum was lost from these stars. In this case, mass transferred from the secondary to the primary would increase the orbital period. Determination of $\dot{M}$ based on measurements of $\dot{P}$ (eg. by Warner and Nather [1971]) were later refuted by Pringle [1975] and Patterson [1984] who argued that such measurements, even if significant, were highly ambiguous.

Patterson calculates values of $\dot{M}$ for 28 CV's. For those with low mass transfer rates ($\dot{M} \lesssim 2\times10^{-10}$ $M_\odot$ yr^{-1}) he uses the disk model of Tylenda [1981a], in which the outer

parts of the disk are optically thin. Patterson first determines M_v, and then uses Tylenda's relationship between continuum spectrum and $\dot{M}$. The method requires knowledge of the distance to a given CV, or its deduction from an empirical equivalent width - M_v relationship. Its main disadvantage is that it is very sensitive to spectral contamination from elements other than the disk.

Horne [1985] has devised a method of "eclipse mapping" to obtain images of CV accretion disks from the shapes of their primary eclipses. A fortunate consequence of this technique is that it yields the temperature profile of a disk, from which the mass transfer rate may be determined to within a factor of 2. Of course, this technique is only applicable to CV's of high inclination which undergo disk-eclipse by the secondary.

iii) Luminosities and Temperatures: Luminosities and effective temperatures can be calculated for CV's, but these have limited meaning if they represent integrations over dissimilar parts of a complex system.

Some estimates of M_v for entire CV systems are quoted by Warner [1976]: $3 \leq M_v$ (mean) ≤ 4.7 for nova remnants, $7.2 \leq M_v$ (mean) ≤ 7.5 for dwarf novae, M_v (mean) $\simeq 4.5$ for nova-like variables. Estimates of effective temperatures for these classes show corresponding variation, and range from 12 000 to 35 000 K. Clearly there are intrinsic differences between the classes; for instance, Warner shows

that nova remnants are probably ten or more times as luminous as dwarf novae.

Oke and Wade [1982] have obtained spectrophotometry for 31 CV's in the range 0.32-1.1 μm, where light from the secondary is dominant. Wide wavelength coverage of this kind makes it possible to identify and subtract the contribution from the secondary.

Horne and Cook [1985] have used Horne's eclipse mapping technique to reconstruct the surface brightness distribution across the disk of Z Cha in outburst. They use a method of maximum entropy, constrained by an assumption of maximum axial symmetry, and obtain excellent (though non-unique) agreement between the model light curves and observed eclipse shapes. Using their disk reconstruction, they find the surface temperature varies from ~ 8 000 K at the outer disk to ~ 40 000 K near the centre, in good agreement with the $T_{eff} \propto R^{-3/4}$ law predicted for a disk in the steady state. They calculate the effective temperature of the white dwarf to be ~ 10^4 K, which is lower than expected for the implied mass transfer rate.

As noted before, Horne's technique can only be applied to those CV's which undergo primary eclipse. For the remaining systems the problem of de-convolution remains, and it is unsurprising that a reliable, repeatable technique for determining the physical properties of these objects has not appeared. Robinson [1976a,1983] bemoans the dearth of reliable information on fundamental CV properties, and

comments that the only one known accurately for many variables is the orbital period.

CHAPTER 2

CLASSIFICATION OF CATACLYSMIC VARIABLES

2.1 CRITERIA

The traditional classification of cataclysmic variables into four main classes is based primarily on their outburst properties. Thus novae are variables that erupt only once, with a spectacular increase in brightness (9-14 magnitudes or more); recurrent novae erupt every 10-100 years with a change 4-9 magnitudes; dwarf novae undergo relatively small brightness changes (2-6 magnitudes) and erupt on timescales of weeks; and nova-like variables are not known to erupt at all. These classes may be further subdivided into subclasses whose membership requirements are again observational: the duration of decline from maximum light, the presence or absence of rapid coherent oscillations, the degree of optical polarization and so on.

More recently, attempts have been made to provide a physical rather than observational means of classification, thereby grouping according to cause and not symptom. Naturally this has proved difficult, but two physical properties have emerged as decisive: mass transfer rate ($\dot{M}$) and primary magnetic field strength. To a lesser extent, orbital period may be a classification tool. I shall discuss all these as they arise in a summary of the features of the various classes and subclasses.

2.2 NOVAE

In their extensive review, Gallagher and Starrfield [1978] define a classical nova as a variable having specific properties. These are:

1) a single increase in brightness of 9 magnitudes or more within a few days (the eruption),
2) changes in brightness on a timescale of 1000 days or less,
3) spectra that imply ejection of material at velocities between 100 and 5000 km s^{-1}, and
4) characteristic spectral changes during eruption.

Characteristic number 1) is the most intruiging; such a spectacular eruption implies a peak luminosity of 10^5 $L_\odot$ or more, and an energy release of ~ 10^{45} ergs in 100 days or less. Only two known processes can yield such energy on so short a timescale: thermonuclear runaway and runaway mass accretion. Most authors (eg. Gallagher and Starrfield [1978], Kenyon and Truran [1983]) favour the former, since it accounts more naturally for the massive energy release from novae, as well as the ejection of mass at high speeds. According to this model, accretion onto the primary builds up an envelope of hydrogen-rich material around the surface of the white dwarf. When this material reaches a critical pressure, thermonuclear burning begins near the degenerate core, and rapidly leads to runaway. The nova's luminosity increases to a maximum, and the liberated energy is

sufficient to eject part or all of the envelope to form an expanding shell.

Starrfield et al [1972] were first to propose the well-known "CNO" cycle of nuclear reactions as the cause of mass ejection. This cycle is summarised in Figure 2.1. Models by Starrfield, Sparks and Truran [1974] using carbon-oxygen white dwarfs show that, at the peak of the outburst, the most abundant of the CNO nuclei are ^{13}N, ^{14}O, ^{15}O and ^{17}F. As can be seen from Figure 2.1, these are all susceptible to β^+-decay, with half-lives between 60 and 600 seconds. Their decays thus release significant energy into the envelope some time after the peak temperature is reached. It is this energy, rather than that released in the initial runaway, that causes mass ejection, which is thus a relatively gentle event. Starrfield et al [1972] predict enough convection within the envelope to transport CNO nuclei to the outer layers where proton capture no longer occurs; when these layers are expelled, they contain enhanced abundances of C, N and O nuclei. These enhanced abundances are well observed (eg. Pottasch [1959], Mustel [1974], Stickland et el [1981]).

Novae can be subdivided into a range from fast to slow novae, depending on the observed rate of decline after eruption. For example, fast nova V603 Aql (outburst in 1918) declined to minimum light within a few weeks, while slow nova HR Del (1967) took more than a year (Gallagher and Starrfield [1978]).

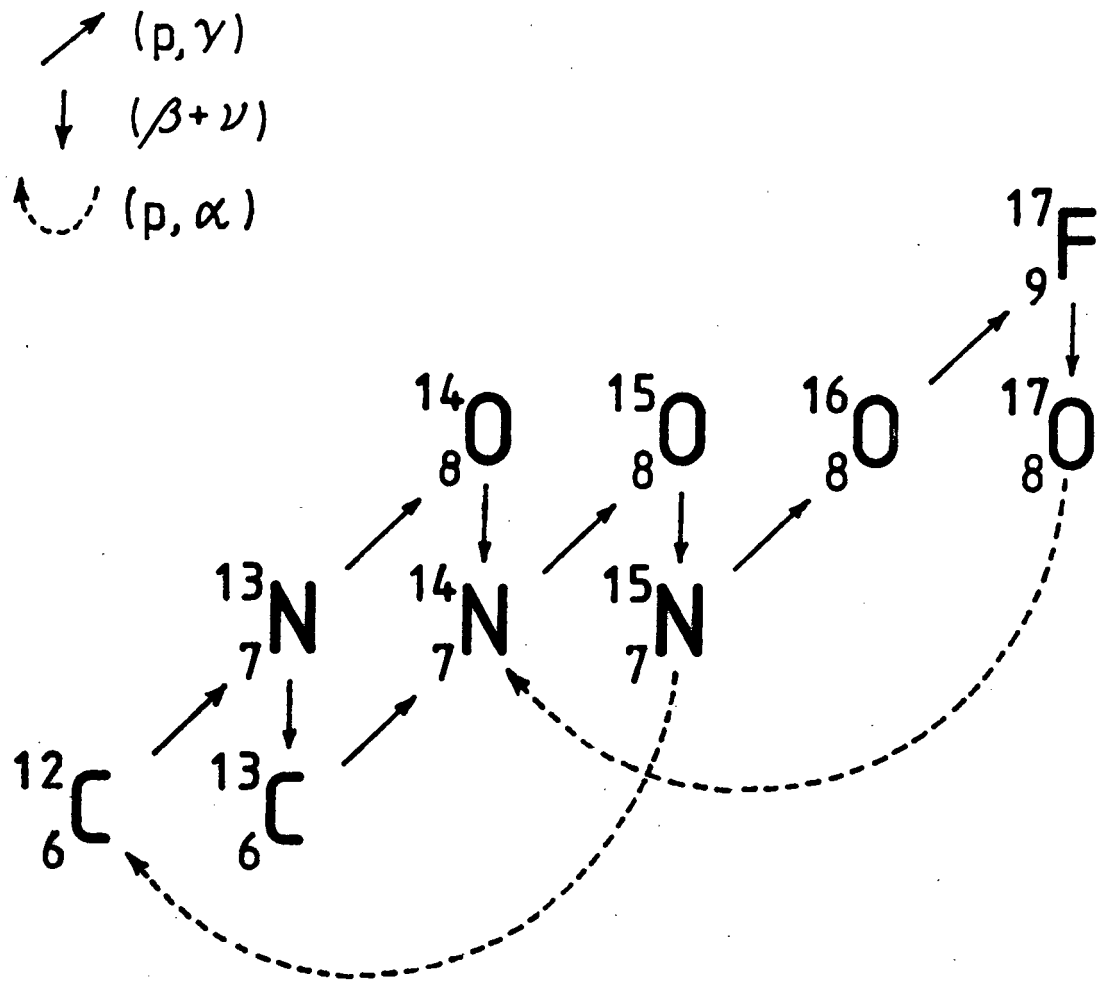

Figure 2.1 The CNO cycle, which is responsible for mass ejection in a nova. The half-lives of the four β-decay nuclei are ^{13}N: 598 s, ^{14}O: 71 s, ^{15}O: 122 s and ^{17}F: 66 s (after Starrfield et al [1972]).

Starrfield, Truran and Sparks [1978] amend their original model to include lower-mass nuclear reactions and an improved treatment of convection. They find that thermonuclear runaway should occur in systems with $\dot{M}$ anywhere from 10^{-5} to 10^{-13} $M_\odot$ yr^{-1}, providing the original hydrogen-rich envelope has enhanced CNO abundances. Their theoretical light curves match those of fast novae quite well. At the same time, Sparks, Starrfield and Truran [1978] successfully model the outburst properties of slow novae by assuming normal solar abundances of CNO in the envelope, and propose radiation pressure as the principal ejection mechanism in this case. Although observations do not consistently support a correlation between nova speed-class and CNO abundances (slow nova DQ Her being a notable counter-example), Truran [1982] indicates that this may be resolved if the strong dependence on white dwarf mass is taken into account.

In terms of the current model, then, a cataclysmic variable will become a nova if its white dwarf accumulates an envelope of critical mass (for a white dwarf of 1 $M_\odot$ and 10^{-2} $L_\odot$ Truran [1982] gives a critical mass of 10^{-4} $M_\odot$). MacDonald [1983] formulates this criterion in terms of upper limits on accretion rate and white dwarf luminosity, themselves functions of white dwarf mass and envelope composition. Once the critical mass is accumulated, temperatures at the base of the envelope rise to $\sim 10^8$ K, and the CNO nuclear cycle begins. The mechanism of CNO

enhancement in the envelope is still highly controversial. Truran [1982] proposes strong convection on a timescale too short for envelope expansion to occur; Kippenhahn and Thomas [1978] suggest chemical mixing due to shear instabilities; Prialnik and Kovetz [1984] favour diffusion. All these models presuppose a carbon-oxygen white dwarf as the source of C and O, which is not entirely supported by evolutionary theories. Only Nariai et al [1980] model a nova explosion on a helium dwarf, and its required mass (0.4 $M_{\odot}$) is unrealistically low for novae. MacDonald [1983] tentatively suggests a helium flash under rather special conditions. Whatever the mechanism, it is extremely efficient, and the nova reaches bolometric maximum within a day, irrespective of speed class.

After bolometric maximum, the nova takes several days to several months to reach visual maximum, depending on the violence of the nuclear runaway. Truran suggests this is a function only of the CNO composition of the envelope, and points to a loose correlation between speed class and rise time. During this time the envelope expands greatly and the outermost parts exceed the escape velocity of the white dwarf, so that the nova at visual maximum has an effective temperature of only ~ 10^4 K and a much enlarged photospheric radius.

Although runaway has ceased, hydrogen burning continues in those parts of the envelope that remain after shell ejection, causing a long phase of constant bolometric

luminosity (again irrespective of speed class). Since this luminosity is of the order of the critical Eddington value, radiation pressure is probably driving a steady rate of mass loss from the envelope (the "optically thick wind"), as modelled by Bath and Shaviv [1976], Ruggles and Bath [1978] and Kato [1983]. Improved models allow the mass loss rate to decrease with time over this phase, in good agreement with optical and radio light curves (Hartwick and Hutchings [1978], Kwok [1983]). As the ejected material thins out, the photospheric radius decreases again and the effective temperature rises. This shifts the continuum radiation towards the ultraviolet, giving rise to a steady decline at optical wavelengths while the bolometric luminosity stays essentially constant (Hartwick and Hutchings [1978], Gallagher and Starrfield [1978]). This phase continues for weeks (fast novae) or months (slow novae) before nuclear burning finally ceases in the envelope remnant. Truran [1982] points out that this timescale is much shorter than that for pure nuclear evolution, which implies (Prialnik, Shara and Shaviv [1978]) that up to 95% of the envelope has been lost.

Towards the end of the phase of constant bolometric luminosity, a nova will sometimes show a sudden drop in the optical light curve, and a corresponding rise in infrared flux (eg. DQ Her, FH Ser). This is generally attributed to blackbody radiation from large ($\geq$ 1 μm) dust grains that form rapidly in the nova shell (Clayton and Wickramasinghe

[1976]). The grains are probably carbon, condensed from the ejected material when the temperature falls below ~ 2000 K, although variations in condensation temperature (and therefore composition) are possible (Bode and Evans [1983a]). Three medium-speed novae have exhibited an unexpected rise in effective dust temperature after infrared maximum, which prompted Gehrz et al [1980] to propose this as a period of grain destruction of duration ~ 100 days. Mitchell and Evans [1984] have suggested electrical charging of grains by ionisation as a controlling mechanism for grain size. This may also explain the observed correlation between speed class and infrared luminosity: fast novae have high bolometric luminosities, extensive ionised shells and thus inhibited grain formation and low infrared excesses (Bode and Evans [1983b]). An alternative model, by Bode and Evans [1980] is that the grains are small (~ 0.01 μm) and already exist prior to outburst. Observations of Nova Aquilae (1982) by Williams and Longmore [1984] and Bode et al [1984] support this view, since early dust emission appeared from regions not yet reached by the nova ejecta. However, this nova may have been atypical of the class, and grain formation is still a controversial issue (Bode and Evans [1981], [1983a], [1983b]).

The final phase of outburst is the return to minimum, at which stage the photometric and spectroscopic properties of the nova become essentially what they were before the eruption (Gallagher and Starrfield [1978]).

2.3 RECURRENT NOVAE

Prialnik et al [1978] comment that all novae may well recur, with outburst interval related to outburst amplitude. An empirical relationship by Kukarkin and Parenago [1934]:

$$A = 0.80 + 1.667 \log P$$

where A is outburst amplitude in magnitudes and P is outburst interval in days, predicts an outburst interval of $P \sim 10^4$ years for a typical 12-magnitude nova. While this represents a gross extrapolation of the observations, the current nova model predicts a similar time interval for buildup of a critical envelope ($\sim 10^{-4}$ $M_\odot$) with a typical accretion rate of 10^{-9} to 10^{-8} $M_\odot$ yr^{-1}. Certainly the model allows for many accretion cycles before significant evolutionary change takes place.

However, recurrent novae are defined as CV's which outburst every 10-100 years, and it is the brevity of this outburst interval which is so difficult to explain. MacDonald [1983] calculates 400 years as the shortest possible accretion time that leads to mass ejection, and concludes that recurrent novae cannot be thermonuclear runaways on accreting white dwarfs. Prialnik et al [1978] are more optimistic, arguing that frequent outbursts may be possible if very little of the heated envelope is ejected with each eruption.

It is possible that the recurrent novae class of variables is a group of physically disparate objects. To date, only five are known: T CrB, RS Oph, T Pyx, V1017 Sgr and U Sco. They range in outburst amplitude from 6 to 10 magnitudes. T CrB and RS Oph contain giant secondaries, while U Sco apparently contains a late-type dwarf (Williams et al [1981], Barlow et al [1981]).

For those recurrent novae containing giants, Shara [1980] proposes that accreted material is rich in ^{3}He, which could heat a degenerate envelope sufficiently to give an outburst every ~ 26 years. However, MacDonald [1983] argues that Shara's model is not energetic enough to give mass ejection. Webbink [1976] regards the outbursts of T CrB as results of episodic accretion from the unstable giant. According to his model, transferred material forms an eccentric ring around the primary. As the ring broadens into a viscous disk, radiation is emitted, and maximum luminosity is reached as the inner parts of the disk meet the outer surface of the white dwarf.

For U Sco, Williams et al [1981] find attributes of a nuclear-powered outburst, namely a fast rise to visual maximum and the presence of high-speed ejecta with CNO enrichment. But they note that these attributes do not exclude an accretion mechanism, and that further observations (preferably distance determinations) are necessary to bring one or other model to the fore.

2.4 DWARF NOVAE

Dwarf novae are those cataclysmic variables whose outbursts are even less spectacular (2-6 magnitudes) and even more frequent (every few weeks or months) than those of recurrent novae. About 300 such systems are currently known. Principally because of their eruption frequency, these stars have contributed more information toward the development of a CV model than those of any other class.

Smak [1984a] summarises the other observational properties that characterise dwarf novae:

1) The emission lines are usually strong, but of low energy (eg. the HeII lines are often missing).
2) Dwarf novae are intrinsically faint, having $M_v \sim 7.5$ (cf. novae with $M_v \sim 4$).
3) The hot spots are relatively bright, often rivalling the luminosity of the whole disk.
4) The orbital periods lie within a well-defined range. More will be said of this characeristic in the next chapter.
5) During outburst, the extra light radiated from the system comes primarily from the disk.

Before reviewing the detailed model(s) of dwarf novae, it is useful to classify them into three distinct subclasses, again according to outburst properties:

a) U Geminorum subclass: These "classical" dwarf novae undergo outbursts of 2-6 magnitudes and 5-20 days duration,

with outburst intervals of 30-300 days (Webbink [1982]). While individual systems often show great variation in these properties (particularly outburst interval), Bailey [1975] finds that the timescale for decay from maximum is roughly constant for a given system, and that it is directly proportional to the system's orbital period.

b) Z Camelopardalis subclass: These stars are similar in their outburst behaviour to the U Gem subclass, but occasionally show an additional feature: long "standstills" of constant brightness roughly one magnitude below maximum light. In Z Cam itself, these standstills occur sporadically and may last for as little as a month, or as much as two years (Mayall [1965]).

c) SU Ursae Majoris subclass: These stars undergo two distinct types of outburst. Their normal outbursts are like those of the U Gem stars, but typically of shorter duration (2-3 days) and much shorter outburst interval (10-30 days) (Webbink [1982]). In addition, they show "superoutbursts" which are about one magnitude brighter than the normal outbursts and at least five times their duration, but occur three times less often (Vogt [1980]). Their most remarkable feature was discovered independently by Vogt [1974] and Warner [1975]. This is the appearance, near supermaximum, of low-amplitude light variations called "superhumps" with perplexing periods typically a few percent longer than the orbital period of the binary star.

Much has been written about the outburst mechanisms of these subclasses, and of dwarf novae as a whole. At the present time, only two viable theories remain.

The first is the so-called "mass transfer burst" (MTB) theory, originally proposed by Bath [1973]. This theory proposes time variation of the mass transfer rate as the cause of outburst. According to Bath [1975], a cool (G,K or M) secondary may become unstable due to the release of recombination energy in the ionisation zones of its envelope, some distance below the surface. This energy makes the outer layers convective, and material from below the ionisation zone is brought up to the Roche lobe where it escapes via the inner Lagrangian point. Thus we have a sudden burst of mass transfer, and a flood of material impacting onto the hot spot of the disk. Bath and Pringle [1985] find that a reasonable outburst will occur only if the mass of this material is at least comparable with that of the whole disk. Assuming this is the case, the material soon forms a nearly circular ring around the white dwarf, roughly at the radius of the hot spot. Thereafter, the ring diffuses on a slower, viscous timescale, causing a sharp rise and then a gradual tailing off in the disk luminosity. Bath and Pringle [1981] show that if the rise time is to be as short as is observed in dwarf novae (~ one day) the disk must be very viscous ($\alpha \sim 1$). The outburst maximum thus corresponds to a "steady state" disk with higher than normal surface density throughout. Thereafter, mass transfer

returns to its quiescent rate and the disk relaxes to its quiescent structure.

At the same time, the secondary undergoes physical changes as described by Bath [1975]. Steady mass transfer at peak rate continues for some time ($\sim 10^3$ s) before the outer, loosely bound envelope is lost and the star relaxes away from its Roche lobe. It then re-expands on a timescale of weeks, the envelope reaching thermal equilibrium as the star again fills its Roche lobe. Associated with these phases are luminosity changes, but these are $\sim 10^4$ times smaller than the changes in the disk, and may be neglected. The significance of the recovery of the secondary is that its duration is proportional to the amount of matter lost, so that this MTB model predicts a correlation between the energy of an outburst and the length of the following quiescent period. Such a correlation is significant in SS Cygni, for which over 600 outbursts have been observed (Bath and van Paradijs [1983]).

The second model of dwarf nova outbursts is the "disk instability" (DI) theory, originally proposed by Osaki [1974] and strongly supported by Smak [1984a]. According to this model, matter is transferred at a constant rate from the secondary, which takes no part in the eruption. Instead, the transferred matter reaches the outer parts of the disk via the hot spot, and accumulates there until an instability in the disk causes it to accrete suddenly onto the white dwarf, producing an outburst. The DI model

accounts easily for the enhanced brightness of the spot relative to the disk in dwarf novae, as well as the observation that the spot does not brighten significantly during outburst (Warner and Nather [1971], Warner [1975]).

A mechanism of disk instability has only fairly recently been found. Bath and Pringle [1982] showed that a disk fed by a constant mass transfer stream can only exhibit outburst behaviour if the z-integrated viscosity, μ, is a double-valued function of surface density, Σ. Such relationships were shown to be feasible in disks by Meyer and Meyer-Hofmeister [1981], who suggested that the double-valuedness is due to opacity changes in regions of the disk where ionisation of hydrogen occurs (at $T \sim 10^4$ K). At such temperatures, there are two possible local disk states: a hot, fully-ionised, high-viscosity state and a cool, mainly neutral, low-viscosity state.

An example of the corresponding μ - Σ relationship (at fixed radius) is shown in Figure 2.2. The convective states up to B and the radiative states up from C are stable; the transition states between B and C are unstable. We assume mass is transferred from the secondary at a steady rate. The disk will evolve on a viscous timescale until it reaches the corresponding steady state configuration, with all parts of the disk having the same local mass transfer rate and corresponding local viscosity μ (a function of R). Suppose this transfer rate is such that the steady state viscosity lies in the unstable region at a certain radius (eg. μ_{ss} in

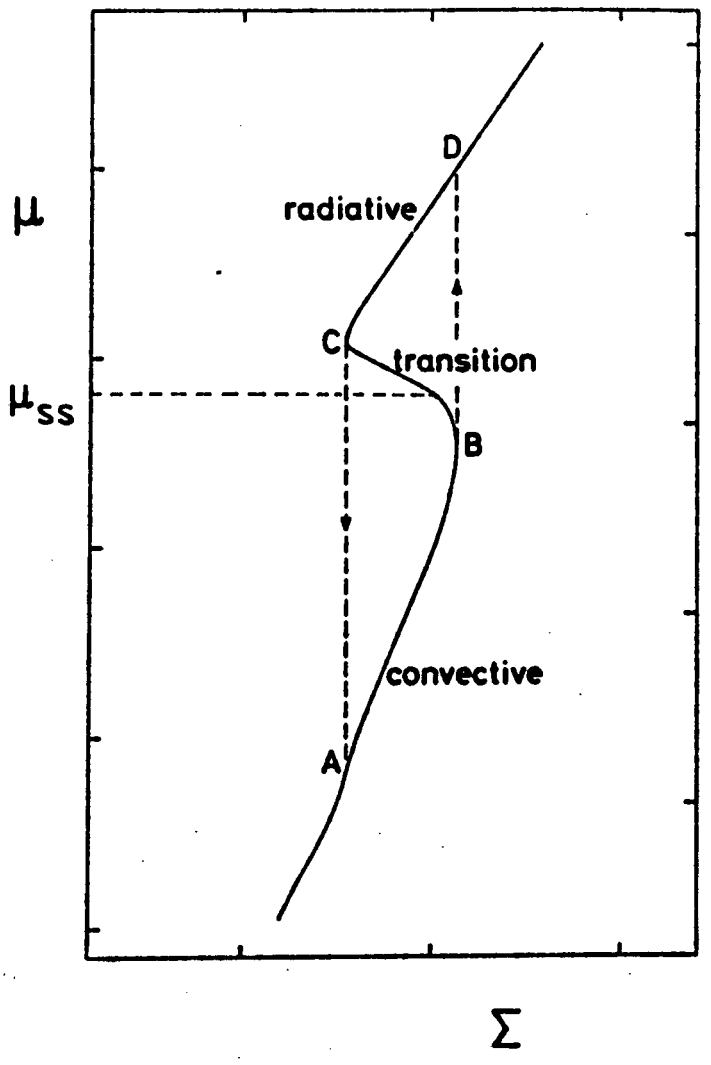

Figure 2.2 Proposed relationship between μ (viscosity) and Σ (surface density) (from Meyer and Meyer-Hofmeister [1981]). μ is also equivalent to local mass transfer rate since viscosity is responsible for inward movement of material.

Figure 2.2). The disk will evolve towards this point, starting, say, on the curve below A. Since the viscosity is less than the steady state value, material accumulates at this radius, increasing the surface density, Σ. The disk evolves upward along the curve A→B. At point B, any further increase in surface density requires a transition (on a thermal timescale) to the radiative state at D. Here the viscosity is so high that material can diffuse inwards rapidly, thereby reducing the local surface density. The disk element slides down the curve from D to C, towards the steady state. At C a transition occurs back to the convective state A, where material begins accumulating again.

On a global scale, instabilities of this type trigger thermal instabilities in neighbouring regions, and an "avalanche" transitional wave of high/low viscosity may move through the disk on a short (thermal) timescale (Papaloizou et al [1983], Bath and Pringle [1985]). Thus the disk as a whole exhibits two types of behaviour: slow accumulation of material (quiescence) and rapid accretion (outburst). For the disk to spend most of the time in the quiescent phase, the mass transfer rate must be just above the maximum for a low-viscosity state (Papaloizou et al [1983]). The details of this behaviour, such as how much of the disk is involved, the extent to which the "wave" will move outward as well as inward, and the resulting time variations of surface density and luminosity, depend sensitively on the precise

formulation of the viscosity, and to a lesser extent on the mass transfer rate. The current hope is thus that successful modelling of light curves will provide insight into the nature and origin of the viscosity. Smak [1984a] summarises the results of full time-dependent calculations, and notes that these models predict two distinct types of outburst. "Type A" outbursts are brought about by higher mass transfer rates. They begin with a toroidal accumulation of material in the outer disk, and an inward-spreading instability. They recur periodically, mimicking the behaviour of U Gem dwarf novae. Since the instability starts from the outer (cooler) parts of the disk and moves inward, Type A outbursts produce a light curve that rises earlier at longer wavelengths. At lower mass transfer rates "Type B" outbursts occur. These begin with a redistribution of surface density in the inner parts of the disk, and an instability which spreads both inwards and outwards. Since the inner disk becomes very hot before brightening, the corresponding light curves rise almost simultaneously at all wavelengths. Depending on how much of the disk becomes involved, the outburst may be of low amplitude and short duration or high amplitude and long duration, rather like those of SU UMa dwarf novae. These repeat in a semi-periodic or even irregular way.

Distinction between Type A and Type B outbursts should thus be possible if the early part of a dwarf nova outburst is monitored in different wavelength bands. The two types

also predict different changes in disk size. Observations of U Gem indicate that the disk expands by about 30% during outburst, and contracts exponentially during decline and quiescence, in good agreement with the Type A model (Smak [1984b]). The Type B outbursts are less easily matched with observed systems.

As a group, these DI models predict a correlation between outburst amplitude and orbital period, in reasonable agreement with observations (Smak [1984b]).

Other authors obtain variations on these model outbursts by taking α to be a function of radius or a function of local ionisation state. Meyer [1984] finds that the rapid rise and slow decay of dwarf nova outbursts can be modelled with transition waves of different speeds, and concludes that α must be a variable parameter. However, the validity of his calculations has been questioned by Papaloizou and Pringle [1985]. Lin et al [1985] show that constant-α models can successfully reproduce the gross features of dwarf nova outbursts, such as the changes in magnitude and the timescales between outbursts. They suggest that allowing α to depend on temperature could provide minor improvements to the generated light curves.

If partial ionisation at $\sim 10^4$ K is responsible for disk instabilities, then outburst behaviour should depend strongly on the effective temperatures of the outer parts of CV disks. Smak [1983] investigates this idea, and finds that T_{eff} depends most strongly on $\dot{M}$ and R_d (the disk

radius). These he estimates for 16 CV's, and plots the results on an $\dot{M}$ - R_d diagram, reproduced in Figure 2.3. The solid line represents the theoretical borderline for ionisation-induced instabilities. Systems lying below this line have parts of their disks at the critical temperature, $10^{3.8}$ K, while systems above it have hot enough disks to escape the instabilities and undergo steady accretion. Despite the large error boxes in the diagram, it is clear that most dwarf novae lie below the line and most novae and nova-like variables (steady accretion objects) lie above it. Exceptions are GK Per, a nova which does exhibit dwarf nova activity (Smak [1982b]), and three borderline cases: SS Cyg, EM Cyg and Z Cam. The latter two systems are Z Cam dwarf novae, and Smak interprets this subclass as genuinely on the stability borderline. Smak [1982b] also notes that, although both $\dot{M}$ and R_d are equally important in determining accretion behaviour, the sizes of CV disks are less disparate than their mass transfer rates so that the latter becomes the principal controlling feature. Smak [1984a] suggests that characteristics 1) and 2) of dwarf novae (see page 34) are both the result of their low mass transfer rates.

Faulkner el al [1983] reach the same general conclusion from theoretical considerations of disk instabilities: the CV subclass into which a given system falls depends primarily on the long-term mass transfer rate. If $\dot{M}$ is low, large parts of the disk will be unstable, and a "classical"

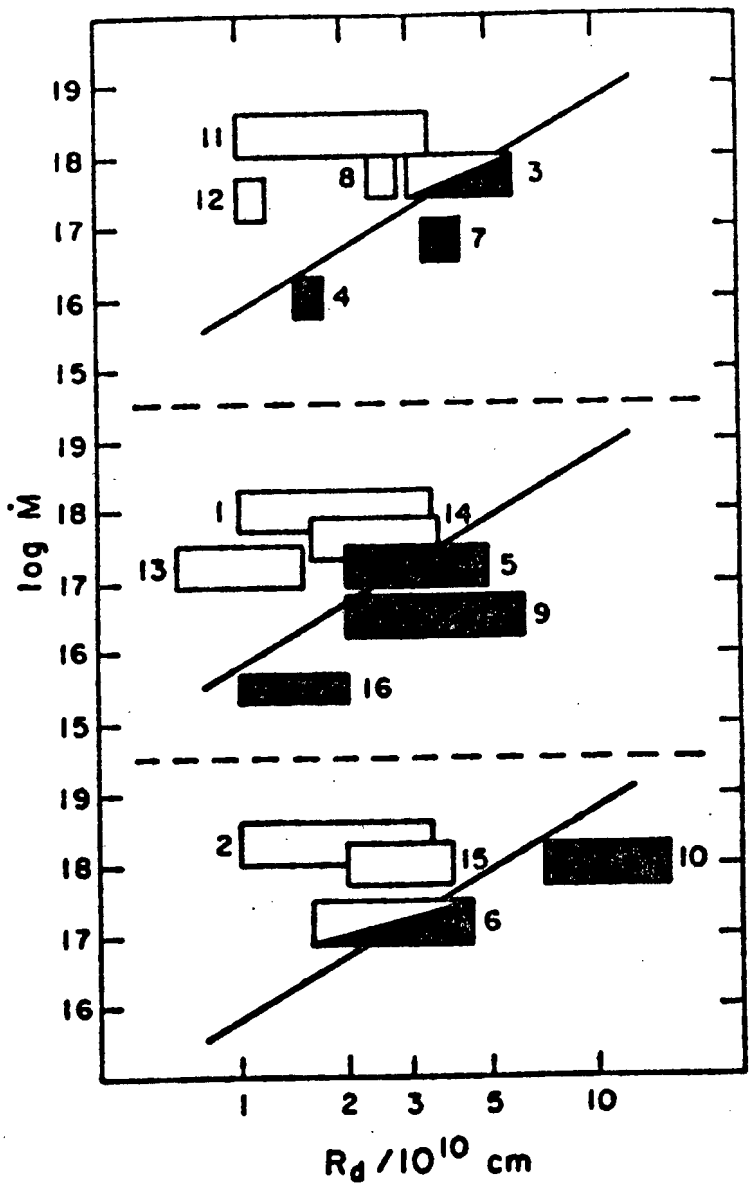

Figure 2.3 The $\dot{M}$ - R_d diagram (from Smak [1983]). Three panels are used to avoid crowding. Open rectangles are novae and nova-like variables; filled rectangles are dwarf novae and half-filled rectangles are Z Cam systems. 1 = V603 Aql, 2 = T Aur, 3 = Z Cam, 4 = Z Cha, 5 = SS Cyg, 6 = EM Cyg, 7 = U Gem, 8 = DQ Her, 9 = RU Peg, 10 = GK Per, 11 = RR Pic, 12 = LX Ser, 13 = RW Tri (faint), 14 = RW Tri (bright), 15 = UX UMa, 16 = ave. ultra-short period CV. The solid line represents the theoretical borderline for ionisation-induced instabilities.

dwarf nova will result. In its quiescent state, much of the disk will be optically thin, giving rise to an emission line spectrum. In outburst, the disk will become optically thick and give rise to an absorption spectrum. On the other hand, if $\dot{M}$ is high, the disk will be stable and optically thick, in a "permanent outburst" state. The system will be a nova or nova-like variable. If $\dot{M}$ is near the critical limit, the system will oscillate between these two behaviours, being sensitive to small $\dot{M}$ fluctuations. Such systems will be Z Cam dwarf novae.

Choosing between the MTB and DI outburst models is not an easy task. As Bath and Pringle [1985] point out, a disk with material accumulated in its outer parts that suddenly becomes very viscous, evolves in exactly the same way as a disk with constantly high viscosity onto which a large quantity of new material is dumped. Thus observations of dwarf novae well into outburst are unlikely to distinguish between the two cases. Both provide the same explanation for Bailey's relationship between decline rate and orbital period: a larger period implies a greater orbital separation, probably a larger disk and thus a slower return to quiescence as material has farther to diffuse.

One of the main difficulties with the MTB model is that the depth of the ionisation zones in the secondary is a function of its mass. The low-mass secondaries of short-period CV's should have such deep ionisation zones that large-scale convection of the outer layers is energetically

unfeasible (Bath and Pringle [1985]). In addition, the disk expansion observed in U Gem and Z Cha during outburst is difficult to explain with the MTB theory. MTB model disks usually contract, as the flood of incoming material has lower specific angular momentum than the outer parts of the disk. Perhaps most troublesome of all, hot spots have not been seen to vary significantly prior to outburst, despite the arrival of a flood of material over a short period of time. Faulkner [1976] is somewhat scathing in his criticism of the MTB theory on this score. Bath et al [1983b] attempt to explain the constant hot spot brightness by invoking deep penetration of the gas stream into the disk, but Smak [1984a] finds this argument less than convincing. Also, the MTB theory proposes steady state conditions at quiescence, but the spectra of dwarf novae in outburst bear a much closer resemblance to the steady state disks of novae at minimum than do spectra of quiescent dwarf novae (Cannizzo et al [1982]). Finally, the most realistic MTB simulations to date (Gilliland [1985]) indicate that mass transfer rates are probably stable on dwarf nova outburst timescales in all CV's with $M_2 \lesssim 1.0\ M_\odot$.

As for the DI model, Pringle and Verbunt [1984] point out that the rate of accretion onto the white dwarf in quiescent dwarf novae may well be too low to generate the observed ultraviolet fluxes. Smak [1984b] suggests a way round this by proposing heating of the white dwarf during outburst, and subsequent re-radiation. This would, however,

require the white dwarf to cool extremely slowly (10^6 - 10^7 s). A second problem is that outbursts of VW Hyi seem to begin in parts of the disk which are rather cool (T ~ 6000 K) to be unstable. Thirdly, the instabilities travel at speeds too high to account for the one-day delay between the optical and ultraviolet rises in dwarf nova VW Hyi. This delay is remarkable: in the optical, VW Hyi brightens by a factor of about ten before any change occurs in the UV (Schwarzenberg-Czerny et al [1985]), an effect too large to be explained by either the MTB or DI model.

Indeed, the two models are not mutually exclusive (Bath and Pringle [1985]). An instability in the disk may well lead to heating and subsequent expansion of the secondary, with a resultant burst of mass transfer. Osaki [1985] has examined this type of feedback instability in detail, and proposes a model for the most enigmatic subclass, the SU UMa dwarf novae. Osaki's model is an extension of one by Vogt [1982], which proposes an elliptical ring of material around the accretion disk as the source of superoutburst and superhumps. According to Vogt, a sudden burst of mass transfer (of duration $\lesssim 10^3$ s) could produce such a ring, and an associated "superspot" on its outer edge. If the orientation of the ring was fixed in space, the binary motion of the system would move the superspot right around the edge of the ring during each orbital period (see Figure 2.4). Clearly the brightness of the superspot would vary around the orbital cycle, reaching a maximum near periastron

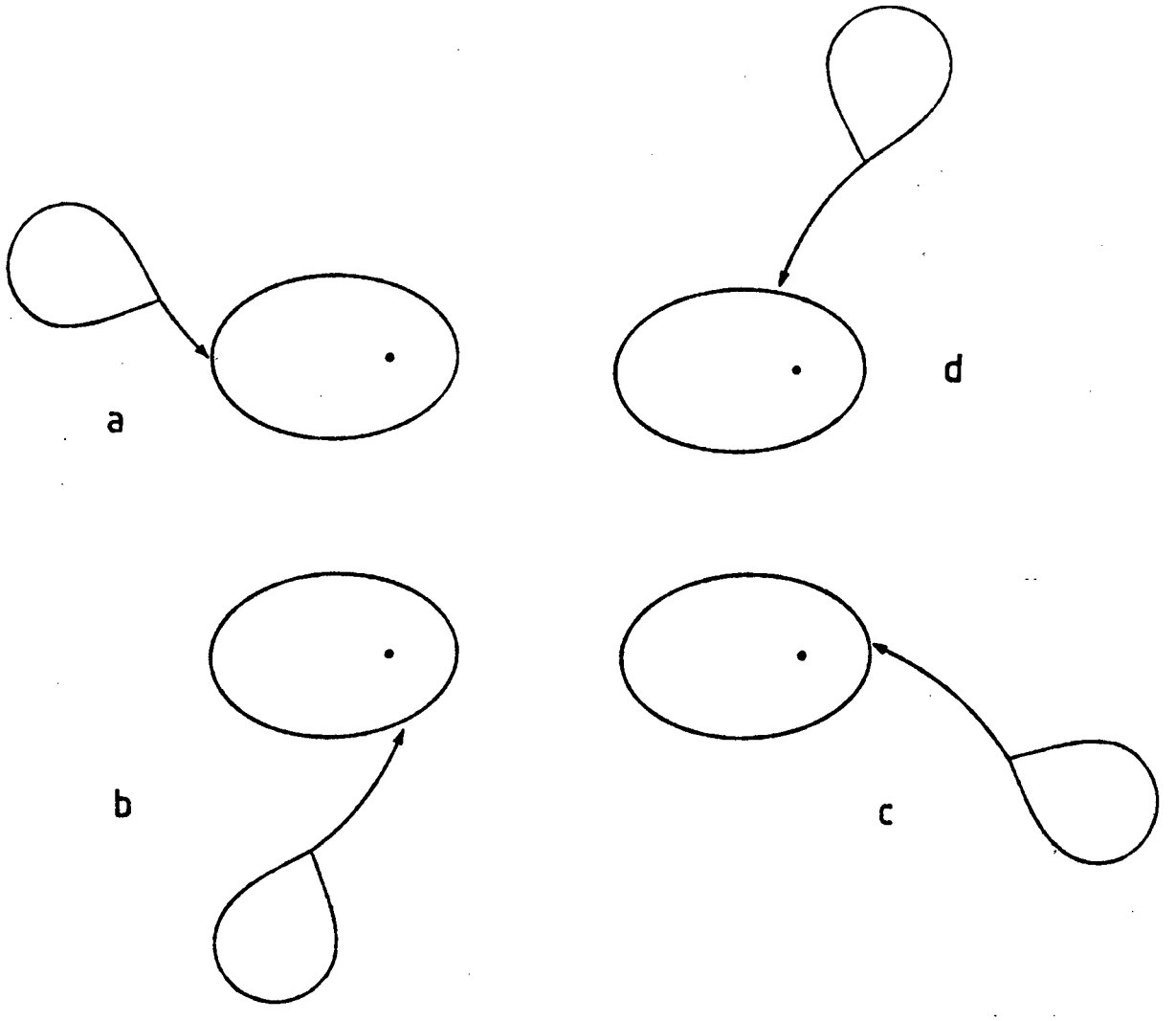

Figure 2.4 Vogt's model of a cataclysmic variable with eccentric disk (not to scale) showing the system configuration at four points in the orbital cycle. Superspot maximum occurs at (c).

where material in the stream falls farthest before releasing its kinetic energy. If the ring were to precess slowly in the prograde sense, the cyclic variation in superspot brightness would increase slightly in period, to give superhumps. At the same time the ring material diffuses inwards to give enhanced accretion onto the white dwarf: superoutburst. Most criticism of Vogt's model comes from Whitehurst [1984] who shows that tidal disruption would destroy such elliptical rings after only a few orbits of material around the primary. Osaki's model, by contrast, allows elliptical orbits to persist because of constant reinforcement. He proposes that far-UV and soft X-ray radiation from the central accretion disk heats the atmosphere of the secondary, thereby stimulating mass transfer. The degree of heating is dependent on the size of the shadow cast on the secondary by the optically thick disk. If the disk is elliptical in shape, the heating effect will be modulated with the orbital period, maximum occurring when the secondary is in the position shown below.

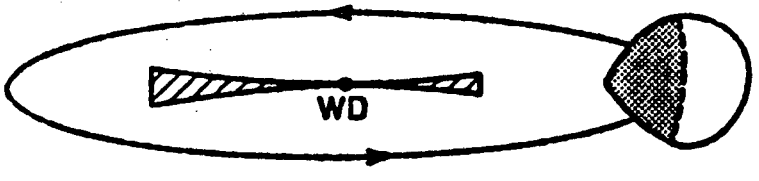

Figure 2.5 The eccentric disk model at position of maximum irradiation of the secondary (from Osaki 1985]).

Like Vogt, Osaki proposes a slowly precessing prograde disk in order to explain the inflated orbital period of superhumps. The beauty of Osaki's model is that the heating mechanism provides positive feedback by enhancing the ellipticity of the disk during each orbital cycle. Osaki calculates the properties of CV's whose disks should be unstable to "irradiation-induced mass-overflow instability". He finds they have low mass transfer rates ($\lesssim 10^{-10}$ $M_\odot$ yr^{-1}) and low secondary masses ($M_2 \lesssim 0.16$ $M_\odot$). Observations indicate that these properties are characteristic of the SU UMa dwarf novae. These systems also lie in the region of the $\dot{M}$ - M_2 diagram where disks are unstable to normal dwarf nova outbursts. Although the two behaviours are thus seemingly unrelated (one being an MTB phenomenon and the other a DI phenomenon), Osaki shows that a normal outburst may trigger a superoutburst, as is generally observed. Finally, he suggests that normal outbursts and superoutbursts do not coincide because the mass transfer rate that is induced by the superoutburst instability is roughly ten times larger than the normal rate, thus shifting the entire disk into a state of steady accretion. Osaki's model successfully accounts for nearly all the observed properties of superhumps, including the gritty problem of the "late superhumps" which appear in VW Hyi at the end of a superoutburst. These humps have the same period as the earlier superhumps, but differ in phase by 180°, and are explained by Osaki as the result of a change in the dominant

superspot-modulating mechanism from mass transfer bursts to variable stream length.

This model still requires more quantitative justification. For example, Osaki notes that the relaxation time taken by the secondary to adjust to a change in mass transfer rate is essentially unknown. A more serious criticism of the model was made by Whitehurst et al [1984]. Their interpretation of the superoutburst light curves of Z Cha led them to conclude that the superhump source was not eclipsed, and must therefore lie on the secondary as proposed in an early model by Warner [1974]. However, careful simulations by Horne [1984] and Smak [1985] have shown this interpretation to be incorrect, since an extended disk source for the superhumps would give shallow partial eclipses consistent with the data.

A third model, originally proposed by Papaloizou and Pringle [1979], requires a small eccentricity ($e \sim 10^{-4}$) in the binary orbit to modulate mass transfer by the observed amount. Clarke et al [1985] show that this may be compatible with uneclipsed superhumps, providing the superhump source occupies a large part of the outer disk. Their simulated light curves look promising, but timescale considerations force the principal superhump source to be the hot spot (with possible penetration into the disk), a restrictively small region.

A fourth model, proposed by Warner [1985b], will be discussed in subsection 2.5(iii), since it relies on the properties of the intermediate polars.

Clearly the mechanism(s) behind dwarf nova outbursts and superoutbursts are still highly controversial, and well-timed observations will be needed to pare and refine current models.

2.5 NOVA-LIKE VARIABLES

This broad class of variables includes all those stars which, despite having obvious CV characteristics, have never been seen to outburst. I shall discuss four subclasses of this group, although alternative subclassifications exist.

i) UX UMa Subclass: Some of these stars (such as UX UMa) are photometrically and spectroscopically indistinguishable from novae at minimum, and Warner [1976] suggests they are simply novae whose outbursts have not been observed. Others (such as CD-42°14462 and BD-7°3007) have broad absorption lines and instead resemble dwarf novae at maximum. Warner and Van Citters [1974] propose that VY Scl may be a Z Cam variable undergoing extended standstill.

Fortunately, these various resemblences can be unified by adopting Smak's [1983] interpretation of all these systems as having high mass transfer rates. Indeed, Sion and Guinan [1983] find further evidence for $\dot{M} \gtrsim 10^{-8}\ M_{\odot}\ yr^{-1}$ in UX UMa stars: the strong optical contribution from a

thick, luminous disk; the low ratio of X-ray to optical flux; and the P Cygni-type profiles of the spectral lines, indicating strong outflowing winds from the disk. Thus UX UMA stars are seen as being in a state of stationary accretion, but precise classification of individual systems is thwarted by our ignorance of their past histories.

ii) AM Her subclass: (also called Magnetic CV's or Polars) Regarded by many authors as a separate CV class, the AM Her stars differ from all the other groups in having a white dwarf primary with a strong magnetic field. To a first approximation this field is a centred dipole; in some cases the dipole is slightly off-centre (eg. Wickramasinghe and Martin [1985] find that an offset of 0.17 white dwarf radii gives a better fit to observations of AM Her), and it produces a magnetic field strength of $2\text{-}3\times10^{7}$ G at the white dwarf surface (Cordova and Mason [1983]).

The effects of this magnetic field are striking. First of all, in most CV's, accretion of material with high angular momentum gradually increases the rotation rate of the primary. In AM Her stars, however, this "spinning up" is completely prevented by magnetohydrodynamic torques exerted by the primary on the secondary, and the two stars are forced into synchronous rotation on relatively short timescales (Lamb et al [1983]). Observations of these stars are continually monitored for synchronism "slippage", and Liebert and Stockman [1985] review evidence for small changes in the orientation of one of the axes (magnetic or

rotational) of the white dwarf in well-studied systems. As yet, no significant long-term phase shifts have been noted, and Bailey et al [1985] find white dwarf rotation synchronous with orbital rotation to one part in 6×10^4 in the polar CW 1103+254. They point out, however, that stable asynchronism may still occur below this limit, as predicted by Campbell [1984] for systems with certain histories of geometry and mass transfer rate.

Secondly, material arriving as usual from the secondary via the gas stream penetrates the magnetic field of the primary until it is stopped by magnetic pressure. Detailed modelling by Liebert and Stockman shows that the material enters an intermediate "threading region" where competing physical processes buffet and shatter it, and finally reaches the point where the field strength is sufficient to divert it out of the orbital plane. The material falls inward along the field lines at high speed, impacting on the primary at one (or both) magnetic pole(s). Accretion is thus localised, rapid and highly energetic.

Thirdly, the magnetic field is of such strength that the primary captures essentially all transferred material, and thus an accretion disk cannot form. Since rotation is synchronous, the relative orientations of primary and secondary are fixed in time, and accretion will occur preferentially onto one of the magnetic poles. Which one dominates, and the extent of its domination, depends on the orientation of the primary with respect to the secondary and

the relative strengths of the dipole field at the two poles. Accretion may even shift from one pole to the other, as in AM Her (Bonnet-Bidaud et al [1985]).

The regions where funnelling occurs, the "accretion columns", are of particular interest, since they are strong sources of radiation with distinctive properties. Just above the stellar surface ($\sim 10^5$ m) supersonically falling material forms a standing shock, and it is here that most gravitational potential energy is released. Temperatures in this region are $\sim 10^8$ K (Wade and Ward [1985]). The emitted radiation has a hard X-ray component, due to bremsstrahlung, and a soft X-ray component of high intensity. The mechanism responsible for soft X-ray production is not altogether clear; Lamb [1985] cites several recent suggestions (including nuclear burning, filamentous accretion flow and energy transport by nonthermal electrons), but shows that reprocessing of high energy radiation by the polar regions of the white dwarf may in fact be sufficient to explain the observed flux. In addition, cyclotron emission from thermal electrons near the poles gives rise to optical and infrared radiation which is strongly polarized. The fundamental frequency of cyclotron emission is given by

$$\nu_c = \frac{eB}{mc} = 2.8 \times 10^{13} \left(\frac{B}{10^7\ \mathrm{G}}\right) \mathrm{Hz}$$

where e and m are the charge and mass of the electron, and c is the speed of light. For field strengths of a few times 10^7 G, the fundamental lies in the infrared. However, opacity is highest for the fundamental, and it is principally the higher harmonics (m ~ 5-15) in the optical region which are beamed to the observer (Bailey [1985]). This radiation is strongly anisotropic, most being emitted in directions perpendicular to the magnetic field. Wade and Ward [1985] point out that field strength determinations for these stars are thus subject to a strong selection effect: if the field is stronger or weaker than a few times 10^7 G, this strongly polarized radiation (the definitive property of AM Her stars) will be shifted out of the optical part of the spectrum.

Under favourable conditions (such as relatively cool cyclotron source), thermal line broadening may be sufficiently unintrusive to allow identification of the individual cyclotron harmonics. This is possible in the case of VV Pup, and enabled Wickramasinghe and Meggitt [1982] to determine directly the magnetic field strength at the emission source as 3.2×10^7 G. The size and shape of this region are somewhat controversial, but simple models depict a flat, "coin-shaped" region of height ~ 10^5 m and diameter ~ 10^6 m (Bailey [1985]). Recent observations suggest that the source of polarized light may be distinct from the X-ray source. Lamb [1985] reviews the evidence and

suggests the most likely position of the polarized light source is in the accretion column above the shock region.

The combination of intrinsic system geometry and inclination angle, i, modulates the radiation from these stars in a complex way. However, nearly all observable characteristics feature an orbital cycle - a direct result of synchronous rotation. The primary may be orientated in such a way that only one pole is ever visible (eg. E 2003+225), or both may be visible at different parts of the orbit (eg. AM Her). Whenever an active pole is visible, circular polarization is observed. Its intensity varies with viewing angle and reaches a maximum when the accretion column is viewed "pole-on". (In practice, the percentage of circularly polarized light may be observed to fall at these low viewing angles, but this is the result of a peak in the contribution of unpolarized light, probably from the photospheres of the two stars (Wickramasinghe and Meggitt [1985]). Thus the degree of circular polarization varies smoothly around the cycle, reaching a maximum of up to 35% in some systems (Barrett and Chanmugan [1984a]). By contrast, the linear polarization appears as a sharp pulse, usually once but sometimes twice per orbital period, and usually coincident with an "edge-on" view of the accretion column. The pulse height may be as much as 16% in CW 1103+182 (Stockman et al [1983]). Variations in behaviour may be seen in a single system. For example, Cropper [1985a] classifies the orbital variations of EF Eri

into two types, possibly characterising single and double pole accretion, and notes that changes from one type to the other may take place within one orbital period. On a timescale of weeks, there is evidence that the accretion column of EI405-451 moves in colatitude by as much as 15° (Cropper et al [1986]).

Unpolarized light from the photospheres of the two stars is usually lost in the background of radiation from the accretion columns and heated polar caps. However, it may be detected during an eclipse of these regions, or when the system is in a state of low luminosity. When detectable, the white dwarf radiation exhibits Zeeman splitting of absorption lines, from which the magnetic field strength may be calculated. In addition, its UV spectrum may be diagnosed to give the effective temperature at its surface. Szkody et al [1985] find $T_{eff} \sim 50000$ K for AM Her, but only $T_{eff} \sim 13400$ K for CW 1103+254. As in other CV's, the secondary is best viewed in the infrared; observations indicate that polar secondaries are late M-type red dwarfs, unusual only in their low masses ($M_2 < 0.20\ M_\odot$) (Liebert and Stockman [1985]). Less well understood are the sources of strong emission lines in AM Her stars. Balmer lines and He II (4686 Å) often comprise a broad component of velocity amplitude 300-400 km s^{-1} (thought to arise in the accretion stream) and a narrow component (apparently from the secondary).

The overall luminosity state of an AM Her star may be "high" or "low", reflecting two distinct rates of mass transfer. Unlike the outbursts of dwarf novae, these changes occur on timescales of months to years, with transitions rapid and the system predominantly in the high state. A transition to the low state is usually accompanied by decreases in the hard and soft X-ray fluxes but an enhancement, if anything, in the polarized cyclotron emission. Liebert and Stockman [1985] attribute this to a reduction in optical depth of the shock region. In one system, H0139-68, a transition to the low state apparently involves a reduction in the mass transfer rate to almost zero, and the light curve becomes essentially unmodulated (Cropper [1985b]).

The origin of such changes in mass transfer is not altogether clear. King and Lasota [1984] point to heating of the secondary by X-rays from the primary, a model qualitatively similar to the model of Z Cam dwarf novae by Meyer and Meyer-Hofmeister [1983]. However, Hameury et al [1985] conclude that models of this type predict equilibrium mass transfer rates that are insufficiently stable on a timescale of years to give the observed luminosity changes in either dwarf novae or AM Her stars. An alternative suggestion comes from Bastian et al [1985], who report on an outburst of 4.9 GHz emission in AM Her. They deduce a local secondary magnetic field of more than 10^3 G, and suggest that its interaction with the primary field could give rise

to various energetic phenomena, including outbursts and long-term changes in luminosity state.

iii) Intermediate Polar Subclass: (and DQ Her variables) This category of CV's has only been recognised very recently, although many of its members have been studied for some time.

As their name suggests, these stars are intermediate between the "non-magnetic" CV's (novae, dwarf novae and the like) and the strongly magnetic polars. Indeed, many of their properties show a compromise between the two extremes, and Warner [1983] suspects an underlying continuous distribution of systems with varying field strengths, most of which have yet to be recognised.

In the standard model, the characteristic feature of an intermediate polar is a primary magnetic field of sufficient strength to channel accreting material near the white dwarf surface, but insufficient strength to ensure synchronous rotation. As in the AM Her variables, accretion columns are probably present above the magnetic pole(s), but these are thought to be much broader than in the polars, covering a total fraction $f \geq 0.5$ of the white dwarf surface (King and Shaviv [1984b]). They still emit X-rays and cyclotron radiation, the latter peaking at wavelengths longward of the optical. However, at a certain height above the white dwarf surface (the "Alfvén radius") the magnetic field is too weak to channel infalling material effectively, and an accretion disk may form. Spectra of intermediate polars show disk

features (Warner [1983] finds $F_\lambda \propto \lambda^{2.2\pm0.2}$) and occasionally hot spot emission (Hassall et al [1981]), although King [1985] expects such disks to be much reduced, containing only a small fraction of the mass transferred at any time.

Since intermediate polars are so complex, it is unsurprising that their light curves and spectroscopic data are particularly difficult to interpret. Only very recently has Warner [1986b] published a detailed summary of the various sources of periodically-varying radiation in these stars, and their contributions to the Fourier power spectrum of the light curve. If the white dwarf surface has areas which differ in luminosity (such as in an intermediate polar), and if it rotates with frequency ω, an observer would see a modulation of the light curve of frequency ω, and shape dependent on the details of the luminosity distribution. In addition, the changing aspect of the rotating system would provide a modulation of orbital frequency Ω. Whereas in polars $\omega = \Omega$, intermediate polars have $\omega \neq \Omega$ and in general they are of the same sign (ie. rotation is prograde) with $\omega > \Omega$. A third modulation arises from primary radiation reprocessed in a region of the system which is fixed in the orbitally rotating reference frame. This region may be the hot spot (Hassall et al [1981], Warner [1986b]) or the atmosphere of the secondary (Motch and Pakull [1981], Patterson and Price [1981], Mateo et al [1985]). The primary light is generally assumed to be the

"beam" of X-rays from the magnetic pole(s). Warner [1986b] comments that the oscillation shapes probably imply a beam of great longitudinal extent, as might be expected from a broad accretion region. Warner also shows that further sources of reprocessed/reflected light within the binary system can combine to give additional modulations of frequency $\omega + \Omega$ and $\omega - 2\Omega$. Thus the presence of various high-speed, coherent oscillations can be expected to characterise intermediate polar photometry.

Unambiguous matching of the observed oscillation frequencies with their theoretical counterparts is far from straightforward, especially since they are seldom simultaneously observable in one wavelength band. In TV Col, for example, optical photometry reveals two periodicities ($P_1 = 0.21631^{d}$, $P_2 = 4.024^{d}$), spectroscopy gives another ($P_3 = 0.228600^{d}$) and recent X-ray observations yield a fourth ($P_4 = 0.023^{d}$). While $P_2^{-1} + P_3^{-1} = P_1^{-1}$, the relationship between these and P_4 is not obvious. Several models have been suggested for this star, which identify P_1^{-1} variously with ω (Hutchings et al [1981], Mateo et al [1985]), $\omega - \Omega$ (Watts et al [1982]) and $\Omega - \alpha$ where α is the precession frequency of a tilted precessing disk (Bonnet-Bidaud et al [1985]). The latter two models invoke retrograde rotation.

The possibility of a slowly rotating white dwarf has been incorporated by Warner [1985b] into a model which uses intermediate polars to explain the behaviour of SU UMa

stars. Warner proposes that $\omega << \Omega$, so that $\Omega - \omega$ (the superhump frequency) is a few percent less than Ω (the orbital frequency). Smak's [1985] analysis of the superhump eclipses in Z Cha shows that the superhump source contributes significantly to the light curve at all times, in support of Warner's model. His results also imply that, if Z Cha is an intermediate polar, the material illuminated by the X-ray beam must be even more extended than the disk. The principal difficulties with Warner's model lie in explaining why the white dwarf should rotate so slowly ($P_{rot} \gtrsim 2$ days), and why this intermediate polar behaviour should only be evident during supermaximum.

The distinction (if any) between intermediate polars and DQ Her stars lies in the measured values of the white dwarf rotation frequency, ω. The former have rotation periods lying longwards of 13 minutes, while the latter have periods in the range 28-71 seconds. However, many authors (eg. Warner [1985a], Lamb and Patterson [1983]) regard the distinction as tentative, and Patterson [1985] suggests that a selection effect may account for the lack of systems with intermediate values of ω.

The intermediate polars undergo changes of luminosity state in the same way as the polars, with the additional possibility of a third, intermediate state. Thorstensen et al [1985] examine the spectroscopic and photometric periodicities in TT Ari, and find that the spectroscopic (presumably orbital) variations show a change in phase of

0.28 cycles when the system goes from an intermediate to a high luminosity state. They interpret this surprising result as arising from a change in the principal emission source from, say, the hot spot to the white dwarf.

With magnetohydrodynamic torque too weak to overcome accretion torque, the primaries of intermediate polars should be continuously "spun up". This is indeed observed in DQ Her and EX Hya, whose spin-up rates of one part in 10^{12} and 4×10^{9} respectively agree with theoretical predictions of Ghosh and Lamb [1979a,b]. Using the observed values of ω and $\dot{\omega}$, Lamb and Patterson [1983] determine the magnetic field strengths of the known intermediate polars to be an order of magnitude smaller than those of the polars, while the fields of DQ Her stars are apparently weaker still. Van Paradijs et al [1985] report a spin-up rate of one part in 1.5×10^{10} in H2252-035, also in agreement with this theory. However, King, Frank and Ritter [1985] point out that the theory also predicts large numbers of intermediate polars with orbital periods less than 2 hours, whereas only one (viz. EX Hya) has been detected. They offer an alternative theory, based on evolutionary arguments, which identifies intermediate polars as predecessors of polars and thus attributes to them magnetic fields of similar strength. This view of supported by Barrett and Chanmugan [1984b], who argue that large orbital separation could disguise the presence of a strong magnetic field. Unfortunately, these three intermediate polars

constitute too small a statistical sample to differentiate between theories at the present time (van Paradijs et al [1985]).

CHAPTER 3

RAPID OSCILLATIONS IN CATACLYSMIC VARIABLES

The presence of high-speed, coherent oscillations in the optical light curves of DQ Her variables has already been mentioned as the most striking feature of these stars. In fact, rapid oscillations have been observed in all CV classes, although there is much variation in the amplitude, period and coherence properties from one system to another. Warner [1986a] provides an up-to-date list of all such CV's.

The coherence of an oscillation is a measure of the constancy of its period and phase with time. Quantitative determination of coherence depends on the mathematical model used, as reviewed by Cordova et al [1984]. If the oscillation is modelled as a damped harmonic oscillator excited by small, random displacements (an "autoregressive" process), then the decay time of the sinusoidal motion gives a measure of its coherence. Alternatively, if it is modelled as an undamped oscillator undergoing random phase disturbances, the coherence can be measured by the average phase walk per cycle. In both cases, random phase changes can appear as period changes in a power spectrum. A third possibility is the superposition of a number of oscillations with closely spaced periods. This representation forces a pulsational model of the physical system (Papaloizou and Pringle [1978]).

The highest coherence measured in CV's occurs in the DQ Her variables, which have oscillation periods in the range 33-71 s and are stable to better than one part in 10^{12} (Lamb and Patterson [1983]). The other intermediate polars follow, with periods of 13-67 minutes and typical stabilities of one part in 10^{10}. Since all these stars are observed sources of hard (2-10 keV) X-rays, it would seem that the model of a reprocessed X-ray beam from a rotating white dwarf (as discussed in Section 2.4) is the most likely explanation for the generation of these oscillations. Penning [1984] gives further support to this model by identifying oscillations in the Hβ, Hγ and He II flux of four intermediate polars with periods compatible with the optical oscillations. Warner [1985a] shows that the model is sufficiently versatile to explain the different phase behaviours of the ω and $\omega - \Omega$ oscillations in intermediate polars: the two oscillations may be in phase at inferior conjunction of the secondary (as observed in H2252-035) or at superior conjunction of the secondary (as in V1223 Sgr), depending on whether the optical contribution is greater from the direct beam or its disk-reprocessed counterpart. This, in turn, depends only on the detailed geometry of the system.

Somewhat less stable oscillations have been observed in several of the UX UMa variables. They all have periods close to 30 s, but these vary slightly from night to night and on occasion the oscillations may disappear altogether.

Of these stars, AE Aqr shows the same modulation (with the same phase) in optical and X-ray flux, suggesting a similar oscillation mechanism to that of the intermediate polars.

UX UMa itself shows such oscillations, and is unusual in that its high inclination angle results in eclipses of the disk, optically dominant in this system, by the secondary. Observations of the oscillations through eclipse show a characteristic phase shift of -360°, ie. the loss of one complete cycle. In this regard, UX UMa is most often compared with DQ Her, which also exhibits rapid oscillations and disk eclipses, but whose phase shift through eclipse is in the opposite sense: one complete cycle is gained. Petterson [1980] points out that the comparison is somewhat unnatural. Oscillations in DQ Her are always visible and feature an extremely constant period and an amplitude of ~ 0.04 magnitudes; those of UX UMa are erratically present at amplitudes less than 0.002 magnitudes and change slowly in period from night to night. However, attempts to explain both phenomena using one model have been relatively fruitful. Nather and Robinson [1974] model the oscillations as arising from travelling waves of non-radial pulsations with $\ell = 2$ and $m = \pm 2$. While this has the advantage of simple symmetry in generating phase shifts of either sign, the predicted phase changes through eclipse do not match the observed data too well. More recently, Petterson [1980] shows that much better fits can be achieved by regarding both systems as special cases of the X-ray beam model of the

intermediate polars. In Petterson's model, as in Warner's [1985a], small differences in geometry (particularly inclination and beam angle) result in surprisingly different behaviours. The model also accounts easily for the unambiguous observation that the whole disk is somehow involved in generating the oscillations. However, attempts to reproduce the oscillation behaviour outside of eclipse have so far met with only limited success (O'Donoghue [1985]).

Moderately coherent oscillations, stable over several hundred cycles, are also seen in some dwarf novae at outburst. Dubbed "DNO's" (dwarf nova oscillations) by Patterson [1981], these still defy satisfactory explanation despite years of dedicated observation. We briefly review their properties and current models of their generation:

DNO's have typical periods of 10-40 s and appear in the optical light curves of dwarf novae over a few days near outburst maximum. While their periods are stable to one part in 10^4-10^6, their phases may show a "random walk" on much shorter timescales (Cordova et al [1980]). The oscillations are pure sinusoids and, in general, only one frequency is present at a time. The oscillation period of a given system is a continuous, two-valued function of its visual luminosity, as shown in the schematic hysteresis-type diagram of Figure 3.1. The total variation in period may be as much as 16% over a single outburst (Cordova and Mason [1982]). A given system may show a correlation between

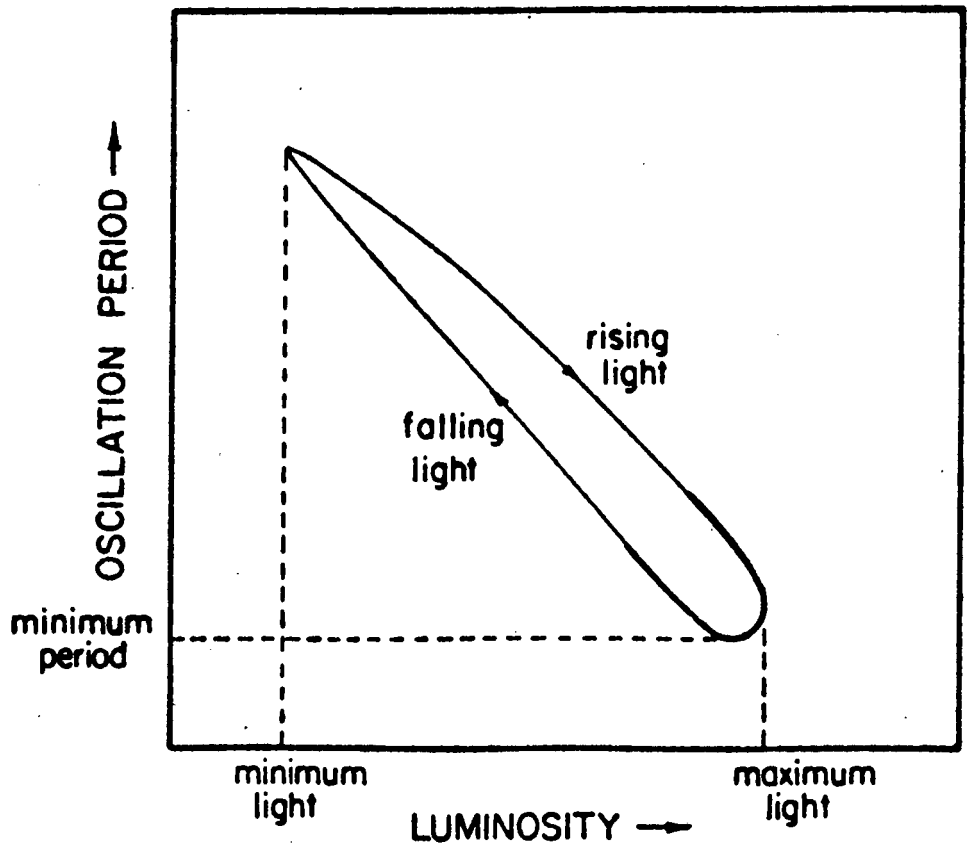

Figure 3.1 Schematic relationship between DNO period and system luminosity during a dwarf nova outburst (dark line) (from Patterson [1981]).

amplitude and coherence (eg. O'Donoghue [1985]). Finally, the amplitudes of the oscillations are low (typically ~ 0.2% of the total optical brightness of the eclipsing system), and variable on timescales of hours, suggesting that they are easily obscured (Warner [1986a]).

Models of oscillation generation fall into two main groups, viz. rotational and pulsational.

i) Rotational Models: The apparent success of the rotating X-ray beam model with the intermediate polars encourages its extension to the case of dwarf novae, especially since the period range of the DNO's corresponds almost exactly with the range of Keplerian orbital periods at the surface of white dwarfs of mass 0.1-1.4 $M_{\odot}$ (Bath [1973]). The most obvious difficulty lies in accounting for the observed changes in this period, since white dwarf rotation is an extremely stable phenomenon. Patterson [1981] points out that a way round this may be found by assuming independent rotation of a thin, outer layer of the white dwarf, but that some difficulties remain. The magnetic rotator model predicts ever-present oscillations at least as stable as the DNO's, but X-ray observations of SS Cyg show pronounced phase jitter at outburst maximum, and no modulation at all during quiescence (Cordova et al [1980]).

A second rotational model has the advantage that it does not require the primary to have an X-ray beam or otherwise non-uniform surface brightness. Bath [1973]

attributes the DNO's to rotating inhomogeneities in the inner disk which are periodically eclipsed by the white dwarf. This would successfully account for the coherence times of the oscillations, since differential disk rotation would be expected to shear out an inhomogeneity within $\sim 10^3$ s (Patterson [1981]). Bath explains the variation of period with luminosity by supposing the inhomogeneities to form at the Alfvén radius, where the inward ram pressure of infalling material is balanced by the outward magnetic pressure from the white dwarf. The position of this equilibrium point depends on the accretion rate, so that the MTB theory of dwarf nova outbursts predicts a decrease in oscillation period with an increased accretion rate, as observed. Unfortunately the quantitative agreement is poor, since the ~ 25% period variations do not mimic the deduced variations of 80% or more in accretion rate (Patterson [1981]).

ii) Pulsation Models: Cyclic variations of period 10-40 s can be generated by a white dwarf pulsating in a non-radial gravity (g-) mode (eg. Warner and Robinson [1972]). Since such pulsations should be far more coherent than the observed DNO's, more recent pulsation models follow rotational models in presupposing a very thin outer skin as the oscillation source (Papaloizou and Pringle [1978]). These g-modes have frequencies given by

$$\nu_\ell = \nu_o \left(1 - \frac{1}{\ell(\ell+1)}\right)$$

where ν_o is the rotation frequency of the stellar interior, and ℓ is a positive integer.

The oscillations arise when modes of different ℓ rotate past each other on the white dwarf surface, giving rise to beats in the local surface temperature. Papaloizou and Pringle [1978] also suggest two alternative pulsation types, both arising in a white dwarf which pulsates and rotates sumultaneously. These are Rosby-type (r-) modes, some of which have large amplitudes only in the outer parts of the star, and g-modes that become trapped near the equator by high rotation rates. Again, it is the recent X-ray observations of SS Cyg that prove most problematic to these models. Interpreted as pulsations, SS Cyg oscillations show large amplitude modes present one at a time and separated by very short time intervals, whereas one would expect a relatively stable spectrum of modes at all times (Cordova et al [1984]). Only WZ Sge, an unusual dwarf nova in several respects, has shown two distinct periodicities simultaneously present in the light curve.

In an attempt to differentiate between these models by determining the source temperature, measurements have been made on the optical colours of the DNO's. Hildebrand et al [1981] find that oscillations in dwarf nova AH Her are much bluer than the continuum radiation. Warner [1986a] notes that the ultraviolet flux in VW Hyi lags behind the visual

flux by about one day during the rise to outburst maximum, and suggests that a monotonic relationship may exist between DNO period and ultraviolet luminosity (cf. Fig 3.1). Both of these results point to the inner regions of the disk as the oscillation source, but unfortunately the data do not support one model over another. Middleditch and Cordova [1982] find that the oscillations in SY Cancri are too blue to be consistent with any simple thermal model, and question the validity of interpretations by users of reduced wavelength coverage.

In addition to DNO's, dwarf novae sometimes exhibit oscillations which are stable for a few cycles only. These are the "quasi-periodic oscillations" or "QPO's" (Robinson and Nather [1979]). They have periods ranging from 30 to 150 s and appear during outburst maximum and subsequent decline to minimum. Their amplitudes are of the same order as those of DNO's, and the dilution of their power over a substantial frequency range makes their detection, even with Fourier Transform techniques, often very difficult.

Patterson [1981] points out that their periods and coherence times usually make DNO's and QPO's easily distinguishable, and proposes that they have different origins. The same view is expressed by Robinson and Nather [1979] who tentatively deduce the source of the QPO's. They rule out the white dwarf with coherence arguments, and the hot spot on the grounds that QPO's in U Gem persist through hot spot eclipse. By assuming that the same mechanism is

responsible for QPO's in both dwarf novae and the X-ray source Sco X-1, they also eliminate the inner disk boundary on energetic grounds, and conclude that QPO's arise in the disk itself, triggered in some way by the increased mass flow associated with outburst. Cox [1981] shows that vertical oscillations of disk material at a given radius would have a period close to the Keplerian orbital period at that radius. Thus the QPO's could well be a superposition of oscillations arising over a sizeable region of the inner disk. If so, the observed coherence times of 3-5 periods could be due to viscosity damping, provided the disk is highly viscous ($\alpha \sim 1$) (Cox and Everson [1982]).

Cordova et al [1980] criticise Robinson and Nather's strict scheme of classification, arguing that the 9-second soft X-ray oscillations in SS Cyg combine most of the features of DNO's, notably their period stability, with the phase incoherence of QPO's. Certainly these oscillations are most puzzling. Cordova et al propose that they arise in the white dwarf/disk boundary layer, where continual formation and decay of local instabilities could yield the observed phase jitter but a relatively constant period. However, it is difficult to imagine how reprocessing of such X-radiation could give rise to the higher phase stability typical of the optical oscillations in SS Cyg. Patterson [1981] suggests that phase coherence may be a superficial measure of stability, citing WZ Sge and AE Aqr as stable oscillators which show random phase change on short

timescales. He also suggests a physical reason for this: the precise moment of intensity maximum depends on the positions of any asymmetric disk features (hot spots or general inhomogeneities), and this dependence is most sensitive for small-amplitude oscillations. Thus minor changes in disk appearance, on timescales of seconds, may be readily visible while not interfering with the long-term stability of beam rotation (Patterson [1980]).

QPO's of much shorter period (1-3 s) have been detected in two AM Her variables, viz. E1405-451 and AN UMa (Cordova and Mason [1982]). These may be due to oscillations of the magnetic flux tubes which channel material onto the white dwarf (Tuohy et al [1981]). AM Her itself occasionally shows QPO's of period 20-60 s (Tuohy et al [1981]). However, Szkody et al [1980] conclude that optical, X-ray and infrared variations in this star show no correlation.

It is thus clear that rapid oscillations are a very widespread phenomenon in cataclysmic variables, and that no single model has yet accounted for their large range of properties. The following chapters highlight two systems whose oscillations may prove particularly useful in discriminating between models.

CHAPTER 4

OBSERVATIONS AND DATA MANIPULATION TECHNIQUES

4.1 OBSERVATIONS

The photometric observations presented in this work were made at the Sutherland site of the South African Astronomical Observatory (S.A.A.O.), using a pulse-counting photometer mounted at the Cassegrain focus of the 0.75 m or 1.0 m telescopes. The instrument is described in detail by Nather and Warner [1971]. In essence, it is an uncooled RCA8644 or Amperex 56DVP photomultiplier tube which records incident photons as electrical pulses of varying height, and a discriminating amplifier which amplifies pulses of intermediate height but excludes the pulses of high and low amplitude caused (respectively) by cosmic rays and thermal excitations within the tube. No cooling was necessary because despite the high quantum efficiency of the tube it gives low dark counts (typically ~ 40 s^{-1}) at 20°C and an operating voltage of 1800 V. Once amplified, the pulses are counted and binned in contiguous time intervals as set by the observer. At the end of each time interval, the total pulse count is recorded on paper-tape or magnetic cartridge. System control is provided by an on-line Nova 3 mini-computer which also handles acquisition, timing and recording of data, and displays it on a VDU screen for immediate value judgement by the observer.

As cataclysmic variables are intrinsically faint, it is vital to maximise the signal-to-noise ratio of real stellar variations, especially if the variations of interest have a short intrinsic timescale (20-80 s in this case). The length of integration intervals was kept sufficiently short to resolve any suspected periodicities with several points per cycle. This was tempered by a need to keep a high photon count per time bin to combat noise levels. In general, intervals of 4-5 seconds were found to be optimal.

With signal clarity the highest priority, use of optical filters was abandoned throughout to increase count rates. Spectral response was thus determined principally by the S11 response of the photomultiplier tube, peaking at approximately 4300 Å. In addition, no comparison stars were monitored so that maximum uninterrupted information on the CV oscillations could be gained. Naturally this precludes accurate magnitude measurements of the variable as well as sensitivity to variations in transparency. The latter can be justified on the grounds that atmospheric variations take place over periods of ten minutes or more, and the resulting features generated in the power spectrum are well-separated from the high-frequency oscillations of interest. Sky measurements were taken at intervals throughout the runs, from every half hour (during stable conditions) to every five minutes (during times of rapid skylight variation).

Full details of the observations appear in subsequent chapters as relevant to the individual stars.

4.2 REDUCTIONS

The data were reduced using a computer program which subtracts sky measurements and adjusts for atmospheric extinction of light at changing elevation, using a mean extinction coefficient of 0.4 magnitudes per air mass for unfiltered light. The reduced data are then scaled to give intensities in counts per second, in order to facilitate direct comparisons between runs of different integration interval. Sky and bad points are set to zero.

The photomultiplier dead-time of 52 ns was not taken into account, since this effect is negligible in studies of low-amplitude oscillations at light levels below 2×10^5 counts s^{-1}.

4.3 FREQUENCY ANALYSIS

The computer program used to look for periodicities in the data was written by D.O'Donoghue using the technique of Deeming [1975]. By analogy with the complex Fourier transform,

$$F(\nu) = \int_{-\infty}^{\infty} f(t) e^{\,i2\pi\nu t}\, dt,$$

Deeming defines the discrete Fourier transform:

$$F_N(\nu) = \sum_{k=1}^{N} f(t_k) e^{\,i2\pi\nu t_k}$$

which does not require equal spacing of the time series t_k. In our case, two arrays are set up: the t_k and the $f(t_k)$, in which are stored the time and photon count of each measurement. Thus it is possible to search for periodicities in widely-spaced data sets. With each distribution of the t_k is associated a unique "spectral window" which may be plotted as a function of frequency to show features that generate aliasing as a result of the data spacing. This facilitates sensible interpretation of the observed Fourier transform, which is the convolution of the true Fourier transform $F(\nu)$ with the spectral window.

Both of the CV's studied in this work exhibit rapid oscillations which vary in period and amplitude on timescales of tens of minutes. This degree of coherence is insufficient to warrant data gaps of a night or more, and so each run has been analysed separately. Thus the spectral windows closely approximate the Dirac comb function characterising evenly-spaced data points, with small deviations due to the deletion of sky and bad points with their corresponding times. An example is shown in Figure 4.1. On several occasions individual runs have been broken down into shorter lengths preceeding Fourier analysis. This technique is useful when an oscillation is stable over part of a run but changes period or loses coherence fairly suddenly.

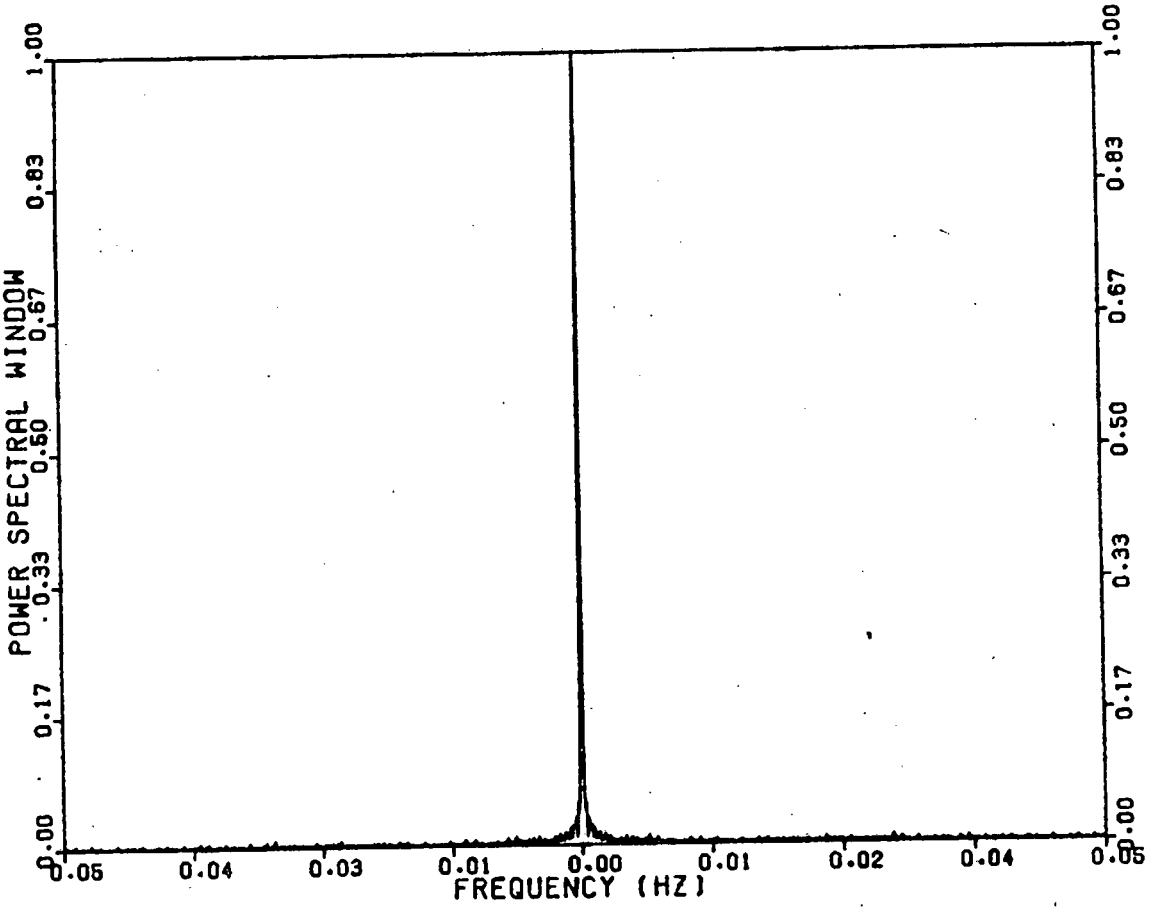

Figure 4.1 Spectral window of run S0130.

4.4 PHASE AND AMPLITUDE DATA

When the period of an oscillation is relatively constant over many cycles, an effective technique of data display is that described by Warner et al [1984]. A representative period is selected to cover that part of the light curve in which the oscillation is stable, and this period is then used in a least-squares fit of consecutive subsections of the data. As each subsection yields a best-fitting value of amplitude (A) and phase (ϕ), their graphic display shows the changing nature of the oscillation with time. Clearly one consequence of this technique is that any real changes in period will also appear as changes in amplitude and phase. For instance, a linear increase of $\Delta\phi$ radians per second indicates the stable presence of an oscillation with period T_{obs} shorter than the fitting period T_{fit} and given by

$$T_{obs} = T_{fit} \times \left(\frac{2\pi}{2\pi + T_{fit}\Delta\phi} \right)$$

A quadratic increase in ϕ signifies a linearly decreasing period, and so on. In all cases the absolute phase is arbitrary; only changes in phase are significant.

The computer program used for this manipulation (written by D.O'Donoghue) allows the user to select the subsection length, the amount of overlap between subsections, and the fitting frequency appropriate for each run. All phase variations are plotted twice, with a 360°

displacement, so that the loss or gain of one whole cycle may be detected.

CHAPTER 5

CPD-48°1577 (IX VELORUM)

5.1 INTRODUCTION

With a visual magnitude of $m_v = 9.8$, CPD-48°1577 is the brightest known cataclysmic variable. It is thus remarkable that it was only recognised as such in 1982 (Garrison et al). Its IUE spectrum resembles those of nova-like variables or erupting dwarf novae, with broad absorption lines of high ionization (Bohnhardt et al [1982]). Optical spectroscopy reveals a typically strong blue continuum and emission cores to the broad Balmer absorption lines, as well as He I, He II and C III-N III emission (Wargau et al [1983]). The UBV colours are similar to those of UX UMa (Garrison et al [1984]). Clearly CPD-48°1577 is a disk-dominated cataclysmic variable.

Wargau et al [1983,1984] calculate preliminary values of the physical parameters of the system, including $i \sim 63°$, $M_1 \sim 0.9\ M_\odot$ and $M_2 \sim 0.5\ M_\odot$.

Studies of long-term variability of CPD-48°1577 by Wargau et al [1984] show irregular brightness changes of amplitude ~ 0.5 magnitudes, but no sign of systematically high or low luminosity phases. This is suggestive of a nova-like variable or old nova, permanently in the "outburst" state of high accretion. Preliminary estimates of the accretion rate of the system vary from $5\times10^{-9}\ M_\odot\ yr^{-1}$ (Sion [1985]) to $7\times10^{-10}\ M_\odot\ yr^{-1}$ (Garrison et al [1984]).

While the higher of these is comparable with the deduced accretion rate in UX UMa (Smak [1983], Sion and Guinan [1983]), stationary accretion is not necessarily excluded by the latter, particularly if the disk is small (Smak [1983]).

Wargau et al [1983] give a preliminary orbital ephemeris for radial velocity minimum, based on five spectra taken on two successive nights:

$$\phi_{min} = JD_{\odot}\ 2445334.562 + 0.187\ E \pm 3 \text{ days.}$$

Their determination of orbital period (4.49 ± 0.07 hours) is slightly longer than the 3.9 ± 0.5 hours calculated by Williams and Hiltner [1984] using least-squares sinusoidal fitting on a single night's V-observations. A third ephemeris by Eggen and Niemela [1984] gives the period as 2.93 hours, based on 26 radial velocity measurements. Each of these determinations relies on a very limited database, and should thus be regarded as uncertain.

Warner et al [1984] report the discovery of rapid, coherent oscillations in CPD-48°1577. They have periods between 24 and 30 s, and were not found by Williams and Hiltner probably because these authors used an integration interval of 10 s.

5.2 OBSERVATIONS

The observations are listed in Table 5.1. The 28 runs yield a total of 82 hours of white light photometry of CPD-48°1577. All runs up to and including S3086 used an RCA 8644 photomultiplier; thereafter an Amperex 56DVP photomultiplier was used. To enable direct brightness comparisons to be made between runs on different telescopes, standard stars of similar colours were observed with each equipment change and the results used to convert mean count rates for all runs to those measurable by the RCA 8644 photomultiplier on the 0.75 m telescope. The resulting count rates are listed in column 9 of the Table.

5.3 RESULTS

Figure 5.1 shows the light curve of run S3048 plotted on two different scales. Figure 5.2 shows the corresponding power spectrum, in which two separate features are visible. One is a narrow periodicity at 25.23 s (3.96×10^{-2} Hz), which is the oscillation reported by Warner et al [1984]. In this run it has a semi-amplitude of 1.0 mmag, typical of coherent oscillations in dwarf novae and nova-like variables. The other is a broad feature, much like the effect of quasi-periodic oscillations, covering a range of frequencies from 0.007 to 0.11 Hz. This feature is in fact generated by telescope drive error, the result of observing an unusually bright variable through a small aperture in conditions of poor seeing. Run S3048 has been selected from the

Table 5.1 Observations of CPD-48°1577

Run No.	Date	$JD_{\odot}$ Start (2 440 000+)	Telescope (m)	Integration Interval (s)	Duration of Run (hours)	Oscillation Period (s)	Oscillation Amplitude (mmag)	Reduced mean Brightness +1000 (c/s)	Observer
S3045	18-11-1982	5291.52718	0.75	5.0	1.73	(30.52)	(1.2)	225	SA
S3048	19-11-1982	5292.50032	0.75	5.0	2.41	25.23	1.0	239	SA
S3050	19-11-1982	5293.49559	0.75	5.0	2.08	25.35	1.0	230	SA
S3052	20-11-1982	5294.44733	0.75	5.0	3.68	25.27	1.2	226	SA
S3075	19-12-1982	5322.52860	1.0	4.0	1.13	26.18	1.4	218	BW
S3080	26-01-1983	5360.51491	0.75	5.0	2.59	-	-	189	SA
S3081	26-01-1983	5361.30846	0.75	5.0	6.86	28.36	1.0	203	SA
S3082A	28-01-1983	5362.54215	0.75	5.0	0.82	-	-	207	SA
S3082B	28-01-1983	5362.57657	0.75	5.0	0.74	-	-	207	SA
S3083A	28-01-1983	5363.29056	0.75	5.0	2.84	28.46	1.2	206	SA
S3083B	28-01-1983	5363.44346	0.75	5.0	4.13	28.71	1.1	210	SA
S3084	29-01-1983	5364.41261	0.75	5.0	4.67	28.92	1.1	212	SA
S3085A	30-01-1983	5365.37642	0.75	5.0	1.81	28.47	1.2	214	SA
S3085B	30-01-1983	5365.48827	0.75	5.0	3.10	28.44	1.0	218	SA
S3086	31-01-1983	5366.28190	0.75	5.0	4.73	29.12	1.0	223	SA
S3236	15-12-1983	5684.44079	1.0	2.0	3.33	-	-	235	BW
S3238	17-12-1983	5686.43669	1.0	2.0	0.70	-	-	235	BW
S3240	18-12-1983	5687.39374	1.0	2.0	4.41	-	-	245	BW
S3242	19-12-1983	5688.41742	1.0	2.0	3.67	-	-	245	BW
S3243	17-01-1984	5717.29373	0.75	2.0	2.27	-	-	230	DOD
S3244	19-01-1984	5718.51313	0.75	2.0	2.47	-	-	230	DOD
S3245	19-01-1984	5719.28559	0.75	2.0	7.98	24.60	0.6	245	DOD
S3247	20-01-1984	5720.45365	0.75	2.0	3.89	24.72	1.3	230	DOD
S3249	21-01-1984	5721.44350	0.75	2.0	0.64	-	-	230	DOD
S3251	22-01-1984	5722.44942	0.75	2.0	2.78	25.09	1.3	230	DOD
S3254	23-01-1984	5723.41557	0.75	3.0	4.59	24.83	1.4	215	DOD
S3283	06-03-1984	5766.44887	1.0	1.0	0.60	-	-	225	BW
S3289	08-03-1984	5768.42571	1.0		1.82	-	-	220	BW

Observers: SA = Sue Allen BW = Brian Warner DOD = Darragh O'Donoghue

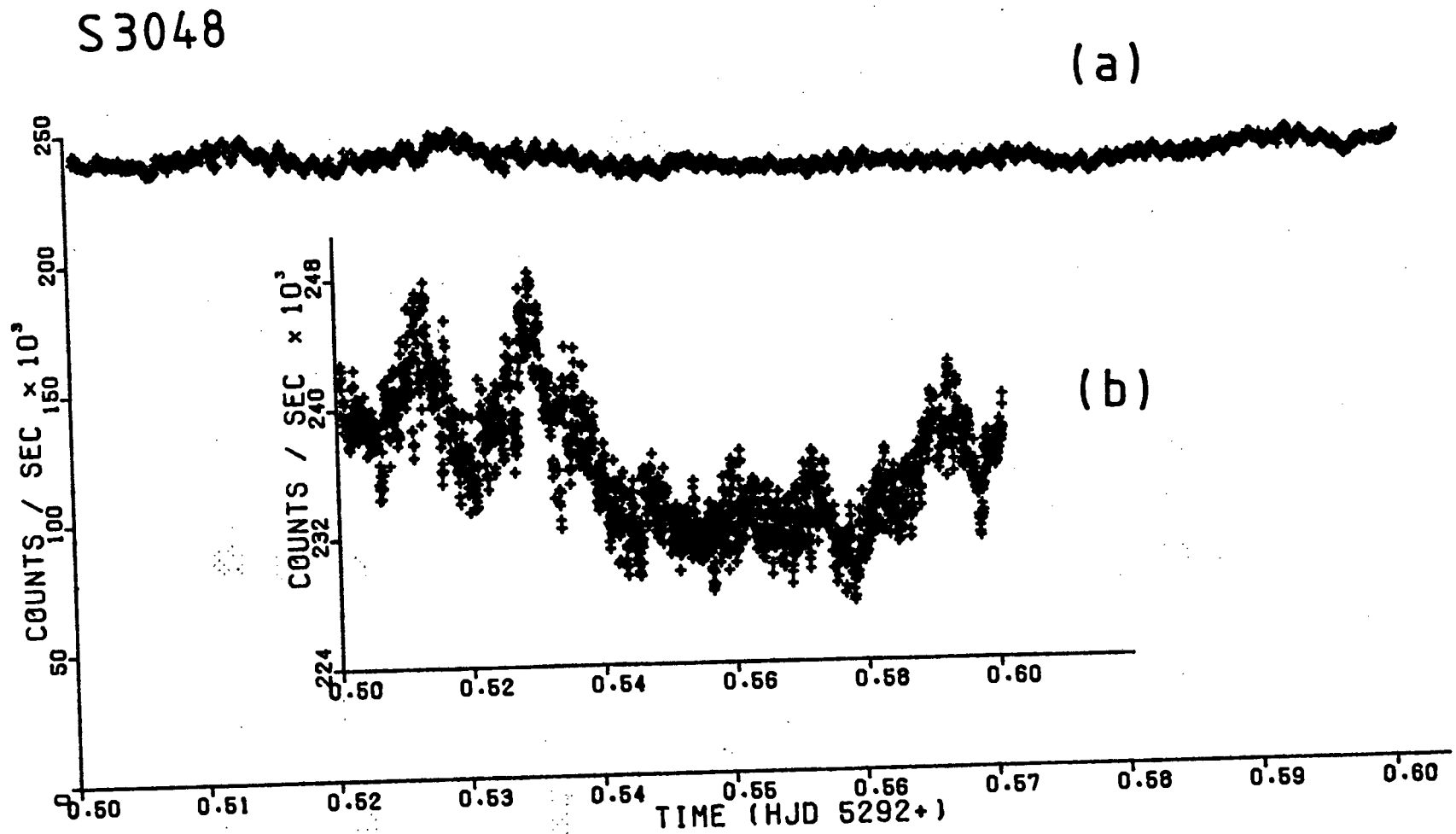

Figure 5.1 Light curve of run S3048 on CPD-48°1577, plotted on two different scales.

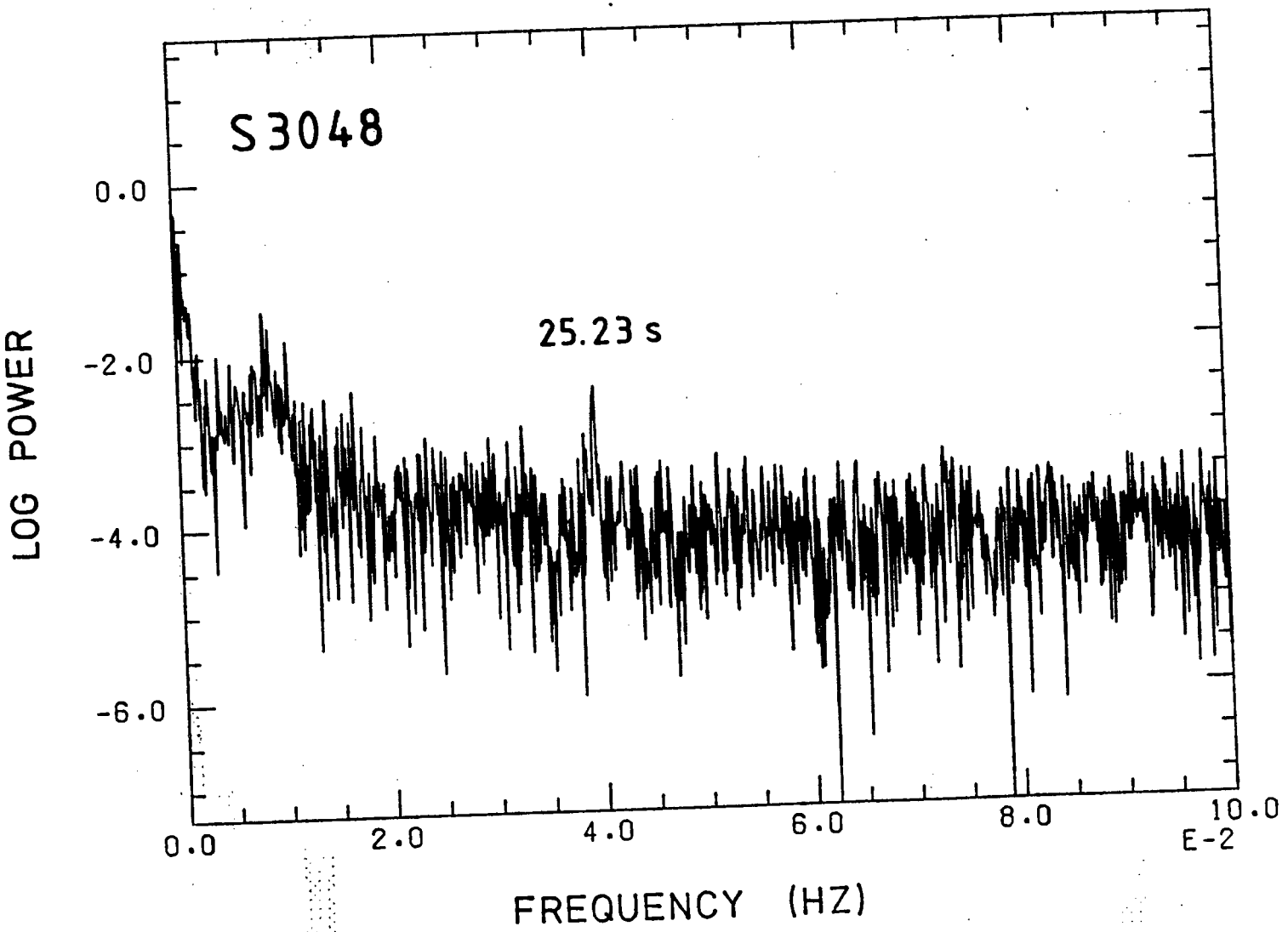

Figure 5.2 Power spectrum of run S3048.

observations listed in Table 5.1 as the worst case of drive error contamination; the 120 s periodicity is apparent in Figure 5.1 as a modulation of the light curve. Even in this case, however, it is clear from the power spectrum that the two features do not mutually interfere, so that the detection and measurement of the coherent oscillation (Table 5.1) can be regarded as reliable.

The much contracted time scale used in Figure 5.1(b) to plot the light curve shows clearly the long-term light variations intrinsic to the star. These variations constitute random flickering of typical peak-to-peak amplitude 0.07 mag, in agreement with observations by Williams and Hiltner [1984].

The coherent oscillations in CPD-48°1577 vary in period and amplitude from night to night, and often are not detectable at all. As with DNO's in other systems, they are sinusoidal to the limits of detection, showing no power at multiples of the fundamental frequency. Columns 7 and 8 of Table 5.1 give the period and semi-amplitude of the oscillations in all runs where they were detectable. These results differ in some cases from those given by Warner et al [1984], since re-examination of the data showed the oscillation amplitudes to be somewhat larger than previously determined. The semi-amplitudes lie in the range 1.0 - 1.4 mmag, except for the very long run S3245 which showed significant variation in period over its total duration (see Fig 5.5) and is thus poorly approximated by a single

sinusoid. On occasions when the oscillations were not detected, estimates of the noise in the Fourier spectra put an upper limit of 0.25 mmag on their semi-amplitude. Rapid oscillations were seen on more than half of the twenty-five nights of observation. This, together with the notable brightness of the system, strongly recommends CPD-48°1577 as a target for extended observation.

It is not clear whether stationary-accretion variables such as CPD-48°1577 exhibit a period-luminosity relationship of the same form as the dwarf novae. In their observations of UX UMa, Warner and Nather [1972] find oscillations of semi-amplitude 2 mmag which undergo a 2% decrease in period and simultaneous 9% increase in white light brightness from one night to the next. Further observations by Nather and Robinson [1974] suggest that the oscillation period in UX UMa may vary on a timescale of weeks, possibly in a cyclic fashion, but these authors do not describe any corresponding variations in system luminosity. Unfortunately such variations are extremely small in comparison with those of erupting CV's, so many more data are required to establish significance.

A period-luminosity graph for CPD-48°1577 is plotted in Fig 5.3. For each run the mean white light intensity, I, was estimated from the fully reduced light curve. The precision of this estimate is limited by slow variations in intrinsic stellar brightness and sky transparency, giving a total uncertainty of approximately 5% as indicated by the

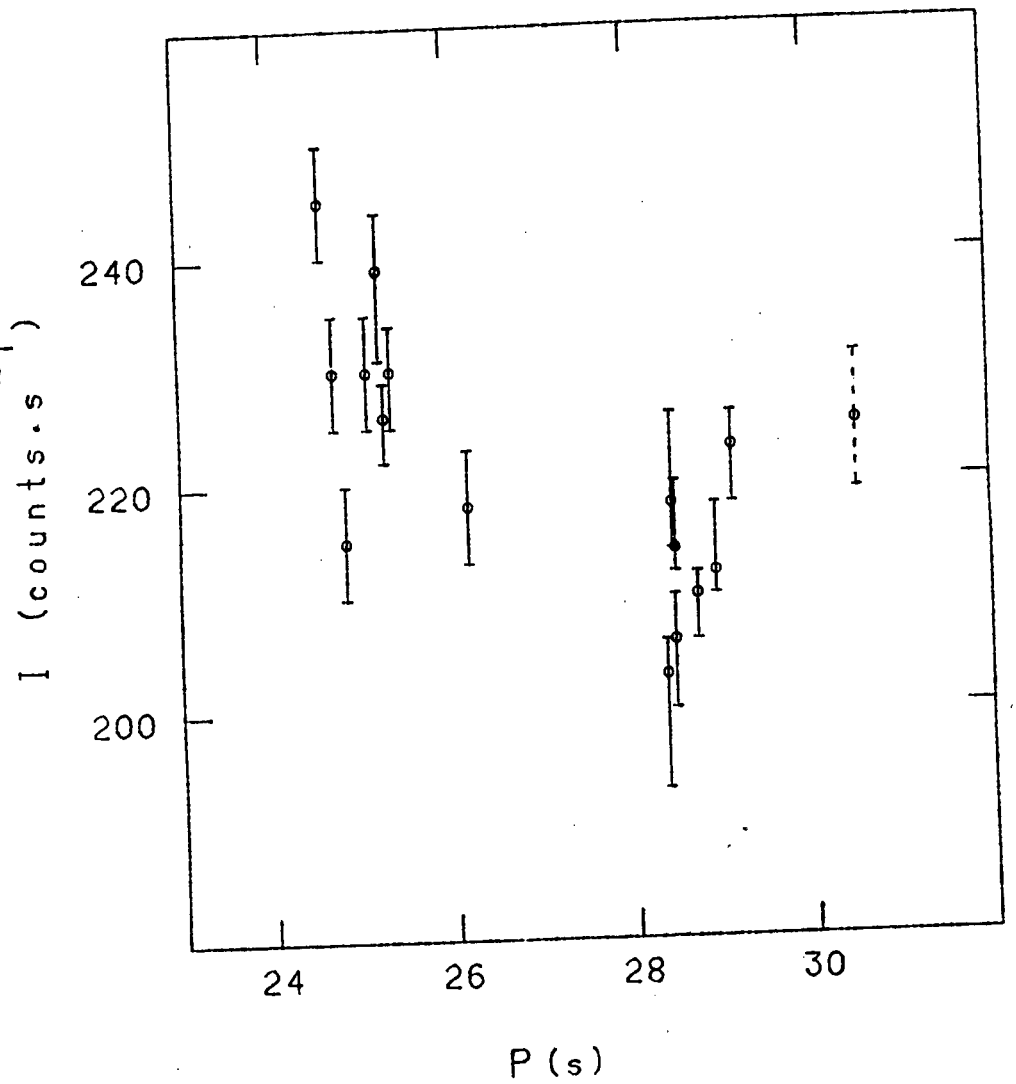

Figure 5.3 Mean white light intensity of CPD-48°1577 versus oscillation period.

vertical error bars. The uncertainty in the periods is < 0.01 s. The point drawn in dashed lines is the oscillation detected in run S3045 and shown in brackets in Table 5.1. Although this oscillation has semi-amplitude 1.1 mmag, there are good reasons for doubting its validity. Comparison of its period with those of oscillations on three successive nights shows a disparity of nearly 20%; nowhere else in the observations of CPD-48°1577 (or any other variable of this type) are there nightly variations of more than 3%. Close examination of the amplitude spectrum also reveals a somewhat narrower peak in S3045 than in the three subsequent runs. Thus we conclude that it is probably a statistical fluctuation in the noise. Its omission from the period-luminosity diagram leaves a clear trend in spite of large scatter. The best line through the graph of log P against log I has gradient $s = -1.7 \pm 0.6$. This is much steeper than the $s \sim -0.2$ for UX UMa or $s \sim -0.25 \pm 0.1$ for typical dwarf novae (Warner et al [1984]), indicating a relatively strong dependence of period on white light intensity.

In all runs which showed the presence of oscillations, Fourier spectra were taken of overlapping subsections of approximately 80 cycles, to give maximum temporal resolution without losing the signal entirely. Fig 5.4 shows the amplitude spectra from three such runs, with time running from bottom to top. Successive subsections have been overlapped by 50% of their length. The oscillations present

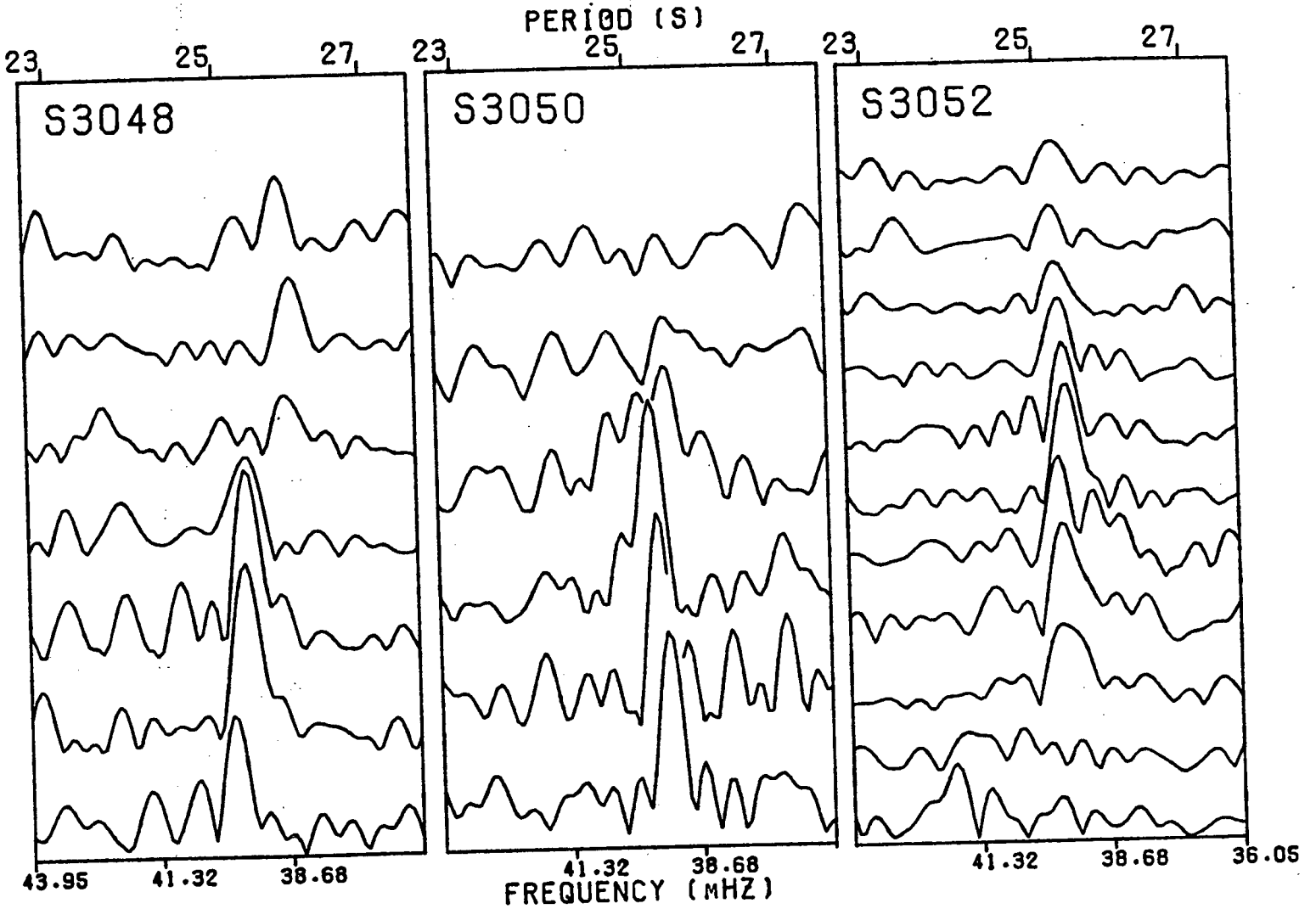

Figure 5.4 Fourier spectra of three runs subdivided into overlapping sections of approximately 80 cycles each.

in S3048 and S3050 disappear near the middle of each run over a period of half an hour or less. In S3052 the oscillations appear some time after the start of the run, persist for about two hours and die away again.

The oscillation period also shows slow variation within a run, as can be seen in Fig 5.5. Here S3245 has been subdivided into subsections of 130 cycles with a 75% overlap. The mean period for the run (viz. 24.60 s) has been used in a least-squares fit of each subsection, and the resulting values of phase and amplitude plotted against time. As explained in Chapter 4, the phase variations imply that the oscillation period is higher than the mean (linear fit gives P = 24.66 s) for the first third of the run, decreases to about the mean value for the middle third, and decreases further to approximately 24.56 s for the last third. Sporadic variation of this magnitude and timescale would amount to a few percent over 24 hours, as is indeed observed. The $\pm$ 1 σ error bars principally reflect the oscillation amplitude, as can be seen from the graph of amplitude against time for the same run.

At high time resolution, CPD-48°1577 occasionally shows a sudden phase shift of -360°. Fig 5.6 shows this effect in three runs, each divided into subsections approximately 20 cycles long with a 50% overlap. The phase shift occurs four times in all, and takes place over a period of 8 to 12 minutes, a factor of four shorter than the extended phase shifts of DQ Her and UX UMa. If the effect is real, it

S3245

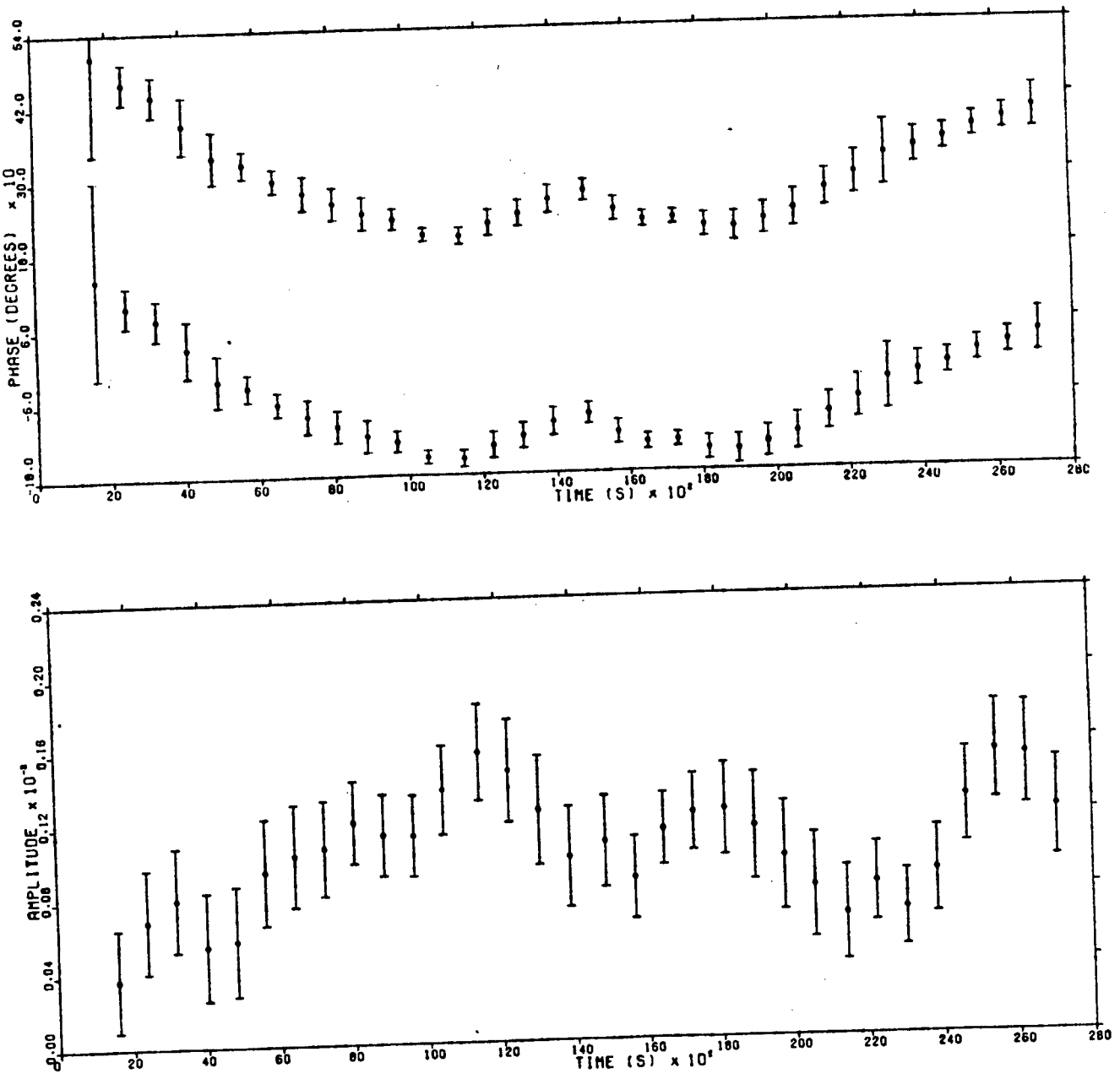

Figure 5.5 Variation of phase and amplitude of oscillations in run S3245. Divisions on phase scale show intervals of 120°.

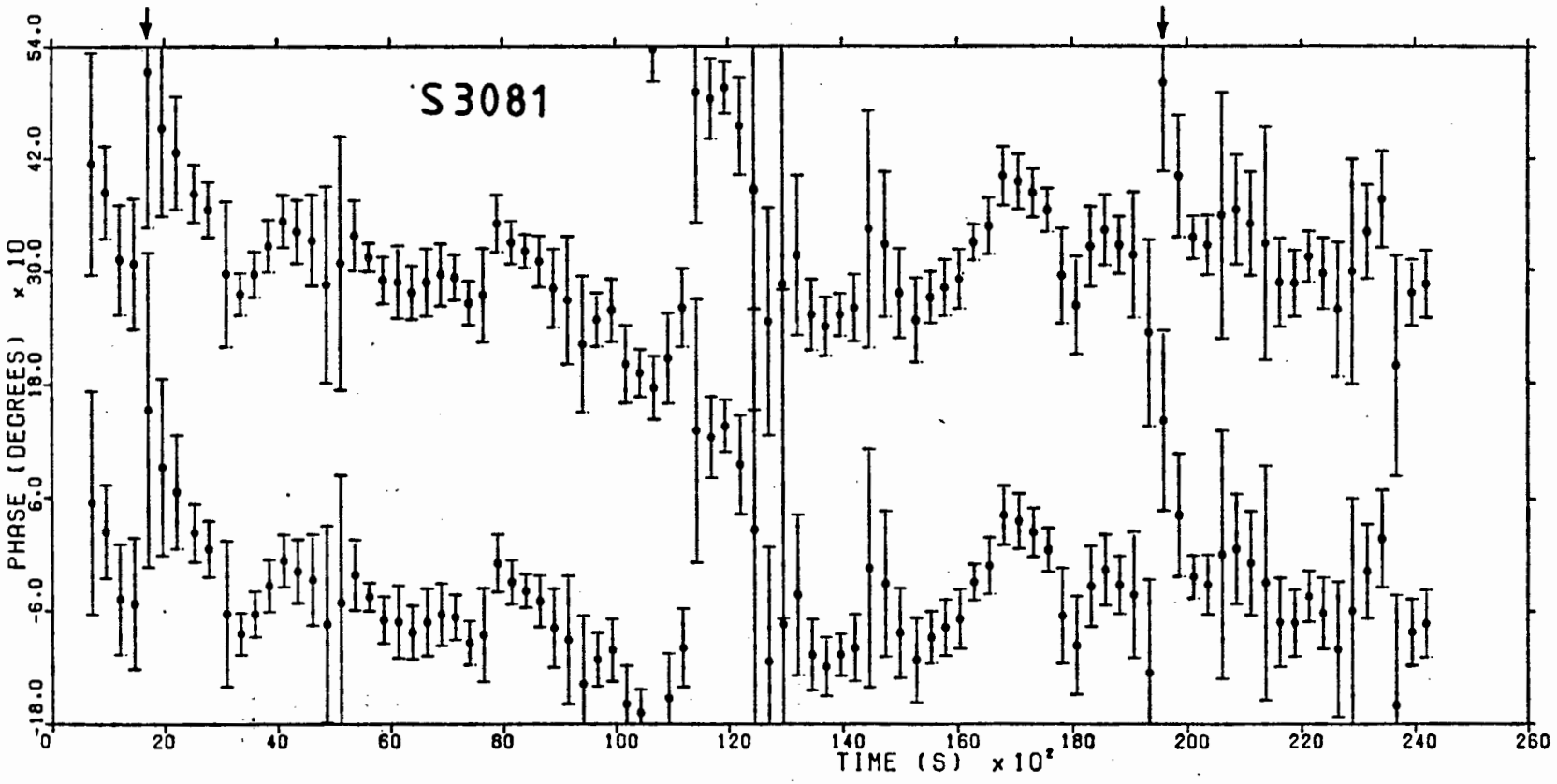

Figure 5.6 High-resolution phase variations in run S3081. Arrows indicate positions of the -360° phase changes.

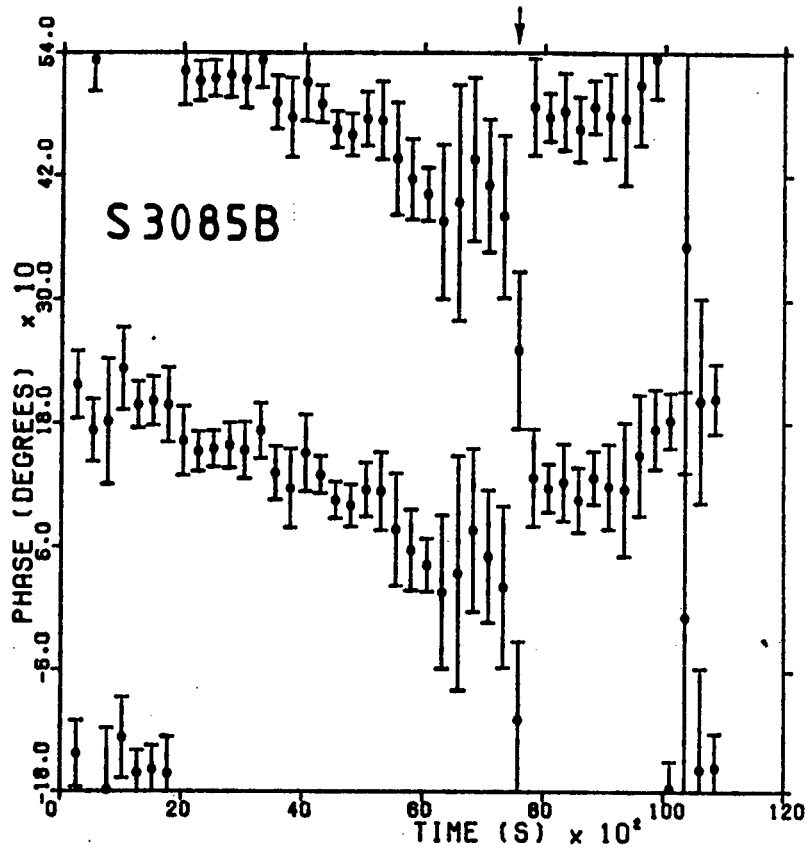

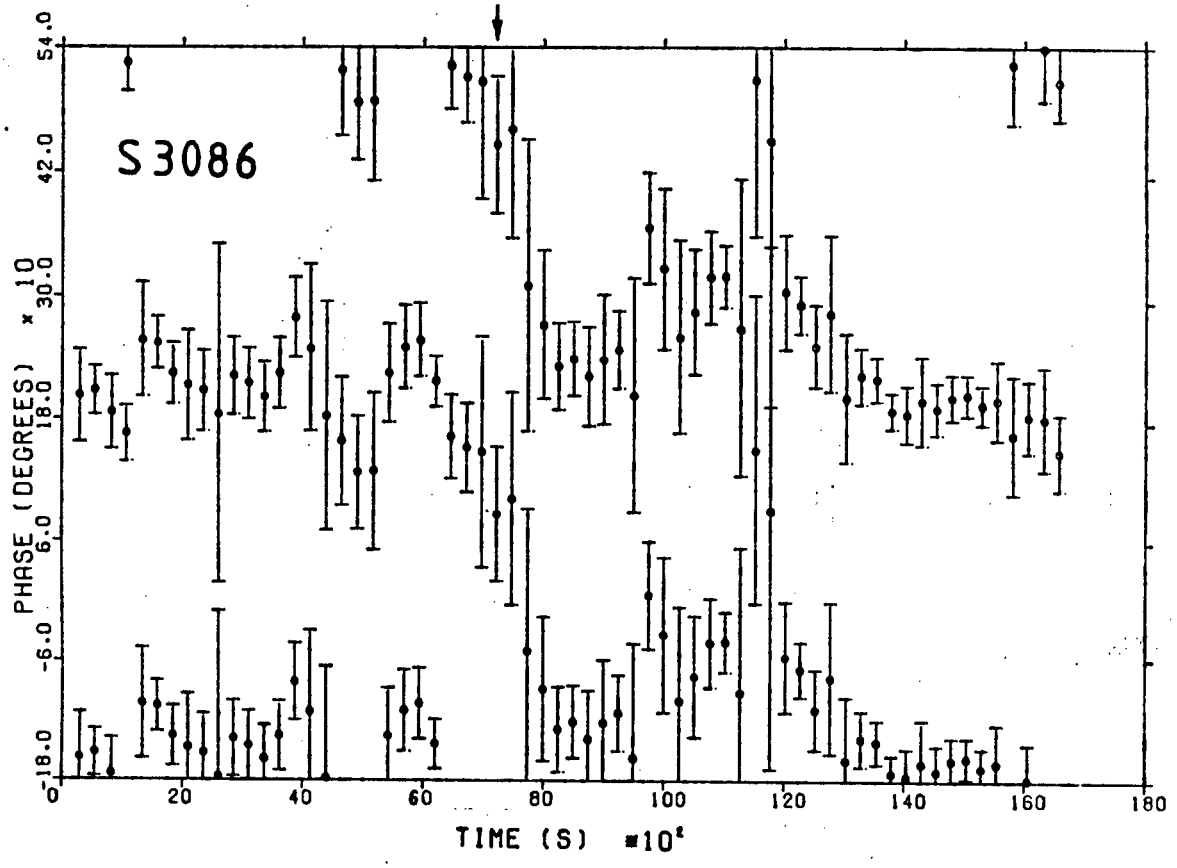

Figure 5.6 (cont.) High-resolution phase variations in runs S3085B and S3086. Arrows indicate positions of the -360° phase changes.

implies that the oscillation source is very small in relation to the disk. Further investigation of the data showed, however, that the occurrence times of the phase shifts are not correlated with any of the published orbital periods; nor are they consistent with an alternative period. Also, there is no apparent correspondence between the phase behaviour and the brightness of the system. At such high temporal resolution the ± 1 σ error bars in Fig 5.6 are unavoidably large, and this author concludes that the -360° phase shifts are probably not significant.

5.4 DISCUSSION

The rapid oscillations in CPD-48°1577 bear strong resemblance to the 9-s oscillations in the soft X-ray flux of SS Cyg. Comparison of Fig 5.6 with Fig 6 of Cordova et al [1980] reveals that both feature independent variation of amplitude and phase, and the nature of the phase variations is very similar in the two systems. Cordova et al find that the phase behaviour in SS Cyg is best modelled as a slow drift in period ($\dot{P} \sim 10^{-5}$ ss^{-1}) combined with a strong random walk due to white noise in this period. At low temporal resolution, CPD-48°1577 shows the same slow period drift of $\dot{P} \sim 10^{-5}$ ss^{-1} (Fig 5.5). This drift may be gradual and steady, or steplike, as in runs S3084 and S3245 respectively. Similar behaviour is seen in the SS Cyg oscillations, and also in the optical DNO's of VW Hyi at supermaximum (Warner and Brickhill [1978]). At high

resolution, CPD-48°1577 shows phase jitter that is qualitatively the same as that of SS Cyg. Quantitative comparison is difficult, since the statistical techniques employed by Cordova et al on X-ray oscillations with a mean amplitude of ~ 30% are not feasible when the amplitude is as low as 0.1%. Fig 5.6 shows less apparent phase jitter than Fig 6 of Cordova et al, but the latter shows independent subsections of four cycles, while the former shows subsections of twenty cycles with a 50% overlap. Increasing the resolution in CPD-48°1577 to a comparable level would yield unacceptably large error bars.

The SS Cyg soft X-ray data provide as yet unresolved constraints on models of oscillation generation (Cordova et al [1980], Chapter 3 of this work). Of great interest is the question of whether the optical oscillation is the tail of the X-ray oscillation spectrum or whether it is reprocessed X-ray radiation. The similarity in coherence and phase properties between the X-ray oscillations of SS Cyg and the optical oscillations of CPD-48°1577 suggests a similar mechanism operating in the two systems, and reinforces the desirability of simultaneous observations of CPD-48°1577 in both wavelength bands. A good opportunity for this may be offered by the Voyager 2 space probe, which has an ultraviolet spectrometer sensitive to radiation from 500 to 1700 Å, and can produce a spectrum every 4 seconds (O'Donoghue [1986]).

CHAPTER 6

Z CHAMAELEONTIS

6.1 INTRODUCTION

Z Cha is a well-studied member of the SU UMa sub-class of dwarf novae. Its special significance as a diagnostic tool arises because it is sufficiently inclined as seen from the earth ($i \sim 80^{\circ}$) to undergo steep-sided primary eclipses (Mumford [1971]). Warner [1974] first interpreted the asymmetrical eclipse profiles of Z Cha at quiescence to show that the eclipse is composite, involving occultation of the hot spot and the white dwarf primary. Until 1981, it was thought that Z Cha was unique in this respect; other CV's show eclipses of the hot spot only (eg. U Gem, EM Cyg) or the accretion disk as a whole (eg. UX UMa). However, since then composite eclipses have also been discovered in OY Car, HT Cas and V2051 Oph (Cook and Warner [1984]).

During outbursts, the eclipses in Z Cha change from being total (flat-bottomed) to partial (rounded), and the profiles become nearly symmetrical and significantly wider. Warner [1974] concludes that the luminostiy increase at outburst (and superoutburst) arises primarily from the disk, which brightens by ~ 3 magnitudes to become the dominant light source.

Detailed analysis of the eclipse profiles of Z Cha at quiescence yields estimates of the geometrical and photometric parameters of the system (Smak [1979], Vogt

[1981], Cook and Warner [1984]). Recently, Horne and Cook have used time-resolved spectrophotometry of the eclipses to construct a two-dimensional mapping of Z Cha in outburst (the method is described in Section 1.4). Thus the eclipses have proved to be a valuable probe into the detailed structure of the primary, disk and hot spot.

Rapid oscillations in Z Cha were first reported by Warner [1974] when the system was at supermaximum in January 1973. Since then, the gross features of Warner's light curves have been re-examined in detail by several authors (including Bath et al [1974], Bailey [1979], Smak [1979] and Vogt [1982]), in attempts to refine a physical model for the system. The present author has selected only those light curves which show the presence of oscillations, in the hope of determining any additional model restraints they may impose.

6.2 OBSERVATIONS

High-speed white light photometry of Z Cha, archived in the Astronomy Department at the University of Cape Town, has been examined in search of periodicities. The original observations have been reduced in the manner described in Chapter 4. The data span a 10-year observational period, and cover a range of brightness from quiescence ($m_v \sim 15$) to outburst ($m_v \sim 11.7$). Most of the data examined were recorded during or near outburst, at which time one would expect a higher probability of finding rapid oscillations,

based on their occurences in other dwarf novae. In Z Cha, normal outbursts are 3 days in duration and recur every 96 days on average, while superoutbursts last approximately 10 days and have a mean spacing of ~ 330 days (Dmitrienko et al [1984]).

Table 6.1 lists all runs included in the search for rapid oscillations. The reduced light curves have been passed through a Fast Fourier Transform program, and any periodicities noted. Those showing periodicities have been put through a polynomial removal of low-frequency trends (described in the following section), followed by a full Fourier Transform. Their periods and amplitudes are given in Columns 8 and 9 of the table. Column 10 gives the approximate luminosity state of Z Cha at the time of observation, as determined from the Circulars of the Variable Star Section of the Royal Astronomical Society of New Zealand.

6.3 RESULTS

Of the 24 runs examined, only two show evidence of periodicities. On both occasions Z Cha was near the end of a superoutburst; S0130 was recorded on the sixth day of maximum light, and S3079 saw the variable well into decline. Although the observations cover the latter parts of four separate superoutbursts in all, only two of these show oscillations. However, the oscillations may appear or disappear on timescales of ~ 10^3 s (Warner [1974] and

Table 6.1 Observations of Z Cha

Run No.	Date	$JD_{\odot}$ of Start (2 440 000+)	Telescope (m)	Integration Interval(s)	Number of Integrations	Duration of Run (hours)	Oscillation Period (s)	Oscillation Amplitude (mmag)	Luminosity State
S0107	08-12-1972	1660.43588	1.0	5.0	2460	3.42	-	-	Quiescent
S0109	10-12-1972	1661.50387	1.0	4.0	1510	1.68	-	-	Quiescent
S0130	08-01-1973	1691.41566	0.5	5.0	2793	3.88	27.7	2.0	Supermax
S0131	09-01-1973	1692.32444	0.5	5.0	1384	1.92	-	-	Supermax
S0132	09-01-1973	1692.44062	0.5	5.0	637	0.88	-	-	Supermax
S2739	19-02-1980	4289.33951	1.0	4.0	3965	4.41	-	-	Early decline
S2740	19-02-1980	4290.27536	1.0	5.0	2828	3.93	-	-	Early decline
S2742	23-02-1980	4293.26876	1.0	5.0	2278	3.16	-	-	Decline
S2745	24-02-1980	4294.40789	1.0	5.0	1290	1.79	-	-	Decline
S2748	25-02-1980	4295.42084	1.0	5.0	1304	1.81	-	-	Late decline
S2860	30-04-1981	4725.21547	0.75	10.0	1048	2.91	-	-	Supermax
S2863	02-05-1981	4727.29722	0.75	5.0	609	0.85	-	-	Early decline
S3068	14-12-1982	5318.45387	1.0	4.0	2720	3.02	-	-	Early decline
S3069	16-12-1982	5320.43509	1.0	4.0	3210	3.57	-	-	Decline
S3071	17-12-1982	5321.42800	1.0	4.0	2509	2.79	-	-	Decline
S3074	18-12-1982	5322.42094	1.0	4.0	2182	2.42	-	-	Decline
S3079	19-12-1982	5323.42366	1.0	4.0	3158	3.51	23.8	1.3	Late decline
S3314	04-05-1984	5825.25181	0.75	5.0	1416	1.97	-	-	Supermax
S3319	07-05-1984	5828.21543	0.75	5.0	1790	2.49	-	-	Supermax
S3321	08-05-1984	5829.23653	0.5	5.0	1291	1.79	-	-	Early decline
S3322	08-05-1984	5829.31207	0.5	5.0	530	0.74	-	-	Early decline
S3462	28-12-1984	6063.45667	0.75	5.0	2236	3.11	-	-	Supermax
S3465	30-12-1984	6065.42990	0.75	4.0	3345	3.72	-	-	Supermax
S3467	31-12-1984	6066.49322	0.75	4.0	2208	2.45	-	-	Supermax

Chapter 3 of this work), and could simply have escaped detection.

The two light curves are shown in Figure 6.1.

In order to use Fourier analysis on the oscillations in Z Cha, the gross trends in the light curve (particularly the eclipse) must first be removed. Four different numerical techniques have been used to do this, and the results compared for suitability. The first is a polynomial least-squares fitting technique, in which polynomials of a given order (in this case second) are fitted to successive non-overlapping sections of the data, and then subtracted from them. These sections were chosen to be ~ 3 cycles in length, sufficiently short to be well fitted by a second-order polynomial at any part of the light curve, yet just long enough to prevent subtraction of the rapid oscillations. The second technique also requires division of the light curve into non-overlapping sections of ~ 3 cycles each, but instead fits a series of cubic spline curves to the means of all the sections, before subtracting. The third is a smoothing and normalisation technique in which each datum is divided by the average of itself and its neighbours. Again, this characteristic "smoothing distance" was chosen to be ~ 3 oscillation cycles of the light curve. Fourth and last is the method of sum and difference filtering (eg. Jenkins and Watts [1969]). Each point on the light curve is added to (or subtracted from) the preceeding point. The effect of iterative addition is to remove the

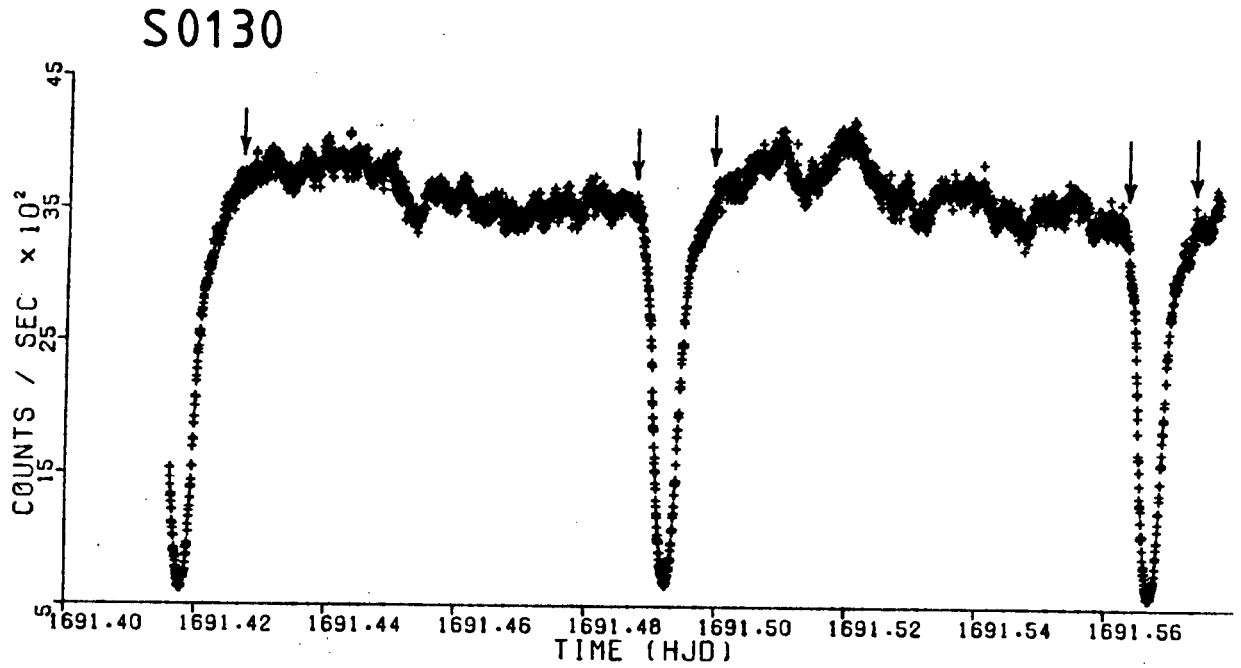

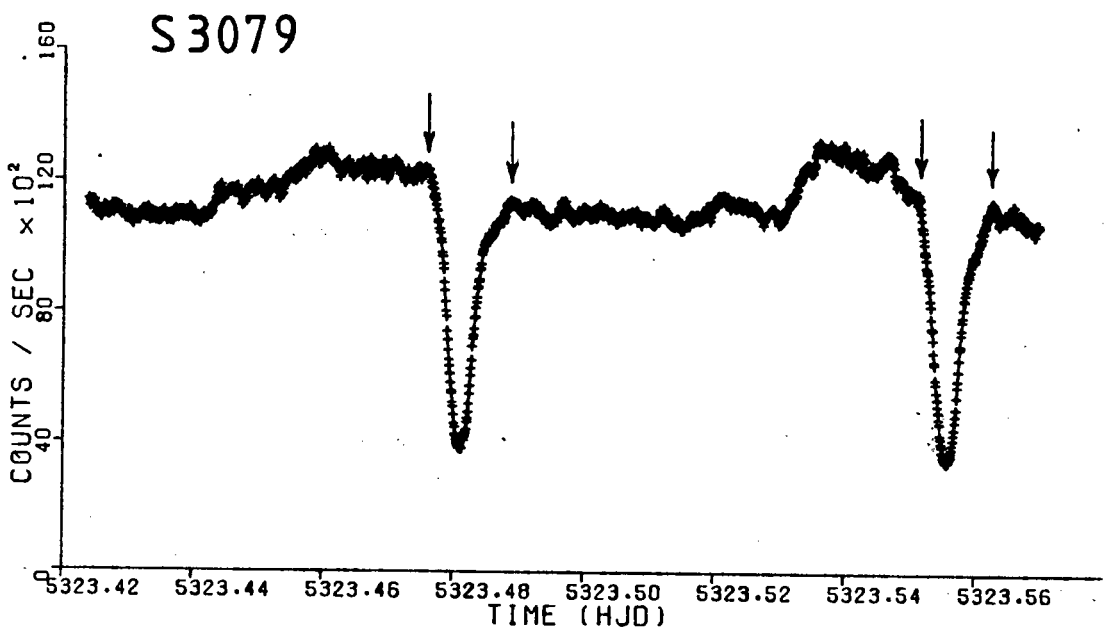

Figure 6.1 Light curves of the two Z Cha runs in which oscillations are present. Arrows indicate the beginning and end of eclipse.

high-frequency trends, while iterative subtraction smears out low-frequency variations. For m summations and n differencings, the result is a band-pass filter which gives maximum response at frequency

$$f_o = \frac{1}{2\pi} \text{ arc cos } \left(\frac{m-n}{m+n}\right)$$

and overall gain as a function of frequency given by

$$G_{m,n}(f) = 2^{m+n} (\cos \pi f)^m |\sin \pi f|^n, \quad -\tfrac{1}{2} \leq f \leq \tfrac{1}{2}$$

(Here f has been scaled so that f=1 is the Nyquist frequency.) In order to enhance the 27.7 s oscillations in run S0130, the values m=45 and n=16 were selected to give a band-pass filter with f_0=0.0342 Hz (29.2 s) and full width at half-maximum Δf=0.0126 Hz (from 24.3 s to 35.0 s). Similarly, m=35 and n=16 were chosen to enhance the 23.8 s oscillations in run S3079, with f_0=0.0473 Hz (21.2 s) and Δf=0.0188 Hz (from 17.7 s to 26.4 s).

Each of these techniques has been applied to the two runs on Z Cha showing rapid oscillations, and comparisons made between the results. As an example, Fig 6.2 shows the phase changes of the oscillations through the second eclipse of run S3079, after removal of low-frequency trends in one of the above-mentioned ways. The temporal resolution is

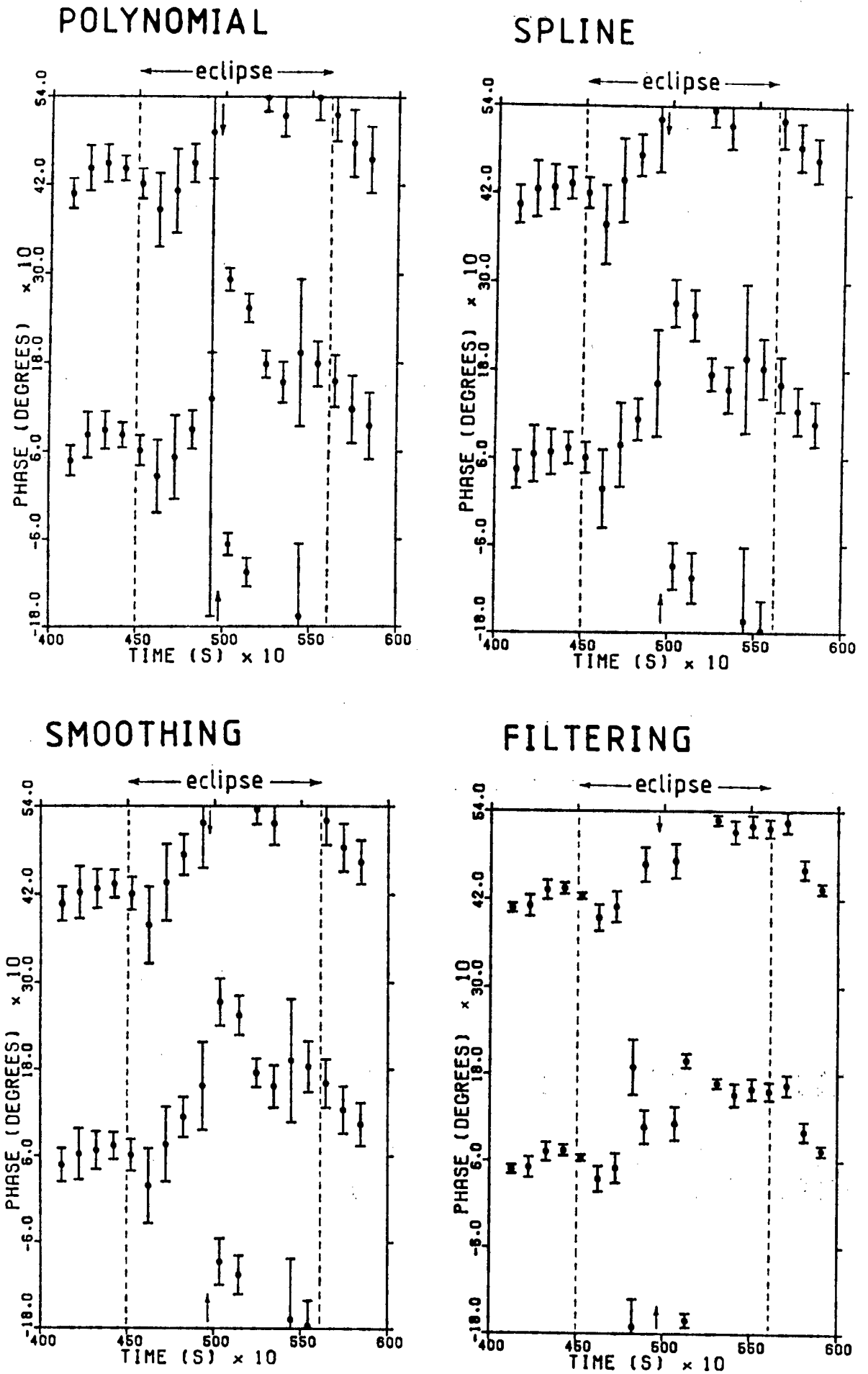

Figure 6.2 Phase changes of the rapid oscillations during the first eclipse of run S3079 showing the results of four different low-frequency filtering techniques. Arrows indicate light minima.

high; each point represents ~ 4.5 cycles, with an overlap of 50%. From the detailed similarity of the plots, it is clear that the four techniques have almost identical effects on the oscillations' phase behaviour. Even the ± 1 σ error bars are of similar height, except in the case of the filtered data, where they are reduced by a factor of approximately 2. This is not unexpected, since the sum and difference filtering technique is the only one to remove high, as well as low, frequencies from the data.

For the analysis of oscillations in Z Cha, we have thus chosen one of the methods as representative of the four. The polynomial fitting technique has been selected as one which gives a fairly realistic measure of the phase uncertainties and also leaves the oscillation amplitudes relatively undisturbed.

Figure 6.3 shows parts of the amplitude spectra of S0130 and S3079 after low-frequency trend removal. The oscillation amplitudes are 2.0 mmag and 1.3 mmag respectively.

The phase behaviour of the oscillations at relatively low temporal resolution is illustrated in Figures 6.4(a) and (b). Each data point represents approximately 30 cycles, and there is a 50% overlap between successive data chunks. It is clear from both the phase and amplitude graphs that for S0130 that the 28-second oscillations are strongly present during the first half of the run, disappear for nearly 15 minutes after the second eclipse, and finally

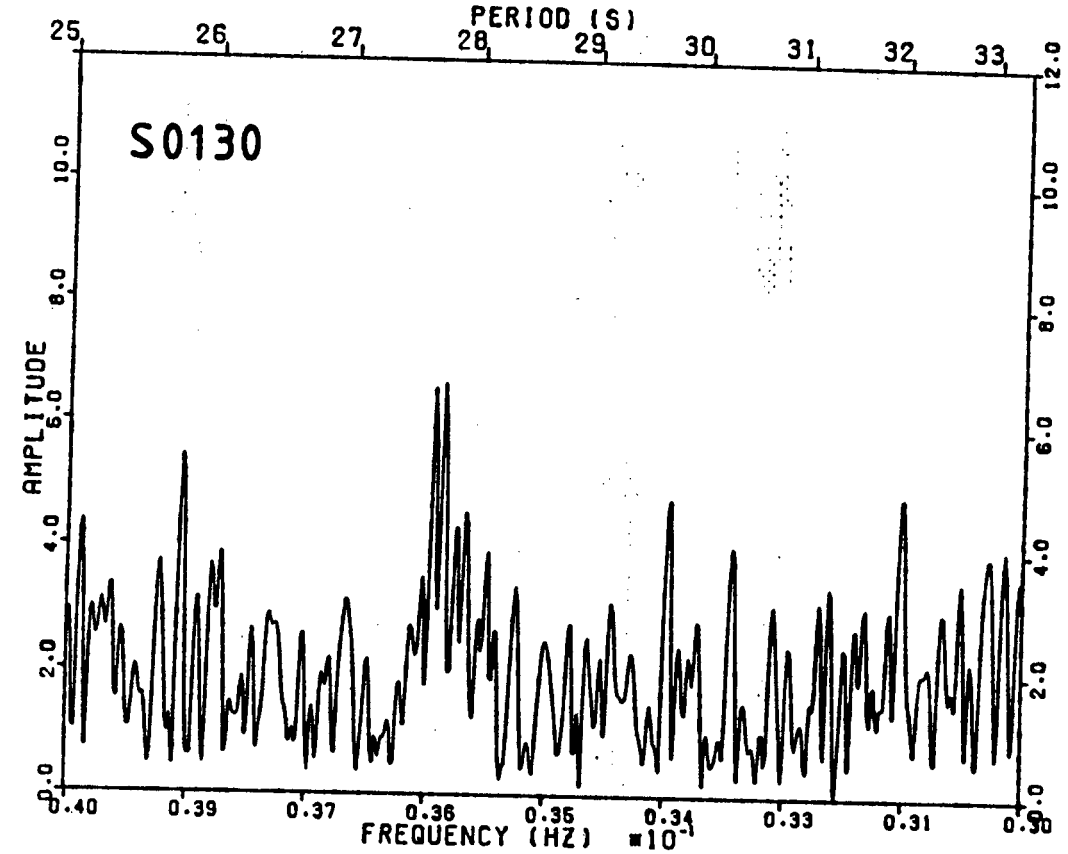

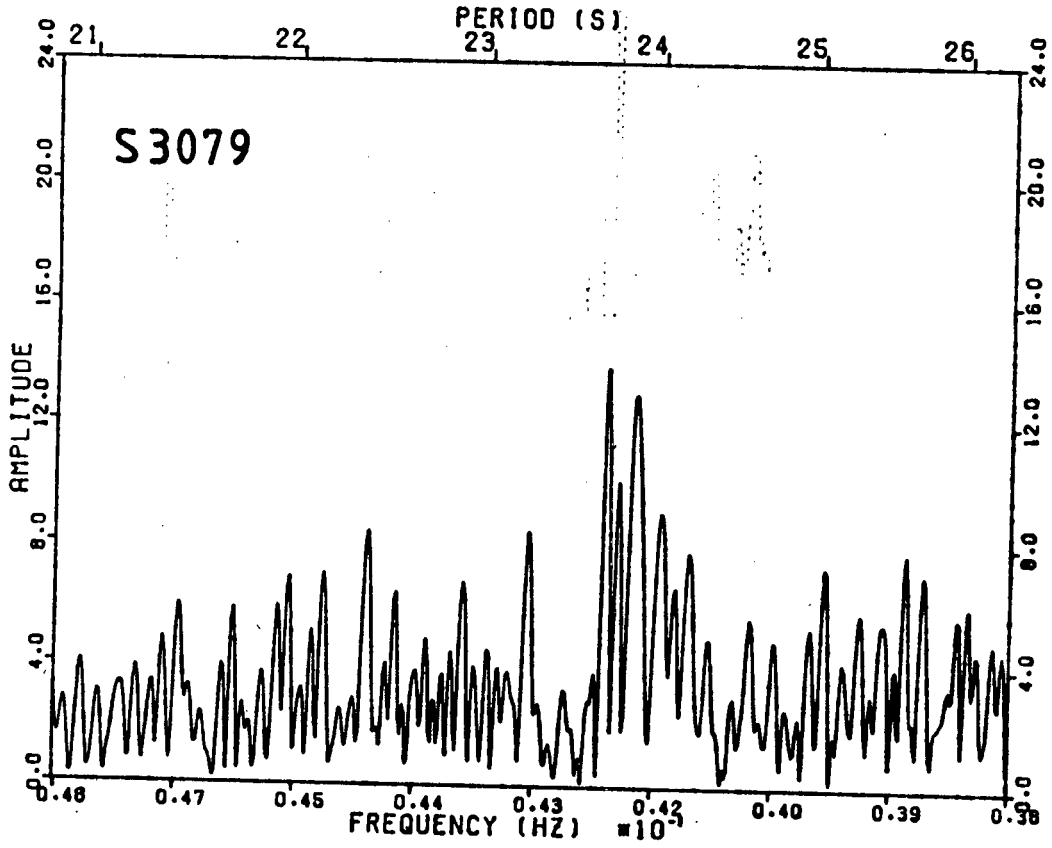

Figure 6.3 Amplitude spectra of runs S0130 and S3079 showing rapid oscillations with periods of 27.7 s and 23.8 s.

S0130

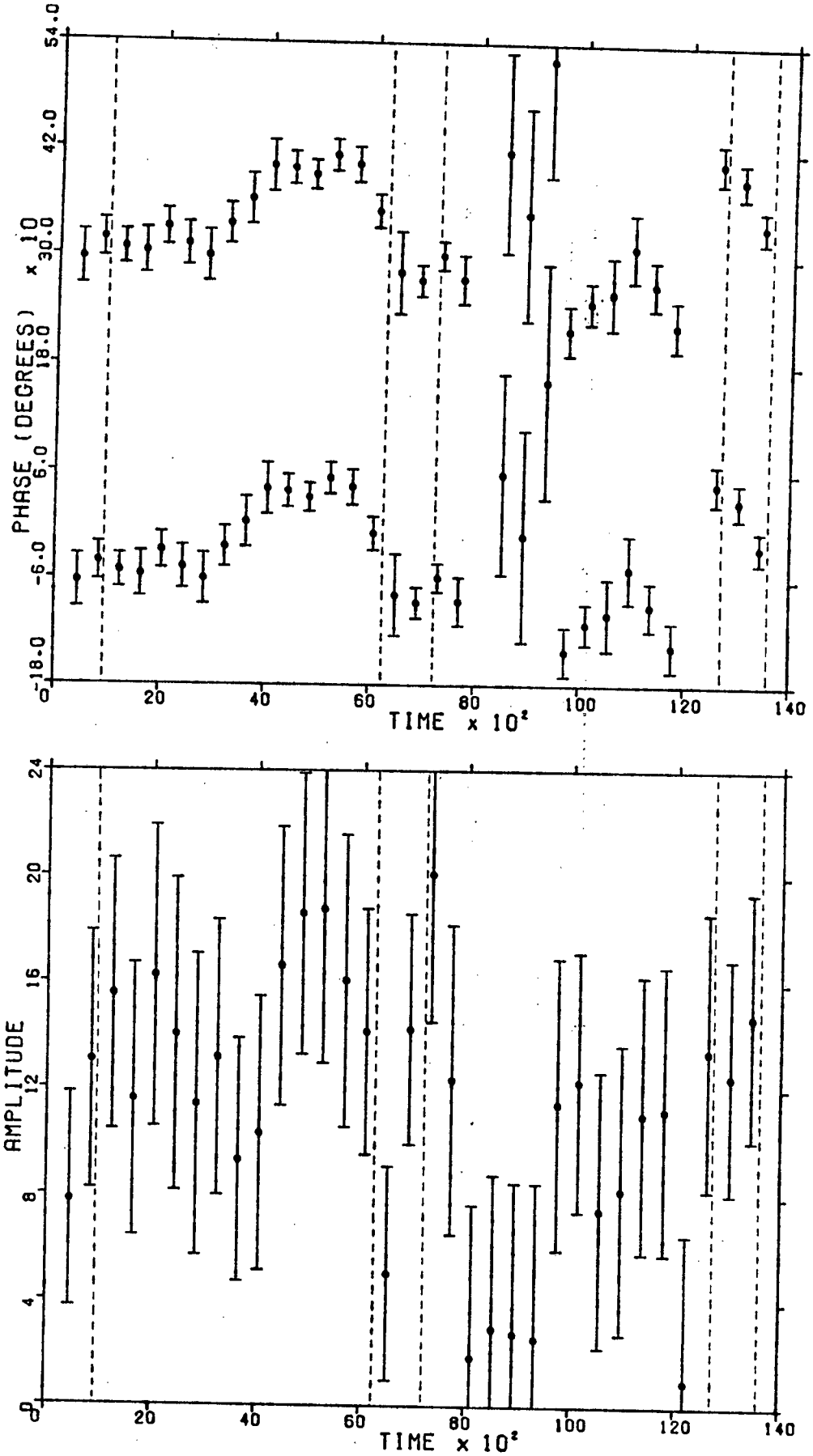

Figure 6.4(a) Variations of phase and amplitude during run S0130. Dashed lines indicate the beginning and end of eclipse.

S3079

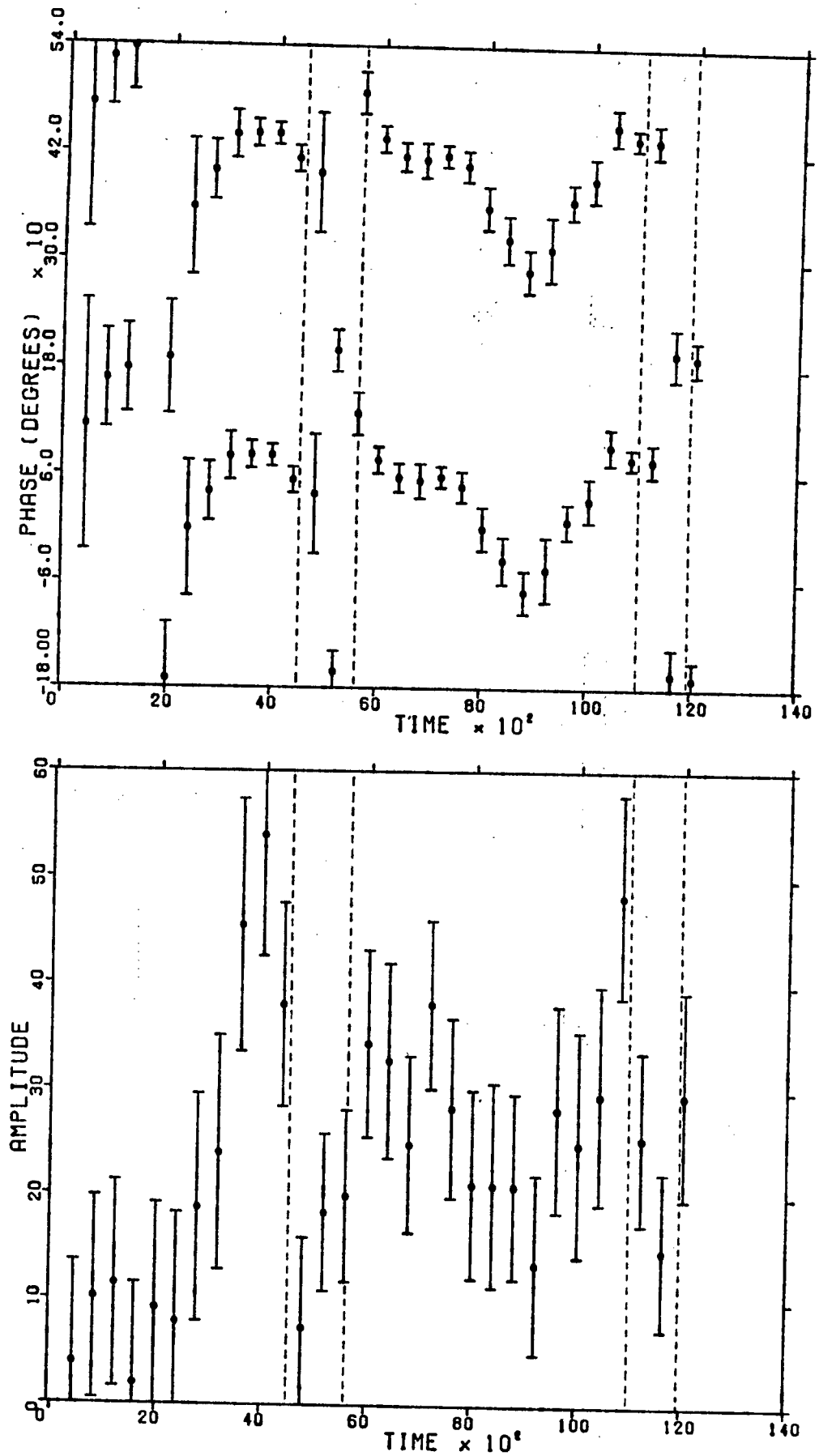

Figure 6.4(b) Variations of phase and amplitude during run S3079. Dashed lines indicate the beginning and end of eclipse.

return at somewhat lower amplitude. Run S3079 shows oscillations increasing in amplitude towards the first eclipse, and persisting thereafter. Where present, the oscillations show typical period coherence of one part in $\sim 10^4$.

At high temporal resolution, the oscillations show very interesting eclipse behaviour. Figures 6.5(a) and (b) show the variations of phase and amplitude during and near each of the five eclipses contained in runs S0130 and S3079. Each data point represents ~ 4.5 cycles, and there is a 50% overlap between successive data chunks. The times of eclipse ingress and egress, as marked by arrows in the light curves of Figure 6.1, are shown in these plots with vertical dotted lines. On occasion the oscillation amplitude within a 4.5-cycle subsection drops so low that a single point has a phase uncertainty greater than 320°. Such points have no statistical significance and tend to confuse the eye. For this reason, the fourth and fourteenth points of the first eclipse in run S0130, and the ninth point of the first eclipse of run S3079 have been omitted from the phase plots.

Although the phase plots are noisy, they appear to show repeatable features through eclipse. The second and third eclipses of run S0130 show a steady decrease in phase of nearly 180° from ingress to mid-eclipse, and a roughly symmetrical phase increase from mid-eclipse to egress. The degree of symmetry is difficult to gauge, as the eclipse shape is sensitive to choice of oscillation period. The

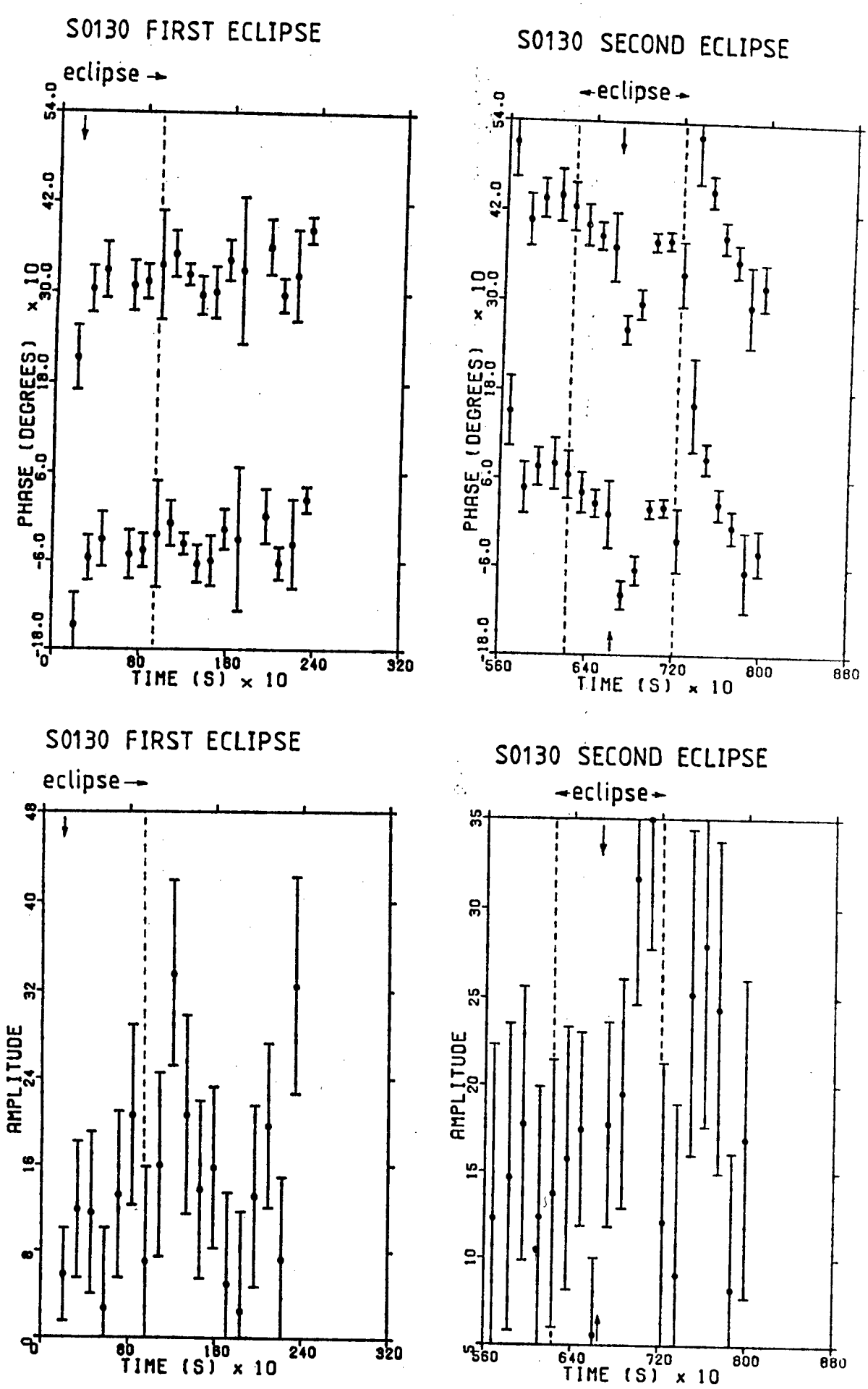

Figure 6.5(a) · Variations of phase and amplitude during first and second eclipses of run S0130. Arrows indicate light minima.

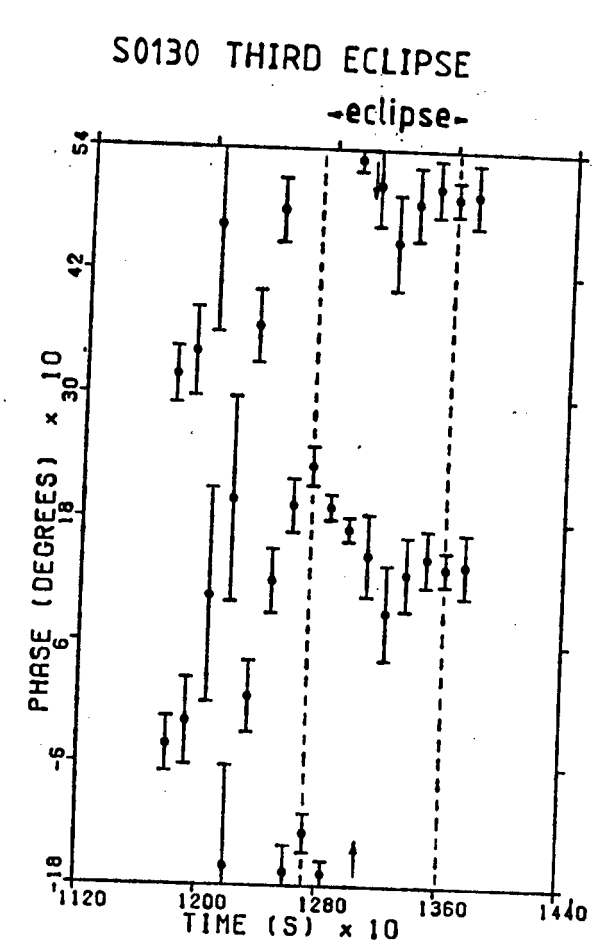

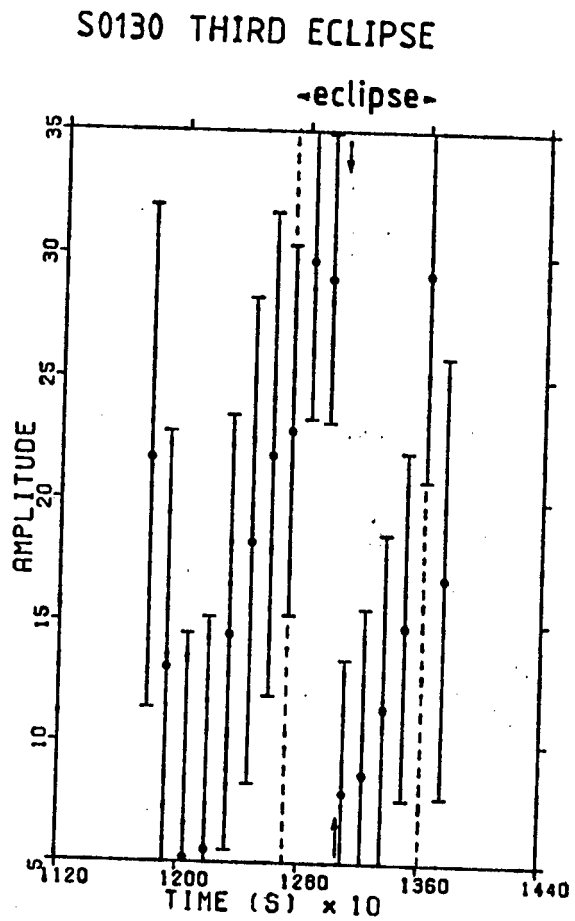

Figure 6.5(a) (cont.) Variations of phase and amplitude during third eclipse of run S0130. Arrows indicate light minima.

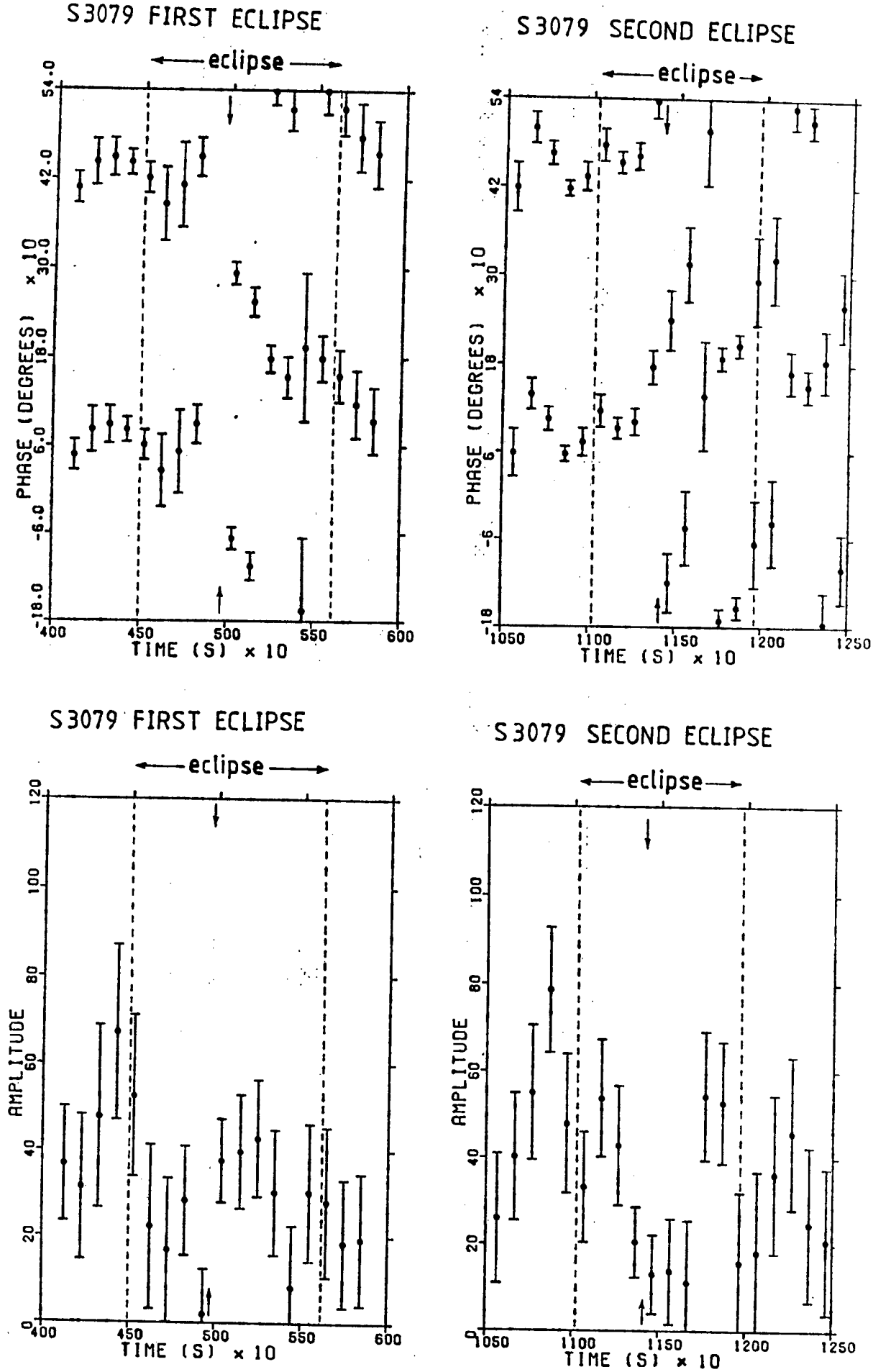

Figure 6.5(b) Variations of phase and amplitude during eclipses of run S3079. Arrows indicate light minima.

first eclipse of this run is also consistent with this phase pattern, although only the second half is available for comparison.

A different behaviour is seen in run S3079. Figure 6.2 shows that in the first eclipse the oscillation phase increases by about 200° from ingress to mid-eclipse, and decreases again from mid-eclipse to egress. The second eclipse (Figure 6.5(b)) is more ambiguous; the phase appears to jump by +180° or -180° at mid-eclipse. However, on the grounds that a 360° phase-shift is not seen in any of the other eclipses of Z Cha, we tentatively conclude that the phase jump from mid-eclipse is -180°, and thus that the second eclipse is qualitatively similar to the first.

It thus appears that the eclipse-related phase changes in Z Cha are repeatable within a run, but that they show longer-term variation. Interestingly, the phase patterns seen in these two runs seem very similar, except that the phase changes are of opposite sign. Such behaviour has not been seen in any other eclipsing cataclysmic variable.

6.4 DISCUSSION

Other than Z Cha, only three eclipsing cataclysmic variables are known to show coherent rapid oscillations, viz. UX UMa, HT Cas and DQ Her. In all four systems the oscillations show phase-shifts that are fully synchronous with eclipse. However, comparison of the Z Cha phase plots with Figure 6 of Nather and Robinson [1974], Figure 15 of

Patterson [1981] and Figure 6 of Patterson, Robinson and Nather [1978] shows that the eclipse-related phase-shifts in Z Cha are far less well defined than those of the other three systems. Table 6.2 lists the oscillation properties of these variables for comparison. The high quality of Nather and Robinson's phase plots is the result of a high sampling frequency and long eclipse duration (roughly proportional to the orbital period), so that the period of phase-shift is spanned by a total of 24 data points per eclipse. In addition, the repeatability of the phenomenon in UX UMa facilitates summations over many eclipses, as is shown in their Figure 6. By contrast, the eclipses in Z Cha are only 16 minutes long, and summation is unfeasible since the eclipses are few in number and feature phase-shifts of changing sign. Both Z Cha and HT Cas show a sharp decrease in oscillation amplitude during eclipse, presumably because the disk dominates the continuum light during outburst and the oscillations arise in the disk. This reduction in amplitude increases the uncertainty in oscillation phase during eclipse, and it is only the relative strength of the oscillations outside eclipse that give HT Cas the unambiguous phase plots shown in Patterson's Figure 15. In DQ Her the oscillations have a typical amplitude of 18 mmag, a factor of ten larger than those seen in Z Cha. Combined with a remarkably high coherence, this effect dominates considerations of period length and eclipse duration, and gives phase plots of very high quality except for the

Table 6.2 Comparison of the Eclipsing Cataclysmic Variables Showing Rapid Oscillations

	Z Cha	UX UMa	HT Cas	DQ Her
Orbital period (hours)	1.79	4.72	1.77	4.65
Eclipse duration (mins)	16	45	13	45
Period (s)	23.8, 27.7	28.5 - 30.0	20.25 - 20.45	71.07
Amplitude (mmag)	1.3 - 2.0	2.0	6.0	18
Amplitude decrease during eclipse	Yes	No	Yes	Yes
Coherence	10^4	10^5	10^5	10^{12}
Phase-shift during eclipse	Variable	- 360°	- 360°	+ 360°
Typical integration interval	4	3	9	4

~ 3 cycles at mid-eclipse where the amplitude drops to < 1 mmag. Clearly it is the low amplitude of the oscillations in Z Cha, combined with their somewhat lower coherence, which put the phase-shifts reported here very near the significance limit.

A further result of the low amplitude of the oscillations in Z Cha is that it is extremely difficult to test for a correlation between period and superhump phase. Such a correlation was found by Warner and Brickhill [1978] in one night's observations of V436 Cen at supermaximum. Inspection of Figures 6.1, 6.4(a) and 6.4(b) reveals a sudden decrease in oscillation period just less than halfway through the first orbital cycle of run S0130, well matched by the drop in the light curve at the end of the superhump. Thereafter, the oscillation amplitude becomes too low for period trends to be discernible. In run S3079, however, the correspondence between changes in period and brightness is poor, and, if anything, suggests an anti-correlation. Thus our results are inconclusive. It is interesting to note that O'Donoghue [1985] finds a correlation between period and superhump phase in V436 Cen on one night, but an equally good correlation between amplitude and superhump phase on the following night, and concludes that a consistent relationship has yet to be established.

Assuming that the eclipse-related phase changes in Z Cha are real, their interpretation requires a precise understanding of the generation mechanism of the

oscillations, and its relationship to the superoutburst phenomenon. At present even the nature of the simplest and best-studied eclipsing oscillator, DQ Her, is not fully understood. O'Donoghue [1985] points out that Petterson's [1980] success in modelling the behaviour of its oscillations is limited to the eclipse region of the light curve, and that the variations in amplitude and phase around the whole orbital cycle have yet to be successfully explained. O'Donoghue attempts to fit the data using an improvement on Chester's [1979] model, which proposes a disk rim of variable thickness due to the bulge of material arising at the hot spot. After varying the size, shape, position and albedo of the bulge, as well as the disk thickness and inclination angle, O'Donoghue concludes that the model is seriously flawed.

Clearly a fully successful oscillation model has yet to appear.

CHAPTER 7

CONCLUSION

Rapid oscillations in cataclysmic variables have been studied since their discovery in DQ Her by Walker [1954]. The number of systems in which rapid oscillations have been observed is now over 30, and yet their nature remains obscure. The extremely high coherences of the DQ Her variables argue strongly in favour of a rotational origin, and models featuring reflection and/or reprocessing of a rotating X-ray beam (eg. Warner [1985a]) seem most promising in explaining these and slightly less coherent sources. However, the most common oscillations, those found in the dwarf novae and some nova-like variables, have coherences too low to be explained by this model and may exhibit random walks in phase on puzzlingly short timescales. Neither pulsation nor rotation models have yet been able to fully account for the period changes in these oscillations.

Since the late 1970's, X-ray satellites such as the Einstein Observatory have provided a further window onto the oscillation mechanism in CV's. In particular, the detection of rapid oscillations in the hard and soft X-ray fluxes of seven systems has encouraged efforts to match intensity variations in both wavebands. While this has been possible with AE Aqr (Patterson et al [1980]), the results are consistent with either a directly observed blackbody spectrum or disk-reprocessed radiation from a much hotter

source. Such ambiguity is not resolved by data from the six other systems, which show poor correlation of period and coherence between their optical and X-ray oscillations. Most puzzling are the quasi-periodic X-ray oscillations in SS Cyg, which, if simultaneous with the coherent optical oscillations, would imply two distinct oscillation mechanisms. To resolve this difficulty, and to determine the degree of reprocessing in oscillating CV's, simultaneous photometry in several wavebands is required. In this regard, CPD-48^{o}1577 may prove especially useful as a very bright system with a high occurrence of coherent oscillations.

The phase behaviour of rapid oscillations through eclipse provides a potentially powerful diagnostic tool. DQ Her, UX UMa, HT Cas and Z Cha are all eclipsing systems which show characteristic phase changes during eclipse. In addition, the duration of these phase changes is in each case the same as the total duration of eclipse, implying participation of the whole disk in the oscillation phenomenon. The similar natures of the phase-shifts is remarkable, since these variables are members of different CV subclasses and their oscillations differ greatly in coherence and frequency of occurrence. It seems probable that similar oscillation mechanisms are operating in these stars, and thus that a successful model of one system might have application to many others. Unfortunately, even the

simplest of these, DQ Her, is not yet fully understood (O'Donoghue [1985]).

The phase behaviour seen in oscillations of Z Cha at supermaximum is particularly complex, showing significant long-term variation. These observations should provide useful model restrictions once a satisfactory model is developed for simpler systems.

A satisfactory model should also account for the appearance and disappearance of oscillations on various timescales in various systems. Warner [1986a] suggests that the occurrence of such changes in CPD-48^{o}1577 on timescales of hours may imply that the oscillations are easily obscured. In addition, they may go undetected in shorter runs because of their low amplitudes in many CV's. However, the striking absence of oscillations in dwarf novae at quiescence points to a more fundamental relationship between outburst state and oscillation amplitude. This is reinforced by the well-known period-luminosity correlation, and also a correlation between coherence and luminosity in some systems (O'Donoghue [1985]). Observations of VW Hyi (Warner [1976]) have shown the appearance of oscillations with similar periods at similar brightnesses, irrespective of whether the variable is at maximum or supermaximum. Z Cha, on the other hand, has only shown oscillations near the end of a superoutburst. Thus the degree of structural similarity between the two outburst states is not yet clear.

The classification of oscillations into "coherent" and "quasi-periodic" appears to be somewhat unsatisfactory, as the soft X-ray oscillations in SS Cyg (Cordova et al [1980]) feature high period stability but low phase coherence. More recently, similar oscillations have been found in the optical light curves of the nova-like variable CPD-48°1577 and the dwarf nova PS74 (O'Donoghue [1985]). In the latter system, the oscillations at maximum and supermaximum are apparently indistinguishable. While these results do not obviously discriminate between the various pulsational and rotational models of oscillation, they do support the disk instability theory of dwarf nova outburst, and suggest stationary accretion flow as the trigger of the oscillations.

REFERENCES

Bailey, J., 1975. *J. Br. astr. Assoc., 86,* 30.

Bailey, J., 1979. *Mon. Not. R. astr. Soc., 187,* 645.

Bailey, J., 1985. *Recent Results on Cataclysmic Variables, ESA SP-236,* p.139, ESTEC, Noordwijk, Holland.

Bailey, J., Watts, D.J., Sherrington, M.R., Axon, D.J., Giles, A.B., Hanes, D.A., Heathcote, S.R., Hough, J.H., Hughes, S., Jameson, R.F. & McLean, I., 1985. *Mon. Not. R. astr. Soc., 215,* 179.

Barlow, M.J., Brodie, J.P., Brunt, C.C., Hanes, D.A., Hill, P.W., Mayo, S.K., Pringle, J.E., Ward, M.J., Watson, M.G., Whelan, J.A.J. & Willis, A.J., 1981. *Mon. Not. R. astr. Soc., 195,* 61.

Barrett, P.E. & Chanmugan, G., 1984a. *Astrophys. J., 278,* 298.

Barrett, P.E. & Chanmugan, G., 1984b. *Mon. Not. R. astr. Soc., 210,* 15P.

Bastian, T.S., Dulk, G.A. & Chanmugan, G., 1985. *Cataclysmic Variables and Low-Mass X-ray Binaries,* p.231, eds Lamb, D.Q. & Patterson, J., Reidel, Dordrecht, Holland.

Bath, G.T., 1973. *Nature Phys. Sci., 246,* 84.

Bath, G.T., 1975. *Mon. Not. R. astr. Soc., 171,* 311.

Bath, G.T., Edwards, A.C. & Mantle, V.J., 1983a. *Cataclysmic Variables and Related Objects,* p.55, eds Livio, M & Shaviv, G., Reidel, Dordrecht, Holland.

Bath, G.T., Edwards, A.C. & Mantle, V.J., 1983b. *Cataclysmic Variables and Related Objects*, p.69, eds Livio, M & Shaviv, G., Reidel, Dordrecht, Holland.

Bath, G.T., Evans, W.D., Papaloizou, J. & Pringle, J.E., 1974. *Mon. Not. R. astr. Soc.*, *169*, 447.

Bath, G.T. & Pringle, J.E., 1981. *Mon. Not. R. astr. Soc.*, *194*, 967.

Bath, G.T. & Pringle, J.E., 1982. *Mon. Not. R. astr. Soc.*, *199*, 267.

Bath, G.T. & Pringle, J.E., 1985. *Interacting Binary Stars*, p.177, eds Pringle, J.E. & Wade, R.A., Cambridge University Press, Cambridge, Great Britain.

Bath, G.T. & Shaviv, G., 1976. *Mon. Not. R. astr. Soc.*, *175*, 305.

Bath, G.T. & van Paradijs, J., 1983. *Nature*, *305*, 33.

Bianchini, A., Hamzaoglu, E. & Sabbadin, F., 1981. *Astr. Astrophys.*, *99*, 392.

Bode, M.F. & Evans, A., 1980. *Astr. Astrophys.*, *89*, 158.

Bode, M.F. & Evans, A., 1981. *Mon. Not. R. astr. Soc.*, *197*, 1055.

Bode, M.F. & Evans, A., 1983a. *Mon. Not. R. astr. Soc.*, *203*, 285.

Bode, M.F. & Evans, A., 1983b. *Q. J. R. astr. Soc.*, *24*, 83.

Bode, M.F., Evans, A., Whittet, D.C.B., Aitken, D.K., Roche, P.F. & Whitmore, B., 1984. *Mon. Not. R. astr. Soc.*, *207*, 897.

Böhnhardt, H., Dreschel, H., Rahe, J. & Wargau, W., 1982. *IAU Circ. No. 3749.*

Bonnet-Bidaud, J.M., Beuermann, K., Charles, P., Marasch, L., Motch, C., Mouchet, M., Osborne, J., Tanzi, E. & Treves, A., 1985. *Recent Results on Cataclysmic Variables, ESA SP-236,* p.155, ESTEC, Noordwijk, Holland.

Bonnet-Bidaud, J.M., Motch, C. & Mouchet, M., 1985. *Astr. Astrophys., 143,* 313.

Campbell, C.G., 1984. *Mon. Not. R. astr. Soc., 211,* 69.

Cannizzo, J.K., Ghosh, P. & Wheeler, J.C., 1982. *Astrophys. J., 260,* L83.

Chester, T.J., 1979. *Astrophys. J., 230,* 167.

Clarke, C.J., Mantle, V.J. & Bath, G.T., 1985. *Mon. Not. R. astr. Soc., 215,* 149.

Clayton, D.D. & Wickramasinghe, N.C., 1976. *Astr. Astrophys., 42,* 463.

Cook, M.C. & Warner, B., 1984. *Mon. Not. R. astr. Soc., 207,* 705.

Cordova, F.A., Chester, T.J., Mason, K.O., Kahn, S.M. & Garmire, G.P., 1984. *Astrophys. J., 278,* 739.

Cordova, F.A., Chester, T.J., Tuohy, I.R. & Garmire, G.P., 1980. *Astrophys. J., 235,* 163.

Cordova, F.A. & Mason, K.O., 1982. *Pulsations in Classical and Cataclysmic Variable Stars,* p.23, eds Cox, J.P. & Hansen, C.J., JILA, Boulder, Colorado, U.S.A.

Cordova, F.A. & Mason, K.O., 1983. *Accretion-driven Stellar X-ray Sources*, p.147, eds Lewin, W.H.G. & van den Heuvel, E.P.J., Cambridge University Press, Cambridge, Great Britain.

Cox, J.P., 1981. *Astrophys. J., 247*, 1070.

Cox, J.P. & Everson, B.L., 1982. *Pulsations in Classical and Cataclysmic Variable Stars*, p.42, eds Cox, J.P. & Hansen, C.J., JILA, Boulder, Colorado, U.S.A.

Crawford, J.A. & Kraft, R.P., 1956. *Astrophys. J., 123*, 44.

Cropper, M., 1985a. *Mon. Not. R. astr. Soc., 212*, 709.

Cropper, M., 1985b. *Ph.D. Thesis*, University of Cape Town, South Africa.

Cropper, M., Menzies, J.W. & Tapia, S., 1986. *Mon. Not. R. astr. Soc., 218*, 201.

Deeming, T.J., 1975. *Astrophys. Sp. Sci., 36*, 137.

Dmitrienko, E.S., Matrienko, A.N., Cherepashchuk, A.M. & Yagola, A.G., 1984. *Soviet Astr., 28*, 180.

Eggen, O.J. & Niemela, V.S., 1984. *Astr. J., 89*, 389.

Eggleton, P., 1976. *Structure and Evolution of Close Binary Systems, IAU Symp. 73*, p.209, eds Eggleton, P., Mitton, S. & Whelan, J., Reidel, Dordrecht, Holland.

Elvey, C.T. & Babcock, H.W., 1943. *Astrophys. J., 97*, 412.

Fabian, A.C., Pringle, J.E. & Rees, M.J., 1976. *Mon. Not. R. astr. Soc., 175*, 43.

Faulkner, J., 1976. *Structure and Evolution of Close Binary Systems, IAU Symp. 73*, p.193, eds Eggleton, P., Mitton, S. & Whelan, J., Reidel, Dordrecht, Holland.

Faulkner, J., Flannery, B.P. & Warner, B., 1972. *Astrophys. J., 175*, L79.

Faulkner, J., Lin, D.N.C. & Papaloizou, J., 1983. *Mon. Not. R. astr. Soc., 205*, 359.

Frank, J., King, A.R., Sherrington, M.R., Jameson, R.F., & Axon, D.J., 1981. *Mon. Not. R. astr. Soc., 195*, 505.

Gallagher, J.S. & Oinas, V., 1974. *Publ. astr. Soc. Pacific, 86*, 952.

Gallagher, J.S. & Starrfield, S., 1978. *Ann. Rev. Astr. Astrophys., 16*, 171.

Garrison, R.F., Hiltner, W.A. & Schild, R.E., 1982. *IAU Circ. No. 3730.*

Garrison, R.F., Schild, R.E., Hiltner, W.A. & Krzeminski, W., 1984. *Astrophys. J., 276*, L13.

Gehrz, R.D., Grasdalen, G.L. & Hackwell, J.A., 1980. *Astrophys. J., 237*, 855.

Ghosh, P. & Lamb, F.K., 1979a. *Astrophys. J., 232*, 259.

Ghosh, P. & Lamb, F.K., 1979b. *Astrophys. J., 234*, 296.

Gilliland, R.L., 1985. *Astrophys. J., 292*, 522.

Greenstein, J.L., 1957. *Astrophys. J., 126*, 23.

Hameury, J.M., King, A.R. & Lasota, J.P., 1985. *Recent Results on Cataclysmic Variables, ESA SP-236*, p.167, ESTEC, Noordwijk, Holland.

Hartwick, F.D.A. & Hutchings, J.B., 1978. *Astrophys. J., 226*, 203.

Hassall, B.J.M., Pringle, J.E., Ward, M.J., Whelan, J.A.J., Mayo, S.K., Echevarria, J., Jones, D.H.P., Wallis, R.E., Allen, D.A. & Hyland, A.R., 1981. *Mon. Not. R. astr. Soc., 197*, 275.

Hildebrand, R.H., Spillar, E.J. & Stiening, R.F., 1981. *Astrophys. J., 248*, 268.

Horne, K., 1984. *Nature, 312*, 348.

Horne, K., 1985. *Mon. Not. R. astr. Soc., 213*, 129.

Horne, K. & Cook, M.C., 1985. *Mon. Not. R. astr. Soc., 214*, 307.

Hutchings, J.B., Crampton, D., Cowley, A.P., Thorstensen, J.R. & Charles, P.A., 1981. *Astrophys. J., 249*, 680.

Jameson, R.F., King, A.R. and Sherrington, M.R., 1981. *Mon. Not. R. astr. Soc., 195*, 235.

Jenkins, G.M. & Watts, D.G., 1969. *Spectral Analysis and its Applications*, p.297, Holden-Day, San Francisco, U.S.A.

Joy, A.H., 1956. *Astrophys. J., 124*, 317.

Kato, M., 1983. *Astrophys. Sp. Sci., 99*, 295.

Kenyon, S.J. & Truran, J.W., 1983. *Astrophys. J., 273*, 280.

King, A.R., 1985. *Recent Results on Cataclysmic Variables, ESA SP-236*, p.133, ESTEC, Noordwijk, Holland.

King, A.R., Frank, J. & Ritter, H., 1985. *Mon. Not. R. astr. Soc., 213*, 181.

King, A.R. & Lasota, J.P., 1984. *Astr. Astrophys., 140*, L16.

King, A.R. & Shaviv, G., 1984a. *Nature, 308*, 519.

King, A.R. & Shaviv, G., 1984b. *Mon. Not. R. astr. Soc., 211*, 883.

Kippenhahn, R. & Thomas, H.C., 1978. *Astr. Astrophys., 63,* 265.

Kraft, R.P., Krzeminski, W. & Mumford, G.S., 1969. *Astrophys. J., 158,* 589.

Kruszewski, A., 1964. *Acta astr., 14,* 231.

Kukarkin, B.V. & Parenago, P.P., 1934. *Perem. Zvezdy, 4,* 251.

Kwok, S., 1983. *Mon. Not. R. astr. Soc., 202,* 1149.

Lamb, D.Q., 1985. *Cataclysmic Variables and Low-Mass X-ray Binaries,* p.179, eds Lamb, D.Q. & Patterson, J., Reidel, Dordrecht, Holland.

Lamb, D.Q. & Patterson, J., 1983. *Cataclysmic Variables and Related Objects,* p.229, eds Livio, M & Shaviv, G., Reidel, Dordrecht, Holland.

Lamb, F.K., Aly, J.-J., Cook, M.C. & Lamb, D.Q., 1983. *Astrophys. J., 274,* L71.

Liang, E.P.T. & Price, R.H., 1977. *Astrophys. J., 218,* 247.

Liebert, J. & Stockman, H.S., 1985. *Cataclysmic Variables and Low-Mass X-ray Binaries,* p.151, eds Lamb, D.Q. & Patterson, J., Reidel, Dordrecht, Holland.

Lin, D.N.C., Papaloizou, J. & Faulkner, J., 1985. Mon. Not. R. astr. Soc., *212,* 105.

Livio, M. & Soker, N., 1984. *Mon. Not. R. astr. Soc., 208,* 783.

Lubow, S.H. and Shu, F.H., 1975. *Astrophys. J., 198,* 383.

Lynden-Bell, D. & Pringle, J.E., 1974. *Mon. Not. R. astr. Soc., 168,* 603.

MacDonald, J., 1983. *Astrophys. J., 267,* 732.

Mateo, M., Szkody, P. & Hutchings, J., 1985. *Astrophys. J., 288,* 292.

Mayall, M.W., 1965. *J. R. astr. Soc. Can., 59,* 285.

Meyer, F., 1984. *Astr. Astrophys., 131,* 303.

Meyer, F. & Meyer-Hofmeister, E., 1981. *Astr. Astrophys., 104,* L10.

Meyer, F. & Meyer-Hofmeister, E., 1983. *Astr. Astrophys., 121,* 29.

Middleditch, J. & Cordova, F.A., 1982. *Astrophys. J., 255,* 585.

Mitchell, R.M. & Evans, A., 1984. *Mon. Not. R. astr. Soc., 209,* 945.

Motch, C. & Pakull, M.W., 1981. *Astr. Astrophys., 101,* L9.

Mumford, G.S., 1971. *Astrophys. J., 165,* 369.

Mustel, E.R., 1974. *Vistas in Astronomy, 16,* 260.

Nariai, K., Nomoto, K. & Sugimoto, D., 1980. *Publ. astr. Soc. Japan, 32,* 473.

Nather, R.E. & Robinson, E.L., 1974. *Astrophys. J., 190,* 637.

Nather, R.E. & Warner, B., 1971. *Mon. Not. R. astr. Soc. 152,* 209.

O'Donoghue, D., 1985. *Proceedings of the 9th North American Cataclysmic Variables Workshop,* University of Washington, Seattle, U.S.A.

O'Donoghue, D., 1986. *Private communication.*

Oke, J.B. & Wade, R.A., 1982. *Astr. J., 87,* 670.

Osaki, Y., 1974. *Publ. astr. Soc. Japan, 26,* 429.

Osaki, Y., 1985. *Astr. Astrophys., 144,* 369.

Paczyński, B., 1967. *Acta astr., 17,* 286.

Papaloizou, J., Faulkner, J. & Lin, D.N.C., 1983. *Mon. Not. R. astr. Soc., 205,* 487.

Papaloizou, J. & Pringle, J.E., 1978. *Mon. Not. R. astr. Soc., 182,* 423.

Papaloizou, J. & Pringle, J.E., 1979. *Mon. Not. R. astr. Soc., 189,* 293.

Papaloizou, J.C.B. & Pringle, J.E., 1985. *Mon. Not. R. astr. Soc., 217,* 387.

Patterson, J., 1980. *Astrophys. J., 241,* 235.

Patterson, J., 1981. *Astrophys. J. Suppl. Ser., 45,* 517.

Patterson, J., 1984. *Astrophys. J. Suppl. Ser., 54,* 443.

Patterson, J., 1985. *Cataclysmic Variables and Low-Mass X-ray Binaries,* p.281, eds Lamb, D.Q. & Patterson, J., Reidel, Dordrecht, Holland.

Patterson, J., Branch, D., Chincarini, G. & Robinson, E.L., 1980. *Astrophys. J., 240,* L133.

Patterson, J. & Price, C., 1981. *Astrophys. J., 243,* L83.

Patterson, J. & Raymond, J.C., 1985. *Astrophys. J., 292,* 535.

Patterson, J., Robinson, E.L. & Nather, R.E., 1978. *Astrophys. J., 224,* 570.

Penning, W.R., 1984. *Prepr. Steward Obs. No. 543.*

Petterson, J.A., 1980. *Astrophys. J., 241,* 247.

Petterson, J.A., 1983. *Accretion-driven Stellar X-ray Sources*, p.367, eds Lewin, W.H.G. & van den Heuvel, E.P.J., Cambridge University Press, Cambridge, Great Britain.

Plavec, M., 1968. *Adv. Astr. Astrophys., 6*, 202.

Pottasch, S.R., 1959. *Ann. Astrophys., 22*, 412.

Prialnik, D. & Kovetz, A., 1984. Astrophys. J., *281*, 367.

Prialnik, D., Shara, M.M. & Shaviv, G., 1978. *Astr. Astrophys., 62*, 339.

Pringle, J.E., 1975. Mon. Not. R. astr. Soc., *170*, 663.

Pringle, J.E., 1981. *Ann. Rev. Astr. Astrophys., 19*, 137.

Pringle, J.E. & Savonije, G.J., 1979. *Mon. Not. R. astr. Soc., 187*, 777.

Pringle, J.E. & Verbunt, F., 1984. *Proceedings of the Fourth European IUE Conference, ESA SP-218*, p.377, ESTEC, Noordwijk, Netherlands.

Robinson, E.L., 1974. *Astrophys. J., 193*, 191.

Robinson, E.L., 1976a. *Ann. Rev. Astr. Astrophys., 14*, 119.

Robinson, E.L., 1976b. *Astrophys. J., 203*, 485.

Robinson, E.L., 1983. *Cataclysmic Variables and Related Objects*, p.119, eds Livio, M & Shaviv, G., Reidel, Dordrecht, Holland.

Robinson, E.L. & Nather, R.E., 1979. *Astrophys. J. Suppl. Ser., 39*, 461.

Rossi, B. & Olbert, S., 1970. *Introduction to the Physics of Space*, p.374, McGraw-Hill, New York, U.S.A.

Ruggles, C.L.N. & Bath, G.T., 1978. *Astr. Astrophys., 80,* 97.

Savonije, G.J., 1983. *Accretion-driven Stellar X-ray Sources,* p.343, eds Lewin, W.H.G. & van den Heuvel, E.P.J., Cambridge University Press, Cambridge, Great Britain.

Schwarzenberg-Czerny, A., 1981. *Acta astr., 31,* 241.

Schwarzenberg-Czerny, A., Ward, M., Hanes, D.A., Jones, D.H.P., Pringle, J.E., Verbunt, F. & Wade, R.A., 1985. *Mon. Not. R. astr. Soc., 212,* 645.

Shafter, A.W., 1983. *Astrophys. J., 267,* 222.

Shafter, A.W. & Targan, D.M., 1982. *Astr. J., 87,* 655.

Shakura, N.I. & Sunyaev, R.A., 1973. *Astr. Astrophys., 24,* 337.

Shara, M.M., 1980. *Astrophys. J., 239,* 581.

Sion, E.M., 1985. *Astrophys. J., 292,* 601.

Sion, E.M. & Guinan, E.F., 1983. *Cataclysmic Variables and Related Objects,* p.41, eds Livio, M & Shaviv, G., Reidel, Dordrecht, Holland.

Smak, J., 1971. *Acta astr., 21,* 15.

Smak, J., 1979. *Acta astr., 29,* 309.

Smak, J., 1982a. *Acta astr., 32,* 199.

Smak, J., 1982b. *Acta astr., 32,* 213.

Smak, J., 1983. *Astrophys. J., 272,* 234.

Smak, J., 1984a. *Publ. astr. Soc. Pacific, 96,* 5.

Smak, J., 1984b. *Acta astr., 34,* 161.

Smak, J., 1985. *Acta astr., 35,* 1.

Sparks, W.M., Starrfield, S. & Truran, J.W., 1978. *Astrophys. J., 220,* 1063.

Starrfield, S., Sparks, W.M. & Truran, J.W., 1974. *Astrophys. J. Suppl. Ser., 28,* 247.

Starrfield, S., Truran, J.W. & Sparks, W.M., 1978. *Astrophys. J., 226,* 186.

Starrfield, S., Truran, J.W., Sparks, W.M. & Kutter, G.S., 1972. *Astrophys. J., 176,* 169.

Stickland, D.J., Penn, C.J., Seaton, M.J., Snijders, M.A.J. & Storey, P.J., 1981. *Mon. Not. R. astr. Soc., 197,* 107.

Stockman, H.S., Foltz, C.B., Schmidt, G.D. & Tapia, S., 1983. *Astrophys. J., 271,* 725.

Szkody, P., Cordova, F.A., Tuohy, I.R., Stockman, H.S., Angel, J.R.P. & Wisniewski, W., 1980. *Astrophys. J., 241,* 1070.

Szkody, P., Liebert, J. & Panek, R.J., 1985. *Astrophys. J., 293,* 321.

Thorstensen, J.R., Smak, J. & Hessman, F.V., 1985. *Publ. astr. Soc. Pacific, 97,* 437.

Truran, J.W., 1982. *Essays in Nuclear Astrophysics,* p.467, eds Barnes, C.A., Clayton, D.D. & Schramm, D.N., Cambridge University Press, Cambridge, Great Britain.

Tuohy, I.R., Mason, K.O., Garmire, G.P. & Lamb, F.K., 1981. *Astrophys. J., 245,* 183.

Tylenda, R., 1981a. *Acta astr., 31,* 127.

Tylenda, R., 1981b. *Acta astr., 31,* 267.

van Paradijs, J., Kraakman, H., van Amerongen, S., Damen, E. & Tjemkes, H., 1985. *Recent Results on Cataclysmic Variables, ESA SP-236*, p.151, ESTEC, Noordwijk, Holland.

Verbunt, F. & Wade, R.A., 1984. *Astrophys. J. Suppl. Ser.*, 57, 193.

Vilhu, O., 1984. *Astrophys. Sp. Sci.*, *99*, 287.

Vogt, N., 1974. *Astr. Astrophys.*, *36*, 369.

Vogt, N., 1980. *Astr. Astrophys.*, *88*, 66.

Vogt, N., 1982. *Astrophys. J.*, *252*, 653.

Wade, R.A. & Ward, M.J., 1985. *Interacting Binary Stars*, p.129, eds Pringle, J.E. & Wade, R.A., Cambridge University Press, Cambridge, Great Britain.

Walker, M.F., 1954. *Publ. astr. Soc. Pacific*, *66*, 230.

Wargau, W., Bruch, A., Dreschel, H., Rahe, J. & Schoembs, R., 1984. *Astrophys. Sp. Sci.*, *99*, 145.

Wargau, W., Dreschel, H., Rahe, J. & Bruch, A., 1983. *Mon. Not. R. astr. Soc.*, *204*, 35P.

Warner, B., 1972. *Mon. Not. R. astr. Soc.*, *160*, 435.

Warner, B., 1973. *Mon. Not. R. astr. Soc.*, *162*, 189.

Warner, B., 1974. *Mon. Not. R. astr. Soc.*, *168*, 235.

Warner, B., 1975. *Mon. Not. R. astr. Soc.*, *170*, 219.

Warner, B., 1976. *Structure and Evolution of Close Binary Systems, IAU Symp. 73*, p.85, eds Eggleton, P., Mitton, S. & Whelan, J., Reidel, Dordrecht, Holland.

Warner, B., 1979. *White Dwarfs and Variable Degenerate Stars, IAU Colloq. 53*, p.417, eds Van Horn, H.M. & Weidemann, V., University of Rochester, U.S.A.

Warner, B., 1983. *Cataclysmic Variables and Related Objects*, p.155, eds Livio, M & Shaviv, G., Reidel, Dordrecht, Holland.

Warner, B., 1985a. *Cataclysmic Variables and Low-Mass X-ray Binaries*, p.269, eds Lamb, D.Q. & Patterson, J., Reidel, Dordrecht, Holland.

Warner, B., 1985b. *Interacting Binaries*, p. 367, eds Eggleton, P.P. & Pringle, J.E., Reidel, Dordrecht, Holland.

Warner, B., 1986a. *Astrophys. Sp. Sci., 118*, 271.

Warner, B., 1986b. *Mon. Not. R. astr. Soc., 219*, 347.

Warner, B. & Brickhill, A.J., 1978. *Mon. Not. R. astr. Soc., 182*, 777.

Warner, B., O'Donoghue, D. & Allen, S., 1984. *Mon. Not. R. astr. Soc., 212*, 9P.

Warner, B. & Nather, R.E., 1971. *Mon. Not. R. astr. Soc., 152*, 219.

Warner, B. & Nather, R.E., 1972. *Mon. Not. R. astr. Soc., 159*, 429.

Warner, B. & Robinson, E.L., 1972. *Nature Phys. Sci., 239*, 2.

Warner, B. & van Citters, G.W., 1974. *Observatory, 94*, 116.

Watts, D.J., Greenhill, J.G., Hill, P.W. & Thomas, R.M., 1982. *Mon. Not. R. astr. Soc., 200*, 1039.

Webbink, R.F., 1976. *Nature, 262*, 271.

Webbink, R.F., 1982. *Pulsations in Classical and Cataclysmic Variable Stars*, p.2, eds Cox, J.P. & Hansen, C.J., JILA, Boulder, Colorado, U.S.A.

Whitehurst, R., 1984. *Mon. Not. R. astr. Soc., 207*, 215.

Whitehurst, R., Bath, G.T. & Charles, P.A., 1984. *Nature, 309*, 768.

Wickramasinghe, D.T. & Martin, B., 1985. *Mon. Not. R. astr. Soc., 212*, 353.

Wickramasinghe, D.T. & Meggitt, S.M.A., 1982. *Mon. Not. R. astr. Soc., 198*, 975.

Wickramasinghe, D.T. & Meggitt, S.M.A., 1985. *Mon. Not. R. astr. Soc., 216*, 857.

Williams, G.A. & Hiltner, W.A., 1984. *Mon. Not. R. astr. Soc., 211*, 629.

Williams, P.M. & Longmore, A.J., 1984. *Mon. Not. R. astr. Soc., 207*, 139

Williams, R.E., 1980. *Astrophys. J., 235*, 939.

Williams, R.E., Sparks, W.M., Gallagher, J.S., Ney, E.P., Starrfield, S.G. & Truran, J.W., 1981. *Astrophys. J., 251*, 221.